Landsvirkjun

LV-2024-010

VATNAJÖKULL: Mass balance, meltwater drainage and surface velocity of the glacial year 2022-23

VATNAJÖKULL:
Mass balance, meltwater drainage and surface velocity of the glacial year 2022-23

Höfundar
Finnur Pálsson
Andri Gunnarsson
Eyjólfur Magnússon
Sveinbjörn Steinþórsson
Hlynur Skagfjörð Pálsson
Andri Björnsson
Steinunn Helgadóttir

Dagsetning
Febrúar 2024

Lykilsíða

Skýrsla LV nr	LV-2024-010	**Dagsetning**	Febrúar 2024
Fjöldi Síðna	0	**Upplag**	1
Dreifing	[x] Birt á vef LV	[X] Opin	[ ] Takmörkuð til [Dags.]
Titill	VATNAJÖKULL: Mass balance, meltwater drainage and surface velocity of the glacial year 2022-23		
Höfundar/fyrirtæki	Finnur Pálsson, Andri Gunnarsson, Eyjólfur Magnússon, Sveinbjörn Steinþórsson, Hlynur Skagfjörð Pálsson, Andri Björnsson, Steinunn Helgadóttir		
Verkefnisstjóri	Andri Gunnarsson		
Unnið fyrir	Landsvirkjun		
Samvinnuaðilar	–		
Útdráttur	Afkoma Vatnajökuls jökulárið 2022-2023 var neikvæð, –1,01 m að vatnsgildi eða nærri tvöfalt meira massatap en í meðalári frá upphafi mælinga. Þetta má að hluta rekja til lítillar vetrarafkomu sem var um 0,26 m undir meðaltali. Fyrri hluti sumars var fremur hlýr og bjartur á austurhluta Vatnajökuls. Sumarleysing var nærri meðaltali á safnsvæðum Vatnajökuls en vel yfir meðallagi á leysingarsvæðum. Leysing á Vatnajökli mældist um 18% umfram meðallag og sumar afkoma jökulsins 2023 reiknaðist –2,5 m eða um 0,4 m undir meðaltali mælitímabilsins 1997–2022, sem er –2,1 m.		
Lykilorð	Afkoma, Vatnajökull, leysing, jöklar		

Samþykki verkefnisstjóra
Landsvirkjunar

Andri Gunnarsson

VATNAJÖKULL:
Mass balance, meltwater drainage and surface velocity of the glacial year 2022_23

Institute of Earth Sciences
University of Iceland
and
National Power Company

Finnur Pálsson
Andri Gunnarsson
Eyjólfur Magnússon
Sveinbjörn Steinþórsson
Hlynur Skagfjörð Pálsson
Andri Björnsson
Steinunn Helgadóttir

RH-02-23

Contents:

Figures:

Tables:

Appendixes:

1. INTRODUCTION

In 1992 (glacial year 1991_92) a program of surface mass balance measurements was started for Vatnajökull by the Science Institute University of Iceland (now Institute of Earth Sciences, IES) in collaboration with the National Power Company (NPC). For the first year the program was limited to the western part of the glacier, but then expanded to include the northern outlets as well. In 1996 this study was further expanded to include southern outlets, with support from The European Union (Framework IV - Environment and Climate, TEMBA project 1996-1997). This program was extended 1998–2000 with further support from EU (Framework IV - Environment and Climate, ICEMASS project, 1998-2000). In 2000-2002 NPC and IES continued the program. In 2003-2005 IES participated in a multinational research project, which was financially supported by The European Union (EVK2-CT-2002-00152 SPICE). IES was responsible for obtaining data sets for calibration of models of the mass balance and dynamics of Vatnajökull. This work was also supported by The National Power Company of Iceland and The National Road Authority and was a continuation of the TEMBA-project of 1996-97 and ICEMASS project 1998-2001.
Since then, IES and NPC have continued a similar program. Mass balance measurements on the southeast outlet Breiðamerkurjökull is financially supported by the National Road Authority.
The aim of the collaborative work of NPC and IES is to improve understanding of the mass balance and melt water runoff from glaciers. This work in combination with energy balance measurements by NPC and IES on Vatnajökull will is used for calibration of models of the surface energy and mass balance of Vatnajökull.
This report describes the field measurements, mass balance, melt water runoff and GNSS survey, for the glaciological year 2022_23.

2. DIARY

May 2-8, 31, June 1-2: measurements of the winter balance, setup of AWSs.
June 21-22: installation of melt wires and maintenance of the lower AWS on Breiðamerkurjökull.
September 12, October 22- 27: summer balance measurements, take down of AWSs;

In all expeditions the locations of mass balance stakes were measured with Kinematic GPS (or fast static GPS) for surface velocity calculation.

The following members of staff of the Institute of Earth Sciences, University of Iceland, carried out the fieldwork on Vatnajökull: Finnur Pálsson, Sveinbjörn Steinþórsson, Eyjólfur Magnússon, Þorsteinn Sæmundsson with Andri Gunnarsson and Steinunn Helgadóttir (National Power Company), Hlynur Skagfjörð (Reykjavík Rescue Team) and Andri Björnsson.
Volunteers in the Iceland Glaciological Society Spring expedition to Vatnajökull helped in the field work in June.

3. MASS BALANCE MEASUREMENTS

The purpose of the mass balance measurements is to describe the temporal and spatial distribution of the components of the mass balance. The mean annual values of the components and their variation from year to year are analyzed and related to meteorological conditions and climatic variability. The results are used in studies of changes in the glacier volume, estimates of meltwater contribution to glacial rivers, mass balance modeling, evaluation of altitudinal and regional variations of mass balance in response to climatic variations, and to assess the hydrometeorological and dynamic response of the ice cap to climate change.

The mass balance was determined by a stratigraphic method, measuring changes in thickness and density relative to the summer surface. The winter balance was estimated by drilling ice cores through the winter layer in the spring. Ablation was monitored from markers; snow stakes were put up on the glacier and wires were drilled down in the ablation area. The summer balance was measured in the autumn.

3.1 Methods

Measurements of the surface mass balance on a large ice cap like Vatnajökull are impractical in terms of cost with conventional techniques and sampling density that are typically used on small glaciers. The spatial variability of the mass balance may, however, be predictable on the flat large outlets of such an ice cap given data on several profiles extending over the elevation range of the glacier. The precipitation generally increases with elevation and decreases with the distance from the coast, but both the distribution of snowfall and redistribution of snow by drift depend on the prevailing wind direction during the winter. The summer melting depends mainly on the altitude and the albedo of the glacier surface. Therefore, we have used observations along a limited number of flowlines which span the elevation ranges of the outlets. Each profile describes the variation with elevation, but together they also describe the lateral variation of the mass balance. Recently, modern over-snow vehicles and helicopters have allowed fast traverses to ensure successful fieldwork despite frequently poor weather conditions. The error for individual point measurement is estimated ~30 cm_{we} for both summer and winter balance. The error for the glacier wide specific mass balance, based on area integral of mass balance, is however considered smaller, since the error for individual survey sites is independent.

The winter mass balance (b_w) is defined as the mass of snow accumulated during the winter months, the summer balance (b_s) is the mass balance during the summer, and the net balance (b_n) is defined as their sum. The specific mass balance is expressed in terms of the equivalent thickness of water. All mass balance components apply to a time interval between given measurement dates, which are not fixed from one year to another. The dates in the autumn are separated by approximately one calendar year, which roughly coincides with the glaciological year defined as October 1st to September 30th. Snow cores are drilled in April-May through the winter layer and profiles of the density are measured. The summer balance is derived in the autumn from measurements of the changes in the snow core density during the summer in the accumulation area and from readings at stakes and wires drilled into the ice in the ablation areas.

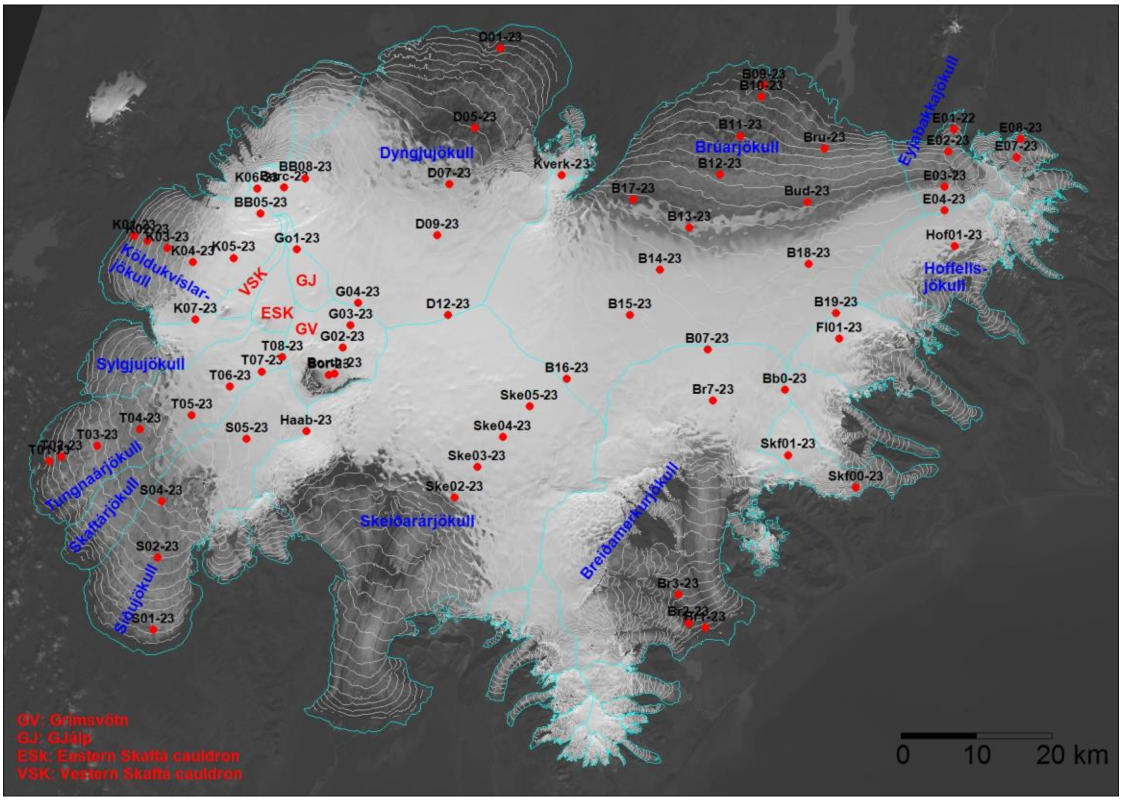

Figure 1. Outlets of Vatnajökull and location of mass balance survey sites 2022_23.

Digital maps are created for winter, summer and net balance for the whole ice cap based on the in-situ measurements. The mass balance is calculated over both the ice and water drainage basins. The summer balance over the water basin is an estimate of meltwater contribution to rivers and groundwater storage. This estimate, however, does not include precipitation that falls as rain on the glacier or snow, which falls and melts during the summer. As conventional for the north hemisphere we define the glaciological year from the start of October to the end of September next year and the period draining meltwater from the glacier during the summer from start of June through September. It would be misleading to include May in the summer period because runoff from the glacier melt in May is delayed due to refreezing during the elimination of the frost in the surface layer.

3.2 Results of mass balance measurements.

Winter mass balance measurements were done at 68 sites in spring 2023 (Fig. 1). The specific mass balance at individual sites is shown in Fig. 2. Most survey sites are on approximate central flow lines at individual outlets. The specific mass balance along the flow lines is given in Fig 3. for the glacier outlets: Síðujökull, Tungnaárjökull, Köldukvíslarjökull, Dyngjujökull, Brúarjökull (west and east), Eyjabakkajökull, Breiðamerkurjökull, SE-Vatnajökull, Skeiðarárjökull accumulation zone and the ice catchment of Grímsvötn.

Digital maps for winter, summer and net balance are shown in Figure 4. The mass balance of individual outlet is discussed in the following subsections.

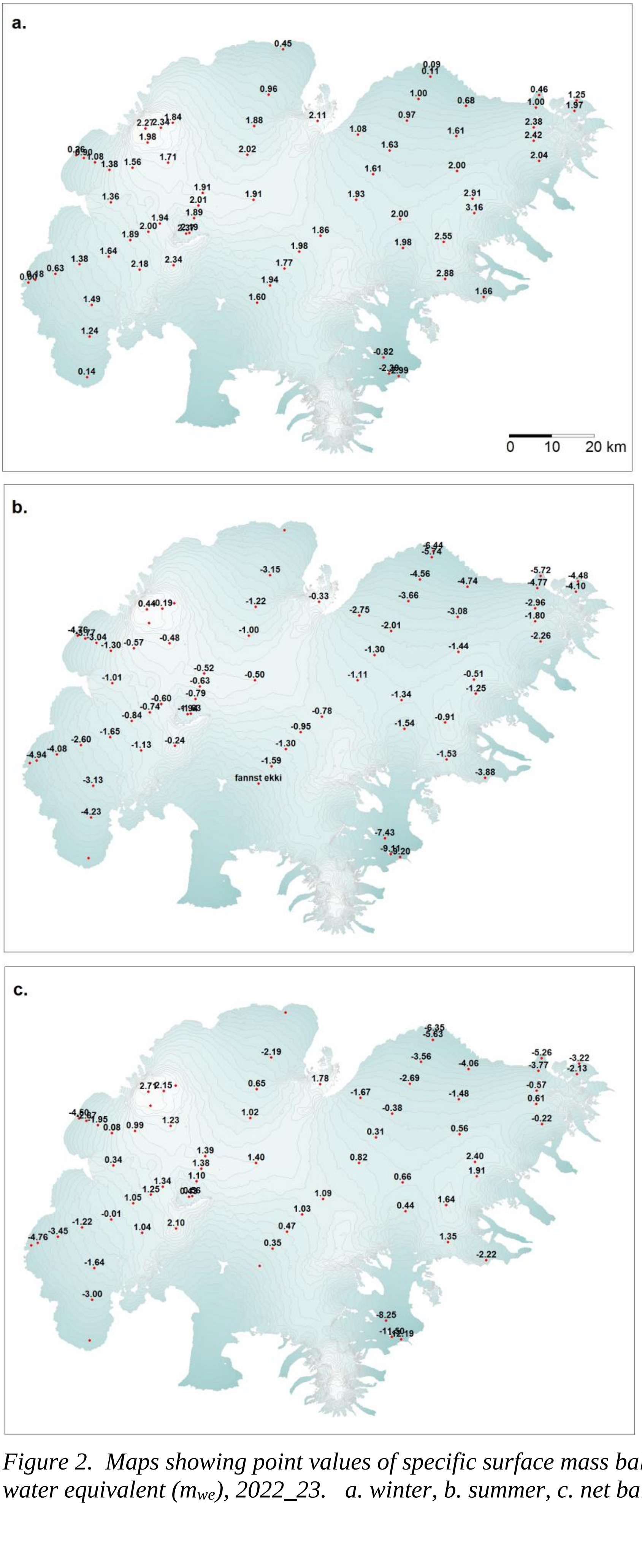

Figure 2. Maps showing point values of specific surface mass balance in m water equivalent (m_{we}), 2022_23. a. winter, b. summer, c. net balance.

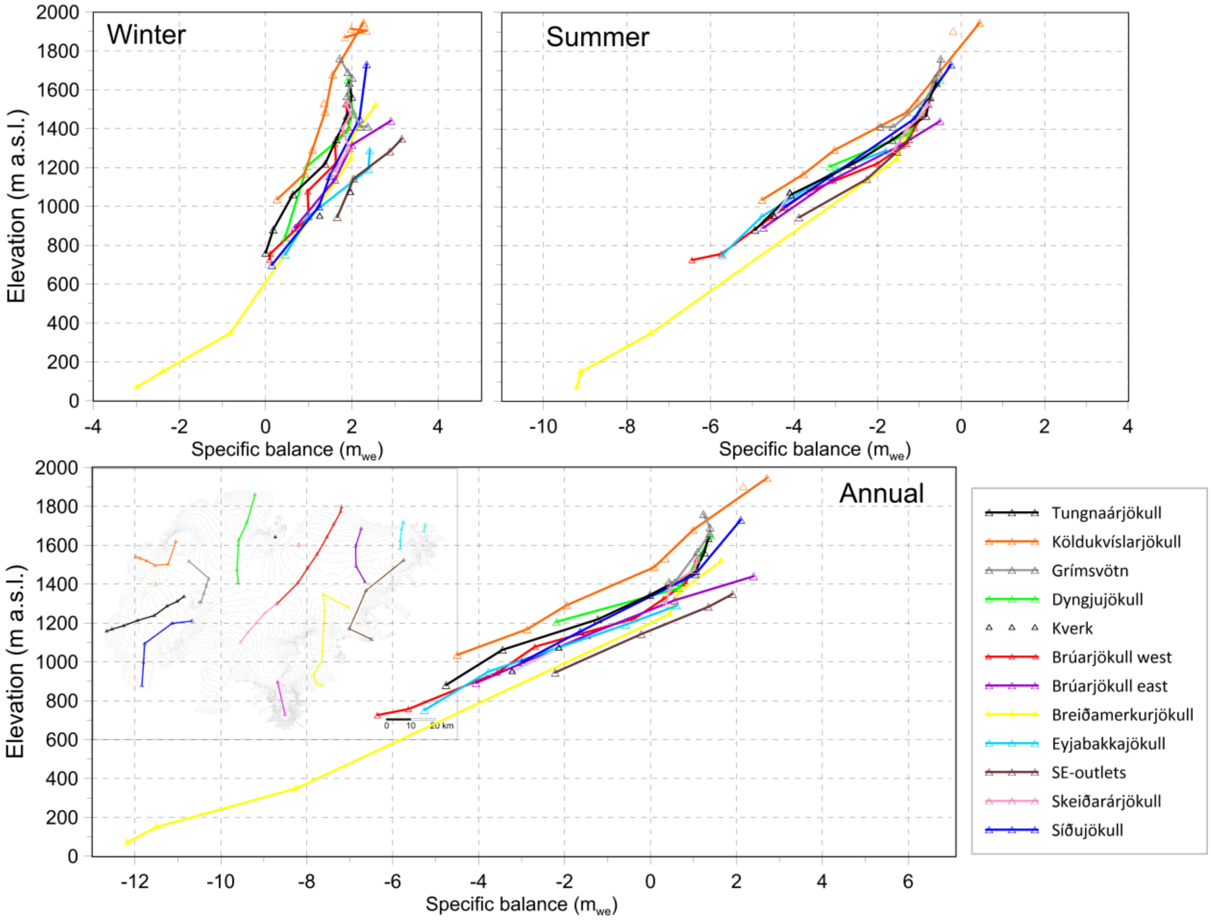

Figure 3. a. Specific mass balance (m_{we}), at survey sites along all mass balance profiles 2022_23.

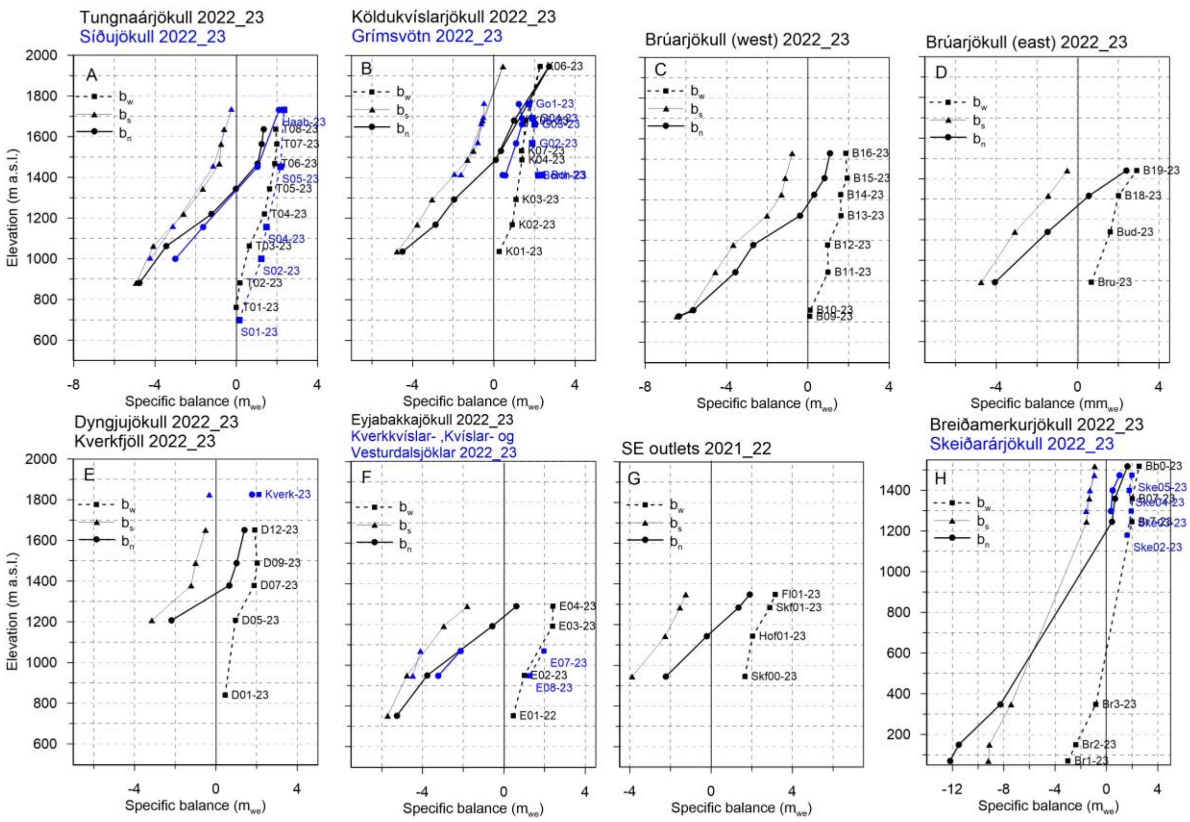

Figure 3. b. Specific point mass balance (m_{we}) 2022_23 as a function of elevation on central flow lines on Vatnajökull outlets.

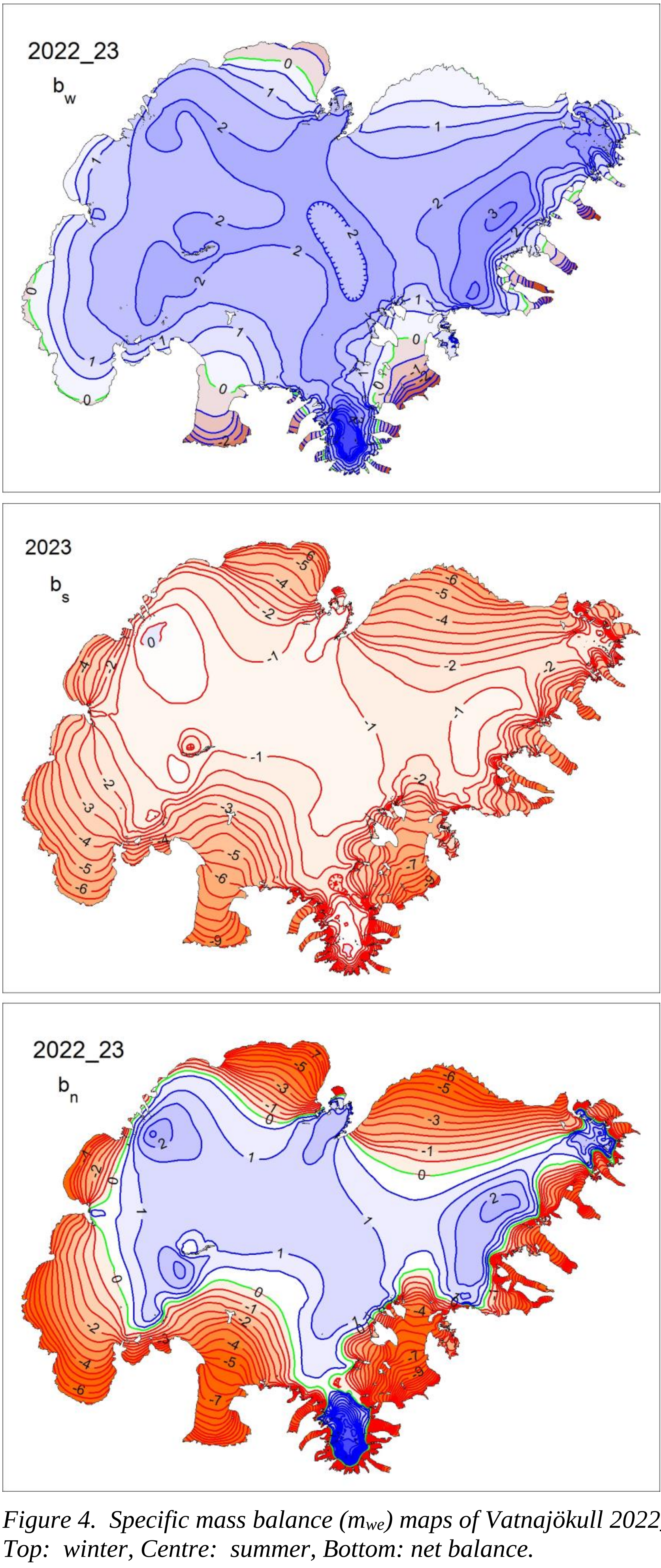

Figure 4. Specific mass balance (m_{we}) maps of Vatnajökull 2022_23. Top: winter, Centre: summer, Bottom: net balance.

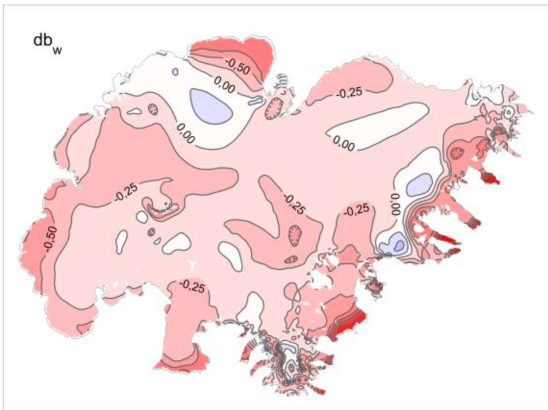

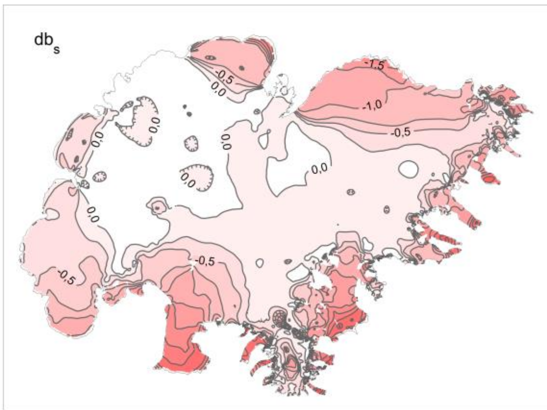

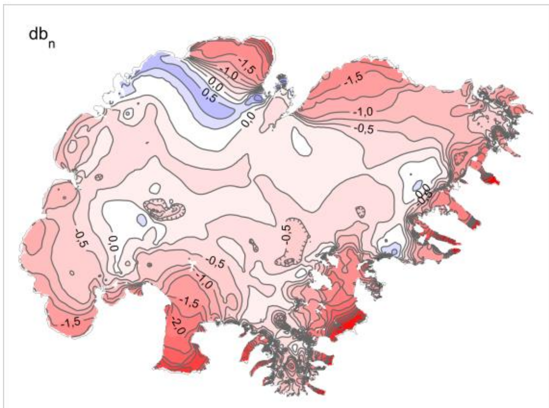

Figure 5. Top left: The difference between winter balance in 2022_23 and the average winter balance 1995_96 to 2021_22. Top right: The difference between summer balance in 2023 and the average summer balance 1996 to 2022. Lower left: The difference between net balance in 2022_23 and the average net balance 1995_96 to 2021_22.

(Blue is higher than average balance and red less than average).

A surface DEM is needed for surface area distribution and delineation of ice divides for individual outlets and catchments. The currently used surface DEM is mostly based on LiDAR survey 2010, -11 and -12 (**Jóhannesson et al. 2013), but the large set of GNSS profiles measured in spring 2023 were used to update the DEM to the 2023 elevation. This DEM was cut to the glacier terminus of autumn 2023, was used in all area distributions; ice and water divides were not reworked. Although of variable accuracy locally the DEM reflects fairly accurate elevation distribution.

The winter of 2022-2023 was rather cold, with winter precipitation less than average in the west (west of Bárðarbunga - Öræfajökull) but closer to average in the east.

Distribution of the winter snow was not typical (see fig. 5). In general, there was by far less snow than average in the lower ablation zones of the icecap, and by far less than average at all elevations in the west and south. Winter melting at the low-lying S-outlets was more than average. The summer was for most part rather warm, very dry and calm, most of the N-Atlantic low-pressure systems passed far south of Iceland. This resulted in an over average summer melt. The warm autumn contributed markedly to the total melt. The warm summer is partly due to warming of the sea water around Iceland by ~1 °C from recent years, now like the conditions in the period 1995-2010.

**Jóhannesson, T., Björnsson, H., Magnússon, E., Guðmundsson, S.,Pálsson, F., Sigurðsson, O., Thorsteinsson, T., and Berthier, E.:
Ice-volume changes, bias estimation of mass-balance measurements and changes in subglacial lakes derived by lidar mapping of the surface Icelandic glaciers, Ann. Glaciol., 54, 63–74, doi:10.3189/2013AoG63A422,2013.

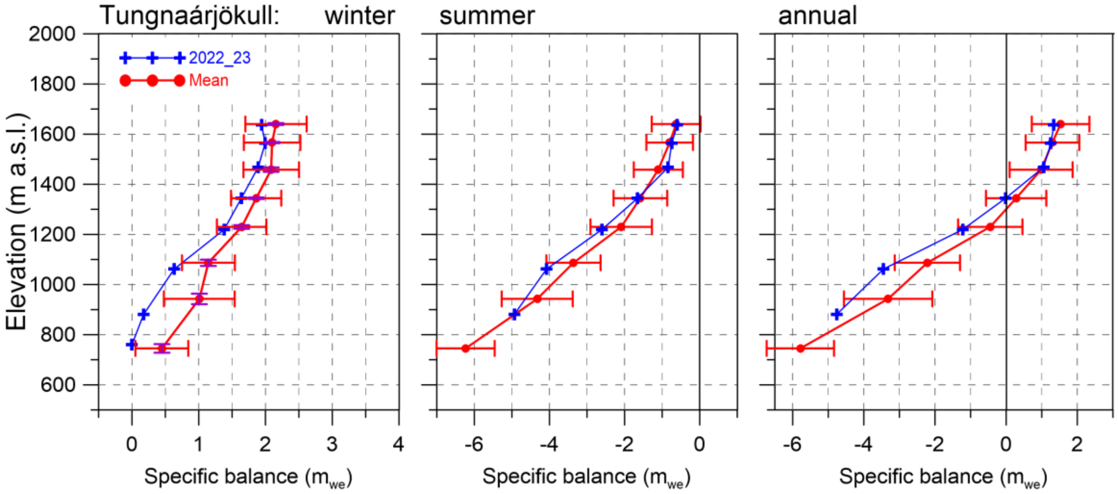

Figure 6. Mass balance at a central flow line of Tungnaárjökull 2022_23 and average mass balance 1991_92 to 2021_22 (the horizontal red lines indicate std. dev of the variability at the survey site during the survey period).

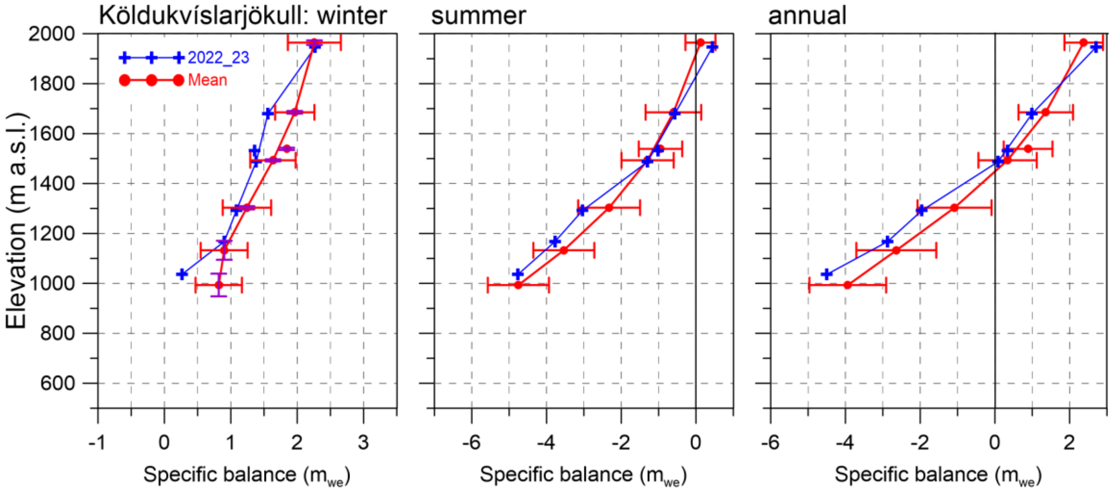

Figure 7. Mass balance at a central flow line of Köldukvíslarjökull 2022_23 and average mass balance 1991_92 to 2021_22.

3.2.1 Tungnaárjökull.

Area = 323 km^2
B_w = 0.38 km$^3_{we}$; b_w = 1.16 m$_{we}$
B_s = -0.87 km$^3_{we}$; b_s = -2.69 m$_{we}$
B_n = -0.49 km$^3_{we}$; b_n = -1.53 m$_{we}$
ELA = 1346 m a.s.l. (at profile)
AAR = 33 %
(The terms are defined at the foot of this page)

Variation of mass balance along a central flow line on Tungnaárjökull is shown in Fig. 6. The winter accumulation was under average at all survey sites, by far so, in the ablation zone. The total winter balance was only 76% of the average. Summer mass loss was not far from average, in total about 2% over the average. This year is the 28th year out of the 32 surveyed with negative net balance on Tungnaárjökull catchment, this time 35% more mass was lost than at average in the survey period.

3.2.2 Köldukvíslarjökull

Area = 284 km^2
B_w = 0.35 km$^3_{we}$; b_w = 1.23 m$_{we}$
B_s = -0.56 km$^3_{we}$; b_s = -1.97 m$_{we}$
B_n = -0.21 km$^3_{we}$; b_n = -0.74 m$_{we}$
ELA = 1478 m a.s.l. (at profile)
AAR = 48 %
Variation of mass balance along a central flow line on Köldukvíslarjökull is shown in Fig. 7. The winter accumulation was less than average in the accumulation zone by about 1. Std.

For each ice catchment basin, B_w, B_s and B_n are water equivalent volumes of winter, summer and net balance, ELA the equilibrium line altitude, and AAR is the accumulation area ratio.

close to average in the mid ablation zone, but almost no snow accumulated below 1000 m elevation. The total winter accumulation was ~83% of the average. Summer mass loss was close to average in the accumulation zone, but by ½ to 1 std. in the ablation zone. all survey sites. In total summer mass loss was ~1% more than average. This year Köldukvíslarjökull net balance was negative, this is the 26th year out of the 32 surveyed with negative net balance; now 58% more mass was lost than in an average year since 1991-92.

3.2.3 Dyngjujökull

Area = 1026 km^2
B_w = 1.53 $km^3{}_{we}$; b_w= 1.50 m_{we}
B_s = -1.85 $km^3{}_{we}$; b_s = -1.80 m_{we}
B_n = -0.32 $km^3{}_{we}$; b_n = -0.30 m_{we}
ELA = 1336 m a.s.l. (at profile)
AAR = 67 %

Variation of mass balance along a flow line on Dyngjujökull is shown on Fig. 8. In the high accumulation zone sites snow accumulation was ~l std. under average, about 1 std. over average in the lower accumulation zone. In the ablation zone snow collection was close to average. The total winter accumulation is estimated 93% of the average of the survey period.
Summer mass loss was almost at average at all survey sites but by about 1 std. over the average at 1200 m. The lowest site has not been visited yet when the report is written. The net balance was negative by -0.30 m_{we} about tenfold the average for Dyngjujökull that is only slightly negative (-0.03 m_{we}).
Dyngjujökull has often had mass balance close to zero, and the net balance has been estimated positive in at least 12 years of the three-decade period of almost continuous mass loss for Vatnajökull as a whole. The inland Dyngjujökull, is the outlet of Vatna-jökull closest to mass equilibrium during the survey period.

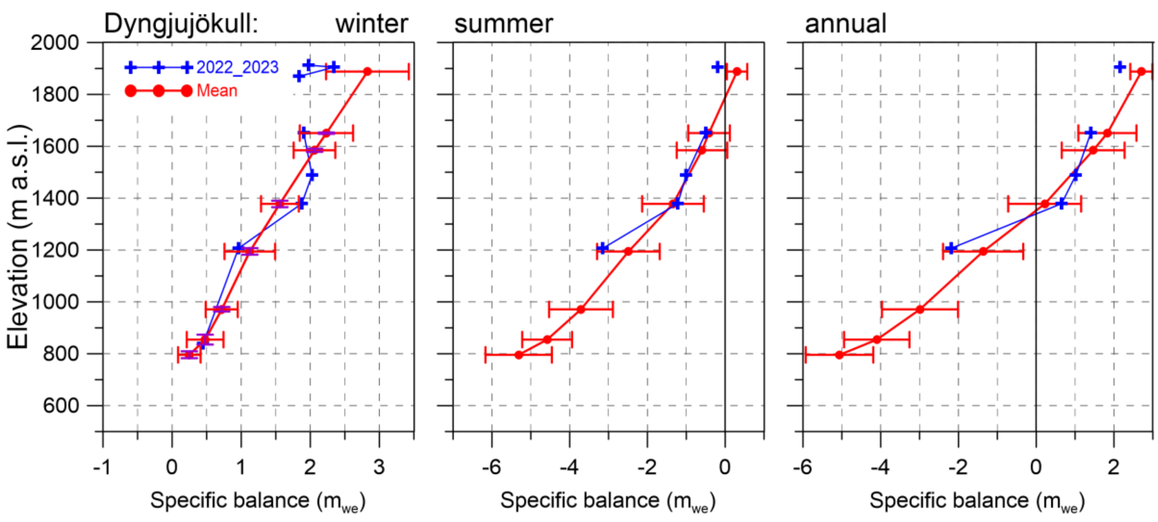

Figure 8. Mass balance at a central flow line on Dyngjujökull 2022_23 and average mass balance 1991_92 to 2021_22 (except 1998_99 – 2003_04 at all but the top elevation).

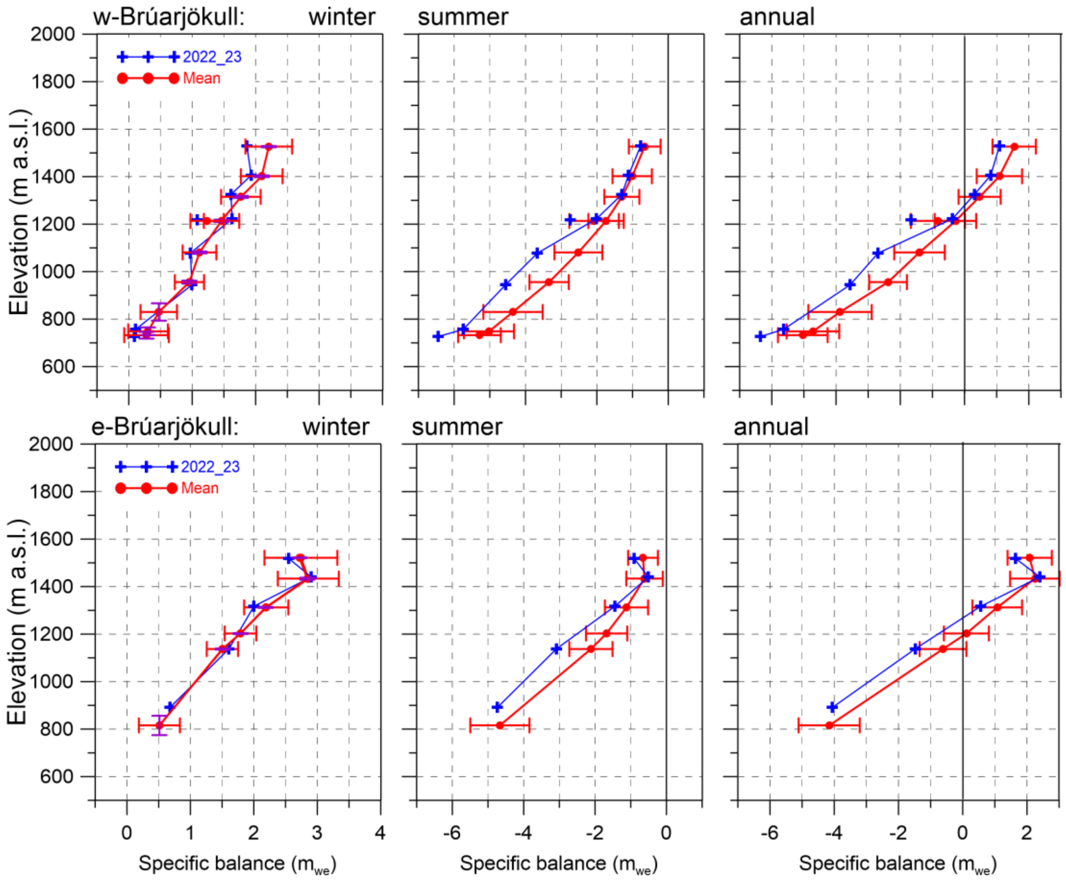

Figure 9. Mass balance at two flow lines on Brúarjökull 2022_23 and average mass balance 1992_93 to 2021_22.

3.2.4 Brúarjökull

Area = 1481 km^2
B_w = 2.30 km^3$_{we}$; b_w = 1.55 m$_{we}$
B_s = -3.36 km^3$_{we}$; b_s = -2.26 m$_{we}$
B_n = -1.06 km^3$_{we}$; b_n = -0.71 m$_{we}$
ELA = 1280 m a.s.l. (western flow line)
ELA = 1268 m a.s.l. (eastern flow line)
AAR = 54 %

Variation of mass balance along the flow lines on Brúarjökull is shown in Fig. 9. On Brúarjökull winter snow collection was not far from average at most survey sites, except in the top western accumulation zone, where it was ~1 std. less than average. The winter accumulation was in total ~96% of the average. Summer mass loss was close to average at most survey sites above 1200 m elevation, but more than 1 std. over than average at all the other sites. In total the mass loss in summer was 19% more than average.
The net balance was close to average in 1200-1400 m elevation range, but at other sites about 1 std. lower at all the other. In total the net balance was negative by 0.71 m$_{we}$. That amounts to about 25 fold that of an average year. During the survey period, there have been 9 years of positive balance and 22 years with negative net balance.

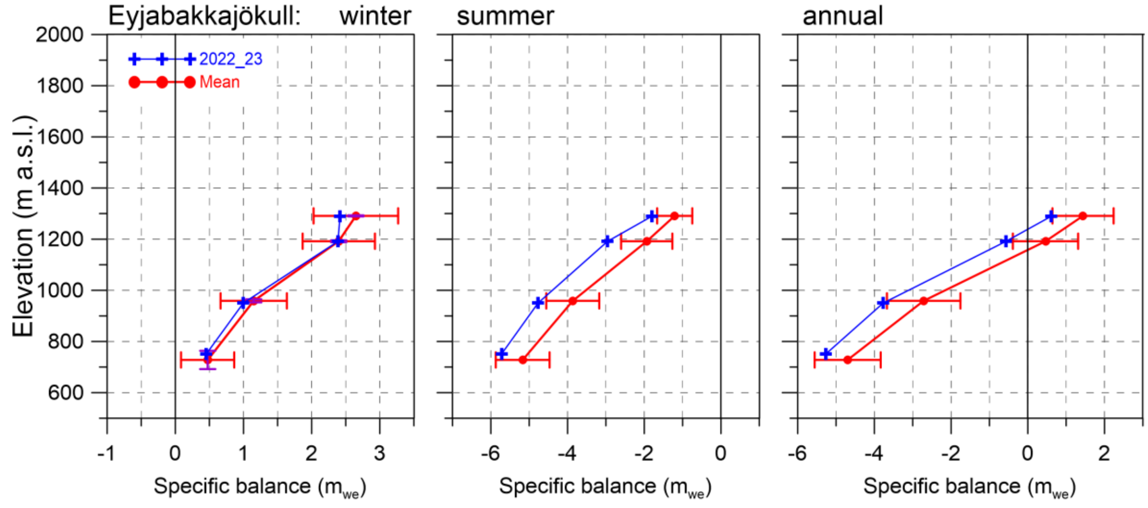

Figure 10. Mass balance at a central flow line of Eyjabakkajökull 2022_23 and average mass balance 1995_96 to 2021_22.

3.2.5 Eyjabakkajökull

Area = 104 km^2
B_w= 0.19 km^3 $_{we}$; b_w = 1.81 m_{we}
B_s = -0.33 km^3 $_{we}$; b_s = -3.23 m_{we}
B_n = -0.14 km^3 $_{we}$; b_n = -1.42 m_{we}
ELA = 1239 m a.s.l. (at profile)
AAR = 38 %

Variation of mass balance along a central flow line on Eyjabakkajökull is shown in Fig. 10. Like Brúarjökull the winter accumulation here was at average at all sites except the highest, where it was less than average. The total winter accumulation is estimated 99% of the survey period average. Summer mass loss was about 1 std more than average at all survey sites. The total summer mass loss was 20% more than average. The net balance was negative by about 1.7-fold that of the average of the survey period and has been negative for all but 3 years of the 28 years of survey.

3.2.6 Breiðamerkurjökull

Area = 875 km^2
B_w = 1.10 km^3_{we}; b_w = 1.26 m_{we}
B_s = -2.55 km^3 $_{we}$; b_s = -2.92 m_{we}
B_n = -1.45 km^3_{we}; b_n= -1.66 m_{we}
ELA = 1200 m a.s.l. (at profile)
AAR = 51%

Variation of surface mass balance along a central flow line on Breiðamerkurjökull is shown in Fig. 11. Winter accumulation was less than

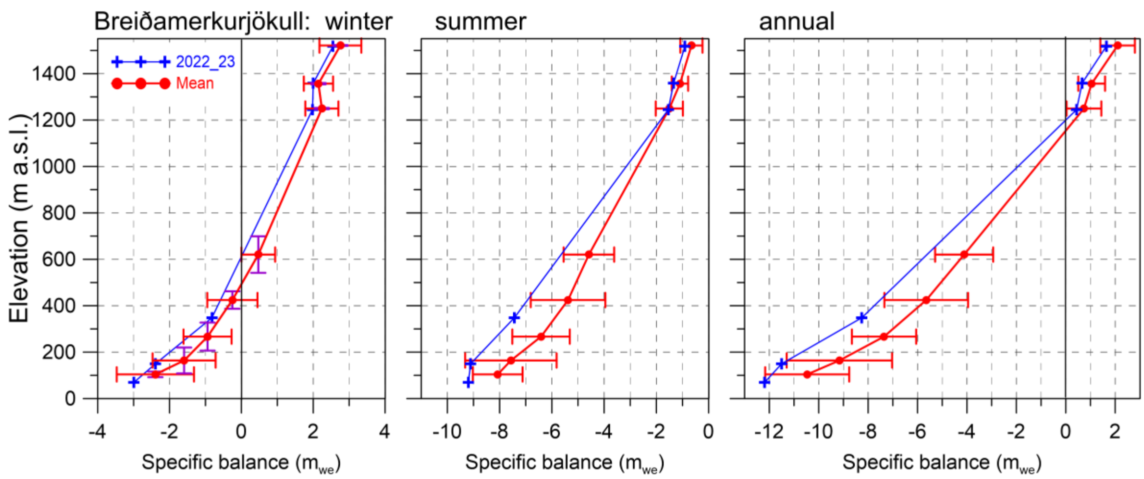

Figure 11. Mass balance at a central flow line of Breiðamerkurjökull 2022_23 and average mass balance 1995_96 to 2021_22.

average at the survey sites in the accumulation zone, but at the lower sites in the ablation zone mass loss in winter was more than average. The total winter balance was ~84% of the survey period average.
Summer mass loss was not far from the average in the accumulation zone), but more than 1 std. over average in the lower ablation zone. The total summer mass loss is estimated 12% over the average during the survey period. The net surface mass loss this year is estimated about 1.5-fold that of an average year.
In addition to mass loss due to surface melt Breiðamerkurjökull loses in the order of 0.5 km^3 (~0.6 m) annually via calving into the marginal lake Jökulsárlón; this mass loss is not accounted for here.

3.2.7 Skeiðarárjökull

Area = 1346 km^2
B_w = 1.87 km^3_{we}; b_w = 1.39 m_{we}
B_s = -3.58 km^3_{we}; b_s = -2.66 m_{we}
B_n = -1.71 km^3_{we}; b_n= -1.27 m_{we}
ELA = ~1250 m a.s.l. (at profile)
AAR = 54
The surface mass balance of Skeiðarárjökull is only measured in the accumulation zone due to almost impassable terrain in the ablation zone both in autumn and spring.
The mb-survey program here was initiated in 2002, although sporadic measurements were conducted in the 1990s. Estimation of mb in the ablation zone for the creation of the mb-maps is based on the survey of the neighboring Breiðamerkurjökull in the east (with similar elevation span) and western neighboring outlet Síðujökull.
Variation of mass balance along the survey profile on Skeiðarárjökull is shown in Fig. 12. Winter snow accumulation was 1 Std. under average at the highest (as was the site B16 located at the ice-divide of Brúarjökull and Skeiðarárjökull in continuation of the Skeiðarárjökull profile). The site at 1300 m however had winter mb close to average; this is likely due redistribution of snow by wind and seen at many other outlets of Vatnajökull this year. The redistribution of snow is more likely in prevailing northly winds and cold temperatures during snow fall.
Summer balance was close to average at the upper sites, and the lowest was not reachable in the autumn due to crevasses. The net balance was about 1 std under average, now due to unusually low winter balance.

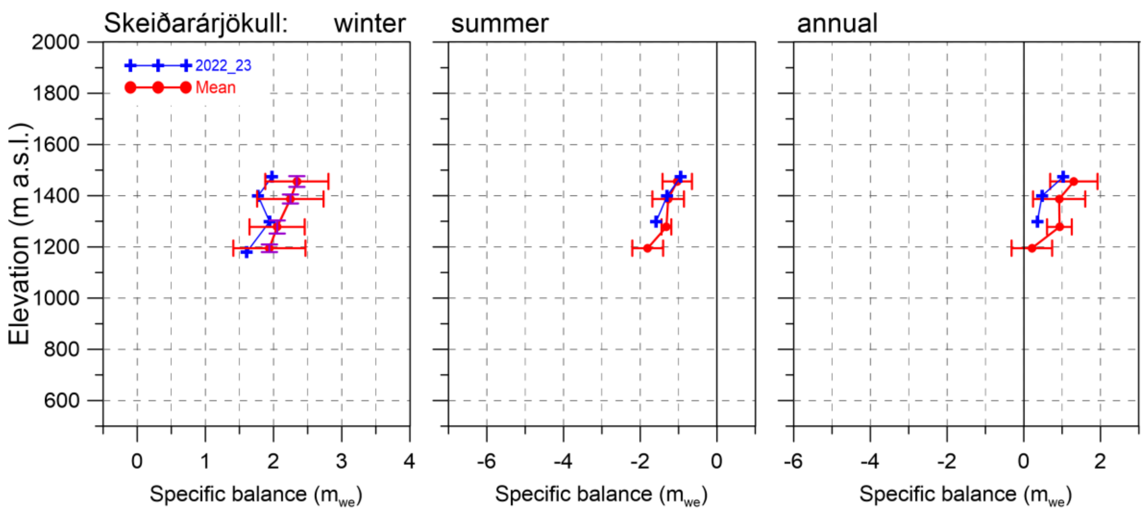

Figure 12. Mass balance at a central flow line of Skeiðarárjökull 2022_23 and average mass balance 2016_17 to 2021_22.

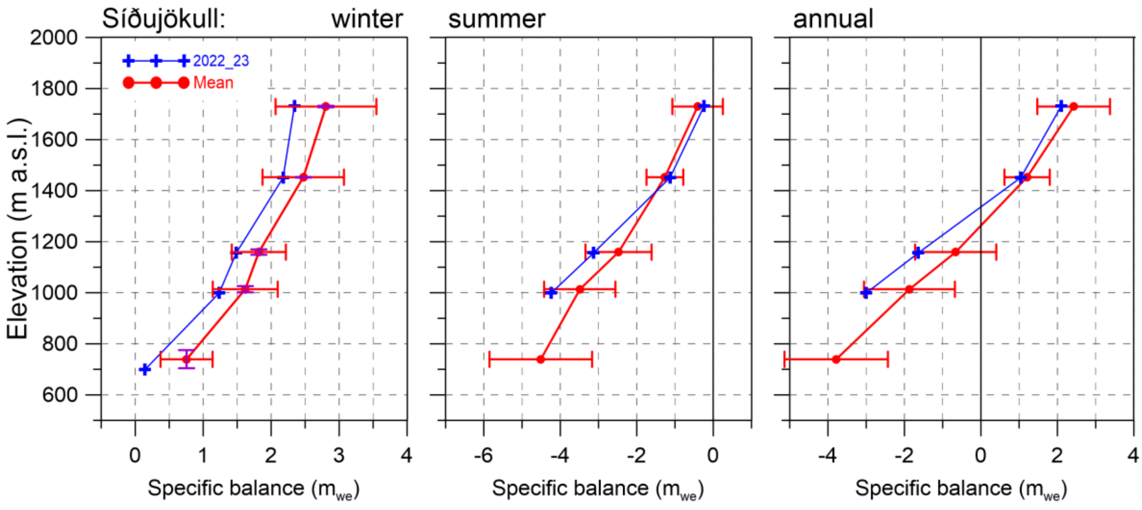

Figure 13. Mass balance at a central flow line of Síðujökull 2022_23 and average mass balance 2004_05 to 2021_22.

3.2.8 Síðujökull

Area = 400 km^2
B_w= 0.55 $km^3{}_{we}$; b_w = 1.38 m_{we}
B_s = -1.26 $km^3{}_{we}$; b_s = -3.15 m_{we}
B_n = -0.71 $km^3{}_{we}$; b_n= -1.77 m_{we}
ELA = 1335 m a.s.l. (at profile)
AAR = 36 %

Variation of mass balance along a central flow line on Síðujökull is shown in Fig. 13.
The winter snow accumulation was well under average at all survey sites. The total winter balance was 86% of the average (since 2004_05). Summer mass loss was at average at the highest sites, but far over the at the lower sites (In autumn the route to the lowest sit3 was impassable). The total summer mass loss was 8% over the average of the survey period. Total mass loss was ~35% more than average during the 18-year survey period. At Síðujökull the only year of surveyed positive net balance was 2014_2015.

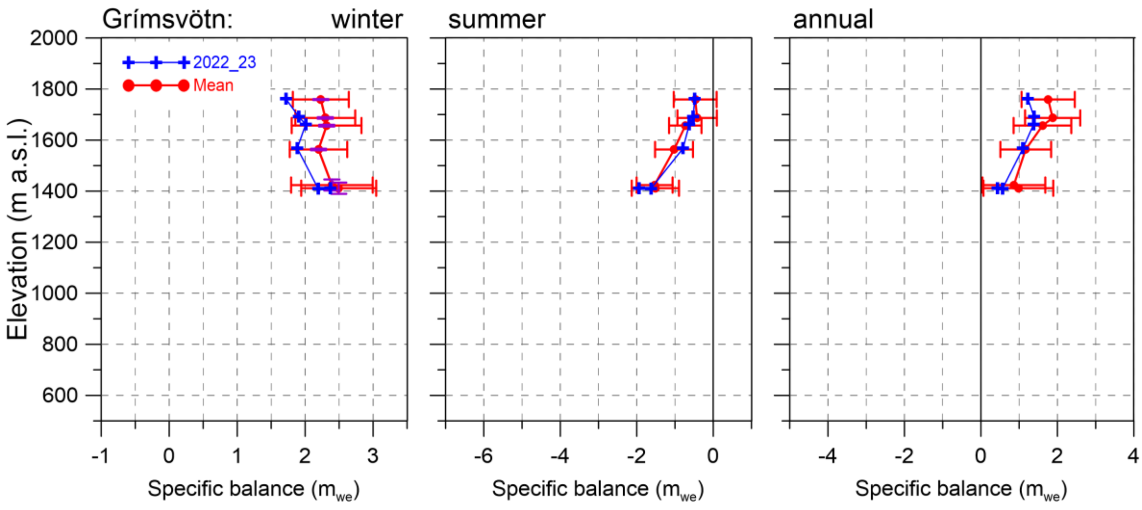

Figure 14. Mass balance at a flow line towards Grímsvötn 2022_23 and average mass balance 1991_92 to 2021_22.

3.2.9 Grímsvötn-Gjálp

Area = 174 km^2
B_w = 0.34 km$^3_{we}$; b_w = 1.99 m_{we}
B_s = -0.13 km$^3_{we}$; b_s = -0.78 m_{we}
B_n = 0.21 km$^3_{we}$; b_n= 1.21 m_{we}

Variation of mass balance at sites close to a flow line from Bárðarbunga towards Grímsvötn center is shown in Fig. 14. Snow accumulation at the survey sites was between ½ - 1 std. less than average, and total winter accumulation 12% less than average. Summer mass loss was close to average at all survey sites; total summer mass loss was 6% more than average. Net balance was positive as always (except 2010), however, now only 78 % of the average.
In addition to surface mass loss in summer, geothermal melt in the Grímsvötn catchment area is on the order of 0.2 km^3 annually. This mass loss is about 1.21 m evenly distributed over the ice catchment, or approximately equal to this year net surface balance. This means that the total balance for the catchment of Grímsvötn is close to zero this year.

The average surface mass balance in the survey period (since 1991-92) is +1.50 m, so assuming the annual 1.21 m loss due to geothermal melt yields an annual surplus of ~0.3 m (0.052 km^3) on average, or ~1.6 km^3. In the Gjálp eruption, within the Grímsvötn ice catchment, over 3.5 km^3 of ice was melted and some, although much less, in the 1998, 2004 and 2011 Grímsvötn eruptions. About half of this has been compensated for by the average total positive surface balance.

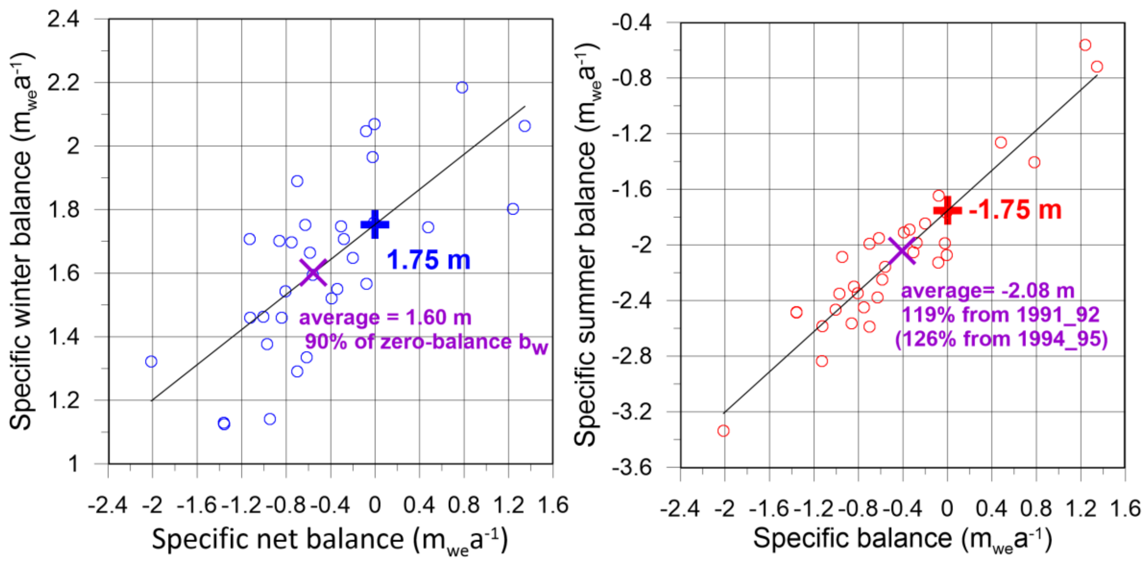

Figure 15. Vatnajökull winter (left) and summer (right) mass balance plotted against net mass balance for the survey period 1991_92 to 2022_23. The + and + and the accompanying numbers, mark the zero-mass balance mass turnover for Vatnajökull (current topography) as estimated from the linear trends shown with thin black lines.

3.3 Vatnajökull: Surface mass balance record

From the digital mb maps (Fig. 4) the glacier wide volumes of winter, summer and net balances for Vatnajökull have been calculated by integration and are as follows:

Area = 7656 km^2
B_w = 11.10 km$^3_{we}$; b_w = 1.46 m_{we}
B_s = -18.74 km$^3_{we}$; b_s = -2.47 m_{we}
B_n = -7.64 km$^3_{we}$; b_n = -1.01 m_{we}
AAR = 53%;

(balance values as a function of elevation are tabulated in appendix D)

The winter of 2022-2023 was rather cold, with winter precipitation less than average in the west (west of Bárðarbunga - Öræfajökull) but closer to average in the east.
Distribution of the winter snow was not typical (see fig. 5). In general, there was by far less snow than average in the lower ablation zones of the icecap, and by far less average at all elevations in the west and south. In many of the outlets over average winter accumulation was measured in the mid elevation range of the accumulation zone, but less than average at higher elevations. This is at least partly due to wind redistribution, but perhaps also by lesser portion falling as rain in autumn due to the colder than average autumn. Winter melting at the low-lying S-outlets more than average. The summer was for most part rather warm, very dry and calm, most of the N-Atlantic low-pressure systems passed far south of Iceland. This resulted in more than average summer melt. The warm 2023 autumn contributed markedly to the total melt. The warm summer is partly due to warming of the sea water around Iceland by ~1 °C from recent years, now similar to the sea temperatures in the period 1995-2010. The total winter balance was ~90% of the average (over the observation period from 1991_92).
The total summer mass loss was almost 20% more than the average of the survey period.
The net balance of 2022_23 was very negative or 2.25-fold the average (over the observation period from 1991_92).
The zero-mass balance mass turnover (mbt) for Vatnajökull (current topography) is estimated from the zero net balance crossover of the linear trend of b_w plotted against b_n and equivalently b_s against b_n (see fig 15.) and found to be close to 1.75 m_{we} (13.4 km$^3_{we}$). The winter balance 2022_23 is ~83% of the estimated zero-mass balance turnover (0-mbt), while the average b_w of the survey period is ~90% of the 0-mbt.
The summer balance of 2023 is -0.72 m (or 42%) more negative than 0-mbt. On average the summer mass loss has been 19% (average of summers 1992-2022) higher than 0-mbt, (26% for the period of 1995-2022).
This clearly shows that the high mass loss of the past 3 decades is governed by too much mass loss during summer rather than too little snow accumulation during winter.
Since 2010, after the 15-year period of high mass loss, the summer and net balance have been highly variable (figure 16.), one year with definite positive mass balance, 2014_15, and a few close to zero or slightly positive: 2010_11, 2016_17, 2017_18 and 2021_22.
The variability of the winter balance is by far more prominent for the outlets closest to sea. That section of the glacier receives precipitation in all south and east wind directions, and thus has high snow accumulation in winters when prevailing paths of the North Atlantic low-pressure systems are just south and east of Iceland.

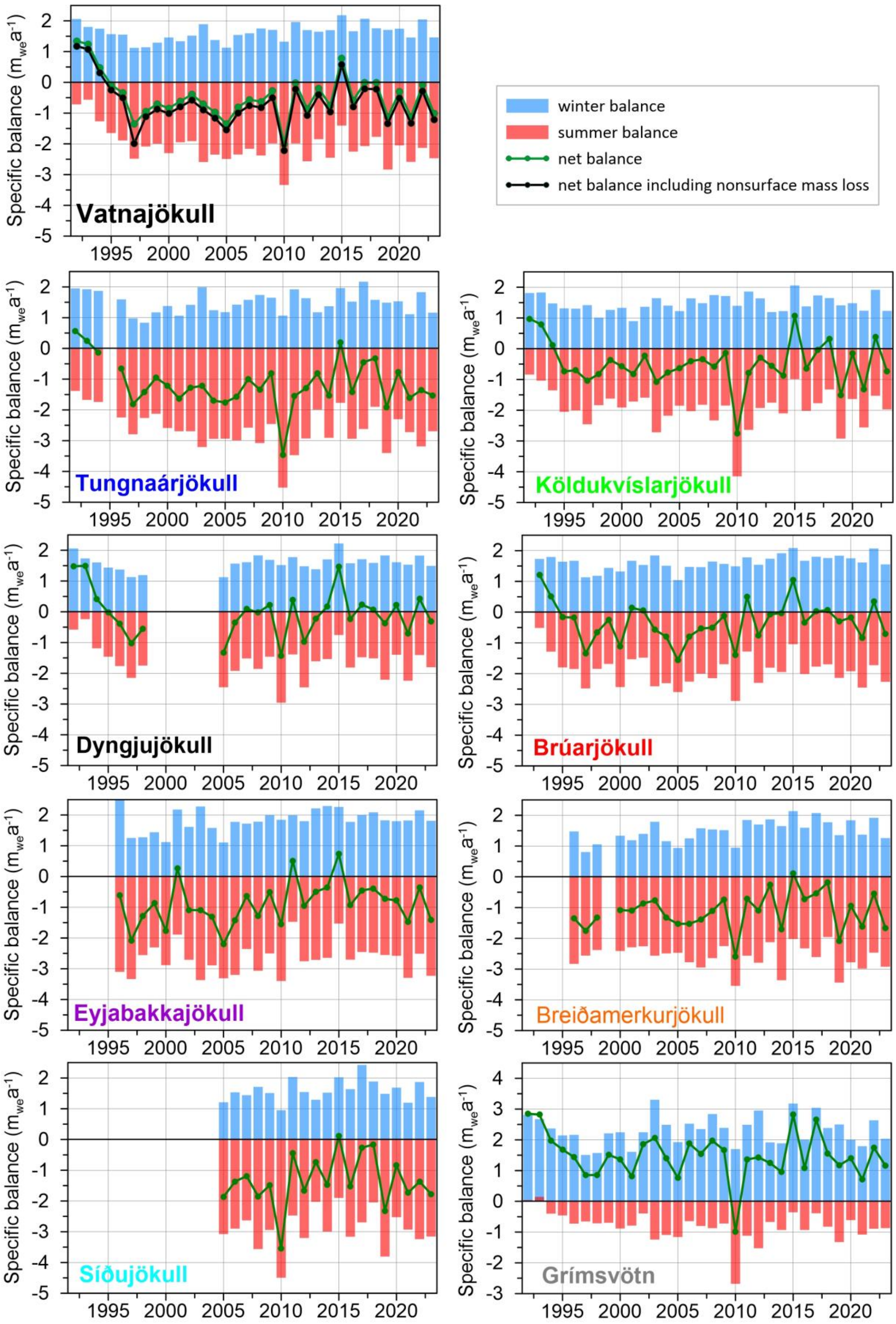

Figure 16. Specific mass balance record for Vatnajökull (top), and selected Vatnajökull outlets 1991_92-2022_23.

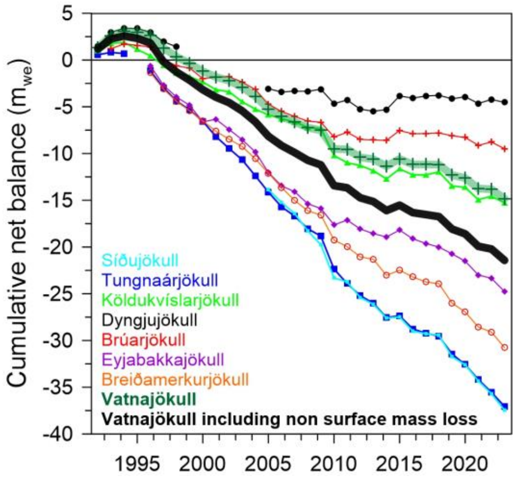

Figure 17. Cumulative specific surface mass balance Vatnajökull and selected Vatnajökull outlets 1991_92 – 2022_23.

The cumulative net balance curves for the outlets of Vatnajökull in Fig. 17 show that all outlets have been losing mass since in most years since 1994_95. In the period of high mass loss, the loss rate is about -0.5 to -0.6 $m_{we}a^{-1}$ for the northern outlets but -1.1 to -1.5 $m_{we}a^{-1}$ for the south and western outlets. After 2010 there is a distinct difference between the north inland (Dyngjujökull and Brúarjökull) and the south and west coastal outlets (Breiðamerkurjökull, Tungnaárjökull and Síðujökull) in that there is a sudden change in the mass balance trend for the northern. The trend changes from -0.5 $m_{we}a^{-1}$ to about zero for the northern while there is little change for the others. The east outlet Eyjabakkajökull behaves like the coastal and is in fact close to sea, while Köldukvíslarjökull in the NV is more like the northern.

The cumulative mb for Vatnajökull is very similar to Köldukvíslarjökull, with a slope of -0.75 $m_{we}a^{-1}$ in the period of high mass loss, but -0.35 $m_{we}a^{-1}$ after 2010.

During the survey period starting in 1991_92 Vatnajökull lost ~131 km^3 of ice or thinned ~15 m due to surface mass loss (summing from the start of high mass loss in 1994_95 yields 159 km^3 or 19 m thinning).

In addition, non-surface mass loss is estimated (calving, geothermal melt, internal friction, eruptions) ~0.21 m_{we} for Vatnajökull in a paper by Tómas Jóhannesson and others (Jóhannesson, T., Pálmason, B., Hjartarson, Á., Jarosch, A., Magnússon, E., Belart,J., et al. (2020). Non-surface mass 1balance of glaciers in Iceland. J. Glaciol. 66,685–697. doi:10.1017/jog.2020.37) which amounts to an ice loss of ~59 km^3 or 7.7 m average thinning since 1994_95.

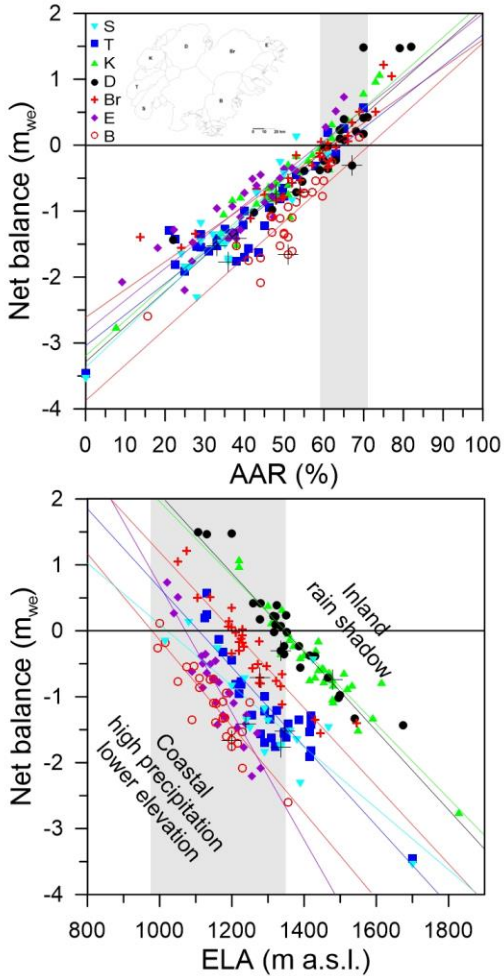

Figure 18. The relation between net annual balance (b_n) and accumulation area ratio (AAR) (upper) and b_n and equilibrium line altitude (ELA), for Vatnajökull outlets during the survey period. (This year's points are marked with a black +).

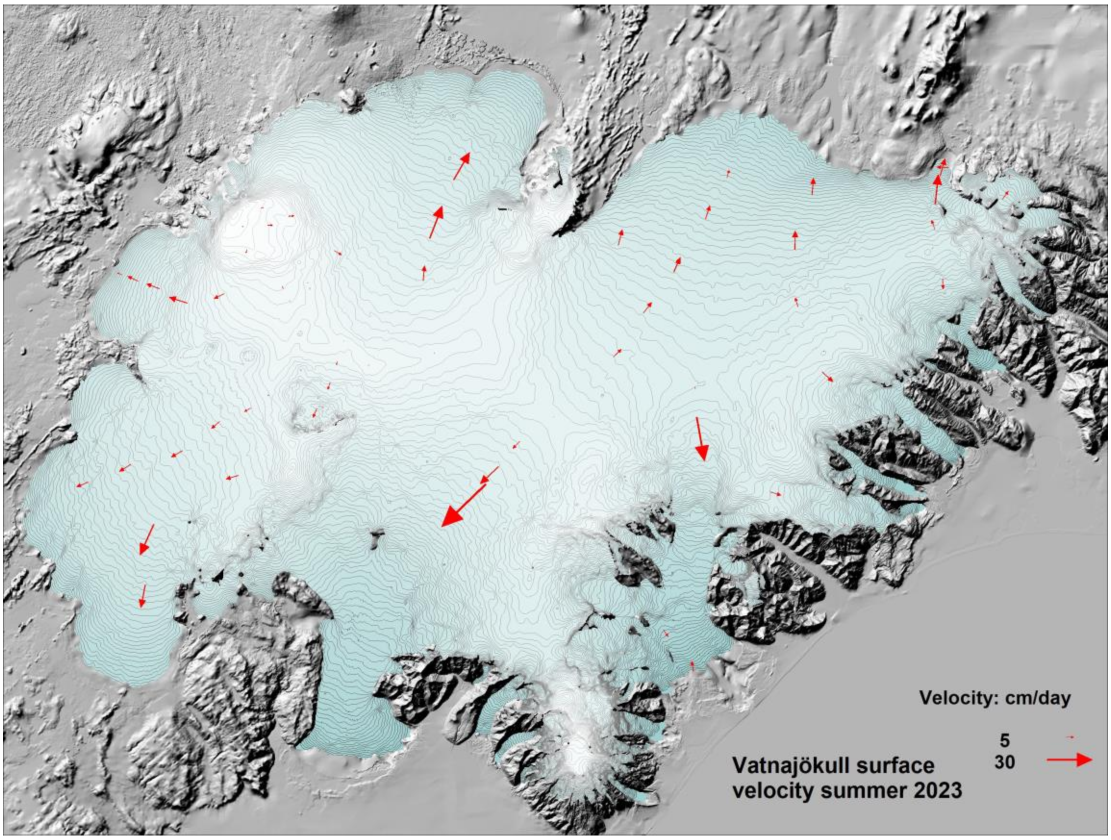

Figure 19. Average summer velocity at survey sites in 2023.

In Fig. 17 the relation of the annual net balance to the accumulation area ratio (AAR) and equilibrium line altitude (ELA) is shown for different outlets over the survey period. The bn-AAR gradient is similar for all outlets, about 0.5 m_{we} for 10% change in AAR. The zero-balance AAR varies for different outlets in the range 60-65%, similar for all outlets except for the southern outlet Breiðamerkurjökull. Breiðamerkurjökull is far from equilibrium, the ablation area is too large. A large part of the outlet has carved 200-300 m deep valley into the former sediment bed, and the surface and bed elevation has lowered accordingly. Similarly, the zero-balance ELA varies from about 1000-1100 m a.s.l. for the southern outlets to 1400 m a.s.l. for the NW outlets. The bn-ELA slope is similar for all outlets -0.6 m_{we} per 100 m, except Eyjabakkajökull with a slope of -1.0 m_{we} per 100 m and Síðujökull with a slope of -.45 m_{we} per 100 m (for Síðujökull possibly due to outliers in the data set).

4. SURFACE VELOCITY MEASUREMENTS

The average summer surface velocity of the glacier surface at the survey sites was calculated from fast static or kinematic GNSS positioning of the ablation stakes/wires (accuracy about ~10 cm). In 2023 all sites were surveyed in spring and autumn and many in June. At a few sites, stakes from previous years were found and resurveyed, making it possible to calculate surface velocity over a year or longer time span. The average summer surface velocity is shown in Figure 19.

At sites close to the glacier terminus very small lateral movement is generally measured. This indicates that the glacier snouts are almost stagnant. In the centre areas of some of the outlets especially close to the equilibrium line, there is an increase in velocity during summer compared to winter. The summer velocity is typically in the order of two-fold the winter velocity. This suggests that basal sliding is increased in the melting season and is of often at the same magnitude as the deformation velocity. To better understand the variable velocity continuous GNSS has been run during summer at several sites.

From previous velocity measurements, surging of outlets has been predicted. Currently the increase in velocity at sites D05 and D07 (Fig. 20.) persists and suggests that Dyngjujökull may surge within a few years. The velocity at sites D07 and D05 is now similar that in 1997 prior to the surge in 1998-2000 and the accumulation zone has thickened. To monitor velocity changes leading up to a surge GNSS instruments were set up in spring to continuously monitor movement at sites D05 and D07.

The data collected allows for post-processing to acquire more accuracy (~dm instead of ~m), but the processing has not been finished when this report is written.

Figure 21. shows the average summer velocity and elevation change record at the survey sites on Eyjabakkajökull. There is a steady increase in velocity at sites E01 and E02 since about 2018. This may be caused by the rapid recession of the glacier snout, and thus steeper surface slopes, formation of a frontal lake and the floating of the ice front. This might be signs of a starting surge, but then speed up at E03 would be expected, which is not the case.

Images of velocity and elevation records for other mb survey sites are displayed in Appendix F.

Most vehicles used in the survey expeditions are equipped with survey type GNSS instruments that collect data while driving. These are post-processed, to yield surface profiles with an accuracy of ~dm in horizontal and vertical. Location of all profiles surveyed in 2023 is shown in figure 22. The profiles have proved of high importance to increase accuracy of remote sensing-based surface DEMs.

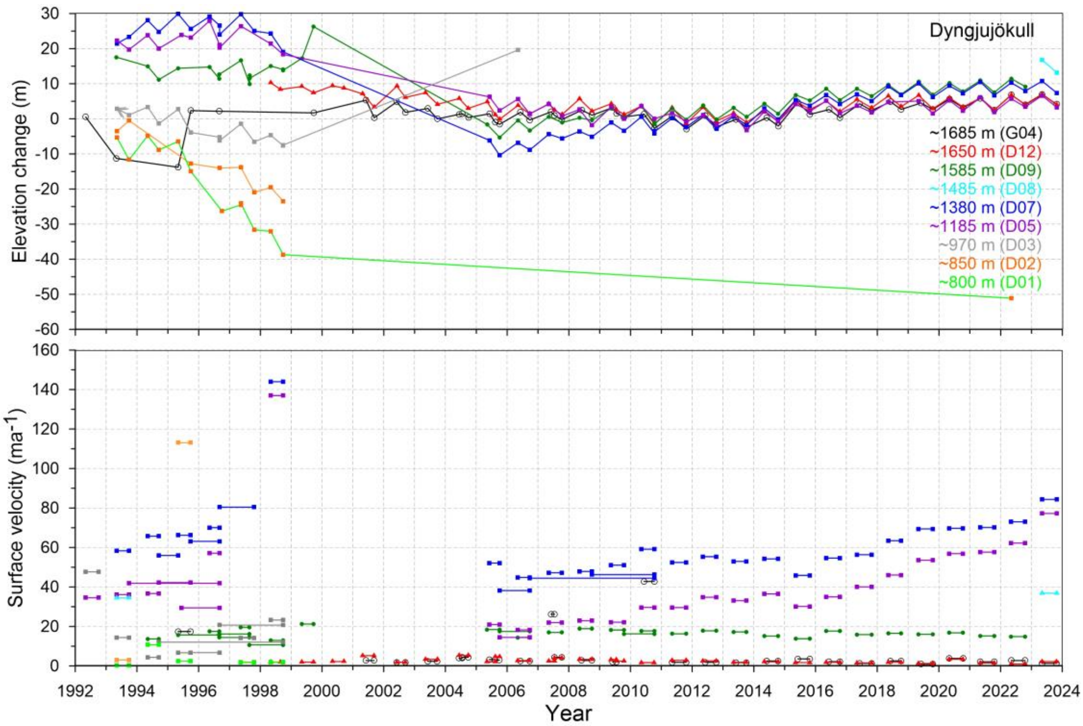

Figure 20. Surface elevation change relative to summer 2011 (upper panel) and average surface velocity (lower panel) at mb sites on Dyngjujökull in 1992 to 2023.

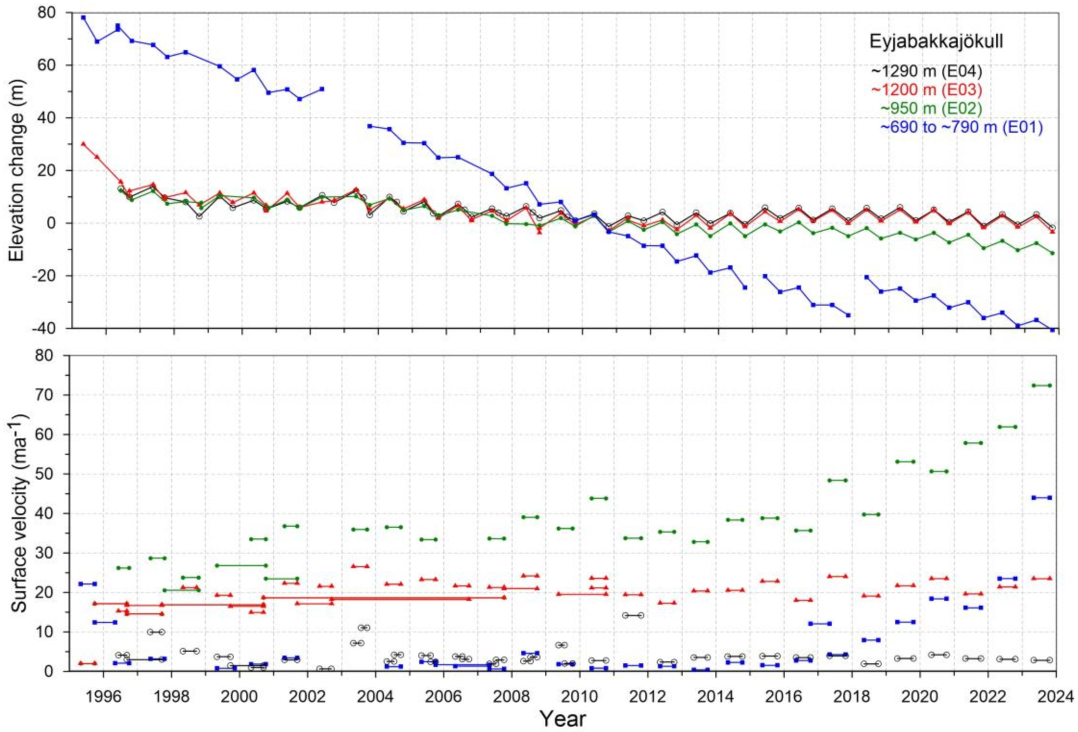

Figure 21. Surface elevation change relative to summer 2010 (upper panel) and average surface velocity (lower panel) at mb sites on Eyjabakkajökull in 1995 to 2023.

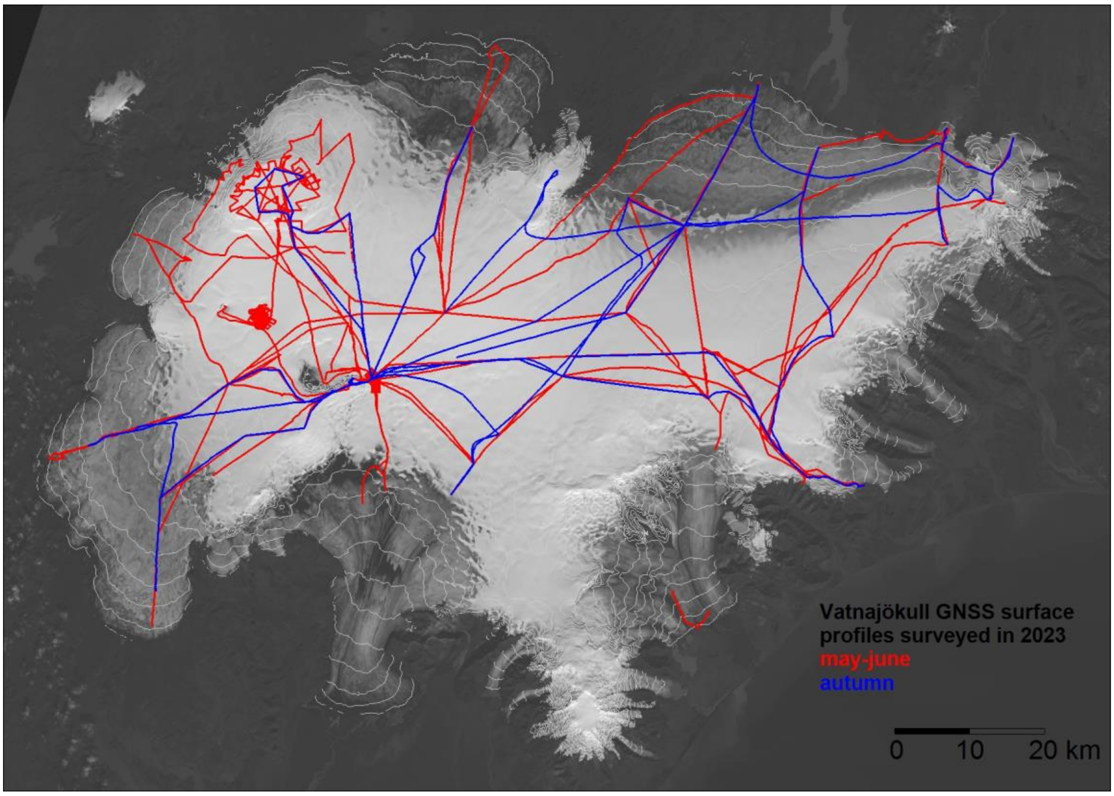

Figure 22. Location of surface elevation profiles surveyed in field trips on Vatnajökull in 2023. Survey in spring is shown in red and autumn survey in blue.

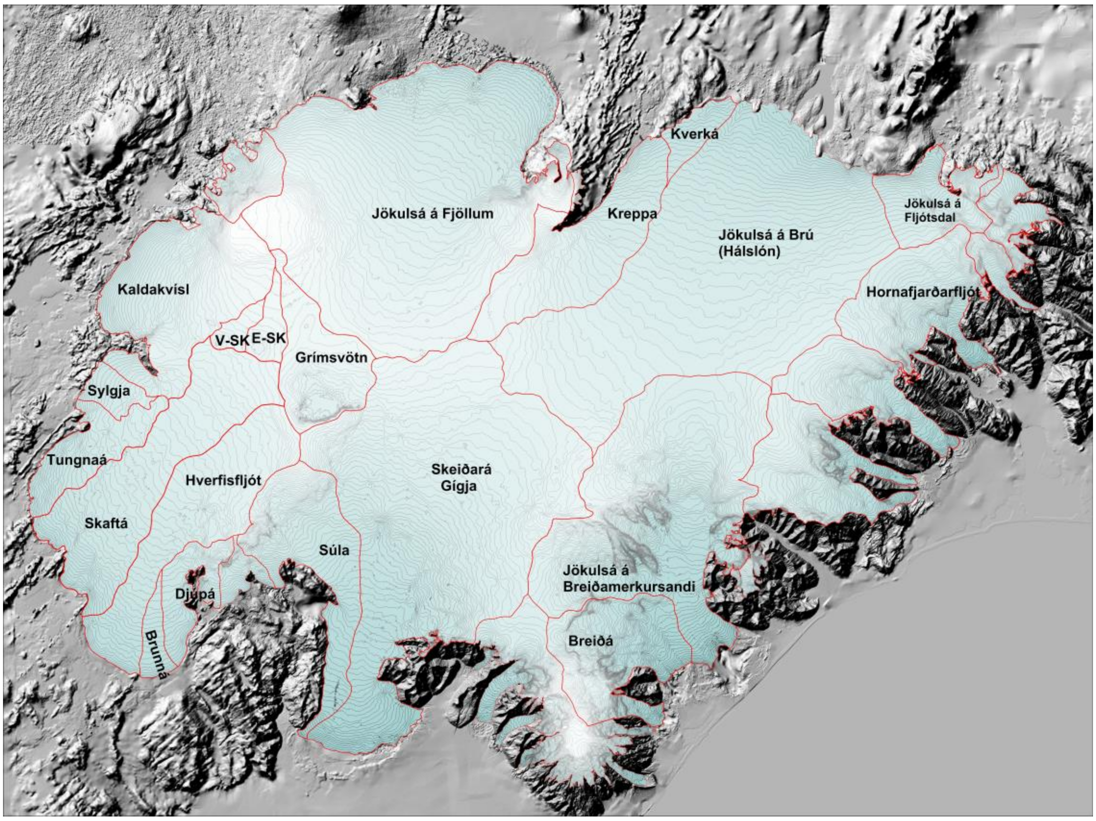

Figure 23. Water divides and drainage basins of selected rivers draining water from Vatnajökull, Súla is since summer 2016 diverted to Gígja.

5. Melt water runoff.

Water divides and drainage basins for rivers draining water from Vatnajökull have been defined from water pressure potential maps. The potential maps were produced from surface (year 2010) and bedrock DEMs.

Figure 23. shows the water divides and drainage areas for selected rivers draining melt water from Vatnajökull. The summer balance over the water basin is an estimate of meltwater contribution to rivers and groundwater storage. This estimate, however, does not include precipitation that falls as rain on the glacier, or snow that falls and melts during the summer. The meltwater contribution can be compared with river runoff at stream flow gauges closest to the glacier. For this comparison, we define the glaciological year from the start of October to the end of September and the period draining meltwater from the glacier during the summer from June through September. It would be misleading to include May in the summer period because runoff from the glacier melt in May is delayed due

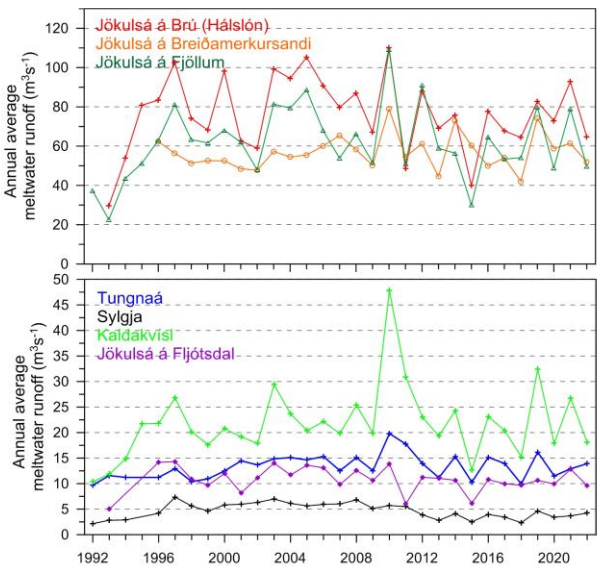

Figure 24. The temporal variation of average annual meltwater runoff to selected river catchments.

Table I. Melt water drainage to selected rivers in summer 2023.

Water Catchment:	Area (km^2)	ΣQ_s ($10^6 m^3$)	Q_s ($m^3 s^{-1}$)	Q_a ($m^3 s^{-1}$)	q_s ($ls^{-1} km^{-2}$)
Vatnajökull	7570	18747	1778,5	594,5	78,5
Tungnaá	104	388	36,8	12,3	117,7
Sylgja	38	122	11,5	3,9	102,1
Kaldakvísl	328	656	62,2	20,8	63,5
Jökulsá á Fjöllum	1109	1959	185,8	62,1	56,0
Kreppa	287	522	49,5	16,5	57,6
Kverka	34	177	16,8	5,6	164,9
Hálslón	1186	2681	254,3	85,0	71,7
Jökulsá á Fljótsdal	121	386	36,6	12,2	101,6
Jökulsá í Lóni	92	289	27,4	9,2	99,4
Hornafjarðarfljót	227	631	59,9	20,0	88,0
Jökulsá á Breiðamerkursandi	686	1783	169,1	56,5	82,4
Breiðá-Fjallsá	220	955	90,6	30,3	137,6
Gígja	1383	3707	351,7	117,6	85,0
Brunná	30	166	15,8	5,3	176,7
Djúpá	70	296	28,1	9,4	133,9
Hverfisfljót	306	765	72,6	24,3	79,3
Skaftá	380	1047	99,3	33,2	87,3
Grímsvötn	171	133	12,6	4,2	24,6
Eystri Skaftárketill	39	20	1,9	0,6	16,1
Vestari Skaftárketill	25	15	1,4	0,5	19,0
Hólmsá	157	463	43,9	14,7	93,7
Heinabergsvötn	214	649	61,6	20,6	96,4
Skjálfandafljót	89	88	8,3	2,8	31,2

ΣQ_s: total summer melt water; Q_s: average runoff (averaged over summer, 4 months, June – September)
Q_a: average runoff (averaged over a whole year); q_s: average runoff per km^2 (averaged over a whole year)

to refreezing during elimination of the cold wave and because of the contribution of the spring snow melt from the highlands to the runoff. Some melting also occurs during winter, especially in the terminus regions of the southern outlets.

Average melt water runoff to different rivers is given in Table I, and temporal variation of the average meltwater runoff in Fig. 24. The average specific runoff (q_s) differs from basin to basin from ~31 to ~176 $ls^{-1}km^{-2}$. This is mainly due to different elevation distributions, for example, the water drainage basins for Tungnaá, Brunná and Kverká are within the ablation zone, while that of Grímsvötn and Skaftárkatlar are high in the accumulation zone.

Runoff as function of elevation, estimated from summer balance, is tabulated for individual water catchments in Appendix E.

6. Conclusions

In the glaciological year 2022_23 the winter balance for Vatnajökull was ~90% of the average in the observation period from 1991_92. Only 7 winters of the survey period have had lower winter balance, but 9 out the 12 recent years have had higher than average winter balance. The average winter balance is 1.63 m_{we} and standard variability is 0.28 m_{we}.

The total summer surface mass loss was 12% over the average since 1995 (19% more than average since 1991_92). During the survey period, only five summers had more surface mass loss. The average summer balance is -2.09 m_{we}, and the standard variability 0.56 m_{we}.

The net balance was negative by 2.25-fold that of the average, and only 7 years have had more surface mass loss. The average net balance is -0.46 m_{we}, and the standard variability 0.56 m_{we}

Since 2010, after the 15-year period of high mass loss, the summer and net balance have been highly variable, even one year with positive mass balance in 2014_15 and close to zero in 2010_11, 2016_17, 2017_18 and 2021_22. In contrast 2018_19 and 2020_21 are both among years with highest surface mass loss of the survey period. It is also noteworthy that 5 years out of the last decade have had more mass loss than the average of the whole survey period.

The cumulative mb for Vatnajökull is very similar to Köldukvíslarjökull, with a slope of -0.75 $m_{we}a^{-1}$ in the period of high mass loss, but -0.35 $m_{we}a^{-1}$ in the period after 2010.

During the survey period starting in 1991_92 Vatnajökull has lost ~131 km^3 of ice or thinned ~15 m due to surface mass loss (summing from the start of high mass loss in 1994_95 yields 159 km^3 or 19 m thinning).

In addition, non-surface mass loss is estimated (calving, geothermal melt, internal friction, eruptions) ~0.21 m_{we} for Vatnajökull in a paper by Tómas Jóhannesson and others (Jóhannesson, T., Pálmason, B., Hjartarson, Á., Jarosch, A., Magnússon, E., Belart,J., et al. (2020). Non-surface mass 1balance of glaciers in Iceland. J. Glaciol. 66,685–697. doi:10.1017/jog.2020.37) which amounts to an ice loss of ~59 km^3 or 7.7 m average thinning since 1994_95.

Glacier surface meltwater runoff in summer 2023 (estimated from summer surface balance only, summer rain and snow that falls and melts during summer, calving and geothermal and internal melting, is not included): to Tungnaá 97% of the average, 103% of the average to Kaldakvísl, 105% of the average to Jökulsá á Fjöllum, 120% of the average to Hálslón, 122% to Jökulsá í Fljótsdal and 108% to Jökulsá á Breiðamerkursandi. (Averages refer to the survey period of each outlet.)

Surface velocity measurements suggest that Dyngjujökull is in the first phase of a surge and may complete a surge cycle within the next few years.

Surface mass balance summary 2022_23:

B_w = 11.10 km^3_{we}
B_s = -18.74 km^3_{we}
B_n = -7.64 km^3_{we}
AAR = 53%

Specific Values:

b_w = 1.46 m_{we}
b_s = -2.47 m_{we}
b_n = -1.01 m_{we}
$b_{n(\text{including other mass loss})}$ = -1.22 m_{we}

Appendix A: Surface mass balance at measurement sites 2022_23.

b_w: specific winter balance, **b_s**: specific summer balance, **b_n**: specific net balance, **l_a**: new snow in autumn (all in water equivalent).

Site	Position Latitude		Longitude		Elévation (m a.s.l.)	Date in spring	Date in autumn	b_w (m)	b_s (m)	b_n (m)	la (m)
B09-23	64	44,483	16	6,1882	726,3	20230505	20231024	0,09	-6,444	-6,354	0,02
B10-23	64	43,682	16	6,7041	757,2	20230505	20231024	0,11	-5,744	-5,634	0,04
B11-23	64	40,939	16	10,484	944,6	20230505	20231024	0,995	-4,559	-3,564	0,16
B12-23	64	38,262	16	14,149	1078	20230505	20231024	0,974	-3,665	-2,691	0,25
B13-23	64	34,578	16	19,637	1222	20230504	20231026	1,63	-2,008	-0,378	0,35
B14-23	64	31,65	16	24,772	1324	20230504	20231023	1,609	-1,303	0,306	0,35
B15-23	64	28,513	16	30,032	1406	20230504	20231024	1,93	-1,114	0,816	0,35
B16-23	64	24,123	16	40,92	1529	20230508	20231023	1,862	-0,776	1,086	0,38
B17-23	64	36,733	16	28,797	1217	20230504	20231023	1,082	-2,747	-1,665	0,39
Br1-23	64	5,9586	16	19,82	70,04	20230501	20231022	-2,99	-9,198	-12,19	0
Br2-23	64	6,354	16	22,523	150	20230501	20231022	-2,39	-9,108	-11,5	0
Br3-23	64	8,4131	16	23,971	348,4	20230501	20231022	-0,82	-7,434	-8,254	0
Br7-23	64	22,143	16	16,939	1245	20230504	20231023	1,98	-1,542	0,438	0,21
B07-23	64	25,797	16	17,481	1359	20230504	20231027	2,001	-1,341	0,66	0,34
Bb0-23	64	22,707	16	5,0412	1519	20230504	20231023	2,55	-0,906	1,644	0,46
Bru-23	64	39,753	15	56,535	891,4	20230503	20231023	0,679	-4,738	-4,059	0,12
Bud-23	64	35,99	15	59,887	1138	20230503	20231023	1,608	-3,084	-1,476	0,37
B18-23	64	31,577	16	0,1205	1317	20230503	20231023	2,002	-1,444	0,558	0,4
B19-23	64	27,978	15	56,008	1441	20230503	20231023	2,906	-0,506	2,4	0,37
D01-23	64	47,868	16	49,975	839,5	20230505		0,45			0
D05-23	64	42,225	16	54,689	1207	20230505	20231026	0,96	-3,147	-2,187	0,35
D07-23	64	38,289	16	59,258	1379	20230505	20231026	1,876	-1,222	0,654	0,36
D09-23	64	34,682	17	1,5194	1489	20230505	20231026	2,025	-1,005	1,02	0,32
D12-23	64	28,975	17	0,1844	1652	20230505	20231024	1,905	-0,501	1,404	0,29
E01-22	64	40,65	15	34,843	751,7	20230503	20231024	0,455	-5,72	-5,265	0,02
E02-23	64	39,108	15	35,996	950,1	20230503	20231024	0,999	-4,77	-3,771	0,11
E03-23	64	36,603	15	36,902	1192	20230503	20231024	2,385	-2,959	-0,574	0,35
E04-23	64	34,938	15	37,179	1289	20230503	20231024	2,415	-1,803	0,612	0,32
K01-23	64	35,177	17	51,88	1036	20230506	20231025	0,265	-4,765	-4,5	0,04
K02-23	64	34,804	17	49,677	1168	20230506	20231025	0,902	-3,773	-2,871	0,16
K03-23	64	34,234	17	46,393	1292	20230506	20231025	1,083	-3,036	-1,953	0,2
K04-23	64	33,211	17	42,246	1487	20230506	20231025	1,38	-1,296	0,084	0,13
K05-23	64	33,446	17	35,458	1679	20230506	20231025	1,558	-0,568	0,99	0,28
K06-23	64	38,354	17	31,313	1946	20230506	20231024	2,27	0,442	2,712	0,42
K07-23	64	29,115	17	42,036	1531	20230506	20231025	1,357	-1,015	0,342	0,27
S01-23	64	7,0163	17	49,974	698,6	20230506		0,143			
S02-23	64	12,165	17	48,986	999,4	20230506	20231025	1,236	-4,233	-2,997	0,08
S04-23	64	16,181	17	48,192	1156	20230506	20231025	1,487	-3,125	-1,638	0,14
S05-23	64	20,515	17	33,993	1451	20230506	20231025	2,176	-1,132	1,044	0,27
Haab-23	64	20,966	17	24,11	1731	20230506	20231025	2,342	-0,242	2,1	0,27

T01-23	64	19,155	18	6,5245	761	20230507		0			
T02-23	64	19,479	18	4,5473	880,8	20230507	20231025	0,176	-4,937	-4,761	0
T03-23	64	20,199	17	58,611	1062	20230507	20231025	0,633	-4,08	-3,447	0,02
T04-23	64	21,336	17	51,529	1219	20230507	20231025	1,38	-2,604	-1,224	0,12
T05-23	64	22,263	17	43,003	1344	20230507	20231025	1,638	-1,652	-0,014	0,18
T06-23	64	24,271	17	36,527	1468	20230506	20231025	1,889	-0,839	1,05	0,2
T07-23	64	25,293	17	31,215	1564	20230506	20231025	1,997	-0,743	1,254	0,21
T08-23	64	26,298	17	27,756	1637	20230506	20231025	1,94	-0,596	1,344	0,26
Bor-23	64	24,938	17	20,154	1412	20230602	20231027	2,37	-1,938	0,432	0,27
Borth-23	64	24,991	17	19,202	1410	20230507	20231027	2,19	-1,626	0,564	0,27
G02-23	64	26,847	17	17,718	1568	20230507	20231024	1,885	-0,787	1,098	0,15
G03-23	64	28,442	17	16,335	1662	20230507	20231024	2,008	-0,628	1,38	0,26
G04-23	64	30,025	17	15,027	1691	20230506	20231024	1,909	-0,523	1,386	0,35
Go1-23	64	33,967	17	24,927	1762	20230506	20231024	1,715	-0,485	1,23	0,37
Skf00-23	64	15,481	15	54,096	945	20230502	20231023	1,66	-3,883	-2,223	0,09
Hof01-23	64	32,349	15	35,83	1143	20230503	20231024	2,04	-2,257	-0,217	0,18
Skf01-23	64	18,017	16	5,0229	1283	20230503	20231023	2,88	-1,532	1,348	1,13
Fl01-23	64	26,164	15	55,632	1349	20230503	20231023	3,16	-1,252	1,908	0,27
Ske02-23	64	15,912	17	0,0657	1179	20230508		1,603	fannst ekki		
Ske03-23	64	18,053	16	56,162	1298	20230508	20231026	1,94	-1,586	0,354	0,35
Ske04-23	64	20,146	16	51,806	1400	20230508	20231026	1,773	-1,299	0,474	0,25
Ske05-23	64	22,234	16	47,234	1473	20230508	20231026	1,975	-0,949	1,026	0,34
E07-23	64	38,412	15	24,703	1070	20230503	20231024	1,966	-4,099	-2,133	0,26
E08-23	64	39,72	15	23,848	948,4	20230503	20231024	1,254	-4,476	-3,222	0,07
Kverk-23	64	38,659	16	40,535	1826	20230601	20231024	2,111	-0,329	1,782	0,49
Barc-23	64	38,407	17	26,762	1905	20230531	20231024	2,342	-0,188	2,154	0,47
BB08-23	64	39,023	17	23,218	1870	20230531	20231024	1,84			0,37
BB05-23	64	36,5909	17	30,7886	1913	20230531	20231024	1,975			0,315

Appendix B: Surface mass balance distribution by elevation in 2022_23.

ΔS : area in elevation range, $\sum\Delta S$: cumulative area above given elevation, b_w: specific winter balance, b_s: specific summer balance. b_n: specific winter balance, ΔB_w: winter balance at a given elevation range, $\sum\Delta B_w$: cumulative winter balance above given elevation, ΔB_s summer balance at a given elevation range, $\sum\Delta B_s$: cumulative summer balance above given elevation, ΔB_n: net annual balance in a given elevation range, $\sum B_n$: cumulative net annual balance above given elevation.

Vatnajökull

Elevation (m a.s.l.)			ΔS (km^2)	$\sum\Delta S$ (km^2)	b_w (mm)	b_s (mm)	b_n (mm)	ΔB_w (10^6m^3)	$\sum\Delta B_w$ (10^6m^3)	ΔB_s (10^6m^3)	$\sum\Delta B_s$ (10^6m^3)	ΔB_n (10^6m^3)	$\sum B_n$ (10^6m^3)
2000	2050	2025	0,3	0,3	5251	-265	4986	1,8	1,8	-0,1	-0,1	1,7	1,7
1950	2000	1975	6,9	7,3	2766	-20	2745	19,1	21,0	-0,1	-0,2	19,0	20,7
1900	1950	1925	41,3	48,6	2281	-25	2255	94,3	115,3	-1,0	-1,3	93,2	114,0
1850	1900	1875	44,3	92,9	2457	-213	2243	109,0	224,2	-9,5	-10,8	99,5	213,5
1800	1850	1825	45,6	138,6	2739	-230	2508	125,0	349,3	-10,5	-21,3	114,5	328,0
1750	1800	1775	54,8	193,4	2334	-325	2008	128,0	477,3	-17,9	-39,2	110,1	438,1
1700	1750	1725	114,4	307,8	2011	-428	1582	230,1	707,4	-49,0	-88,2	181,1	619,2
1650	1700	1675	217,3	525,1	2000	-530	1469	434,7	1142,1	-115,3	-203,5	319,4	938,5
1600	1650	1625	373,6	898,7	2009	-617	1392	750,7	1892,8	-230,6	-434,1	520,1	1458,6
1550	1600	1575	357,9	1256,6	2003	-721	1281	717,0	2609,8	-258,3	-692,4	458,8	1917,4
1500	1550	1525	421,2	1677,8	1979	-842	1137	834,0	3443,8	-354,9	-1047,3	479,1	2396,5
1450	1500	1475	452,5	2130,4	2018	-983	1034	913,3	4357,1	-445,2	-1492,5	468,1	2864,6
1400	1450	1425	502,9	2633,3	2086	-1100	986	1049,3	5406,4	-553,3	-2045,8	496,0	3360,6
1350	1400	1375	540,3	3173,6	2044	-1256	787	1104,6	6511,0	-678,9	-2724,7	425,7	3786,3
1300	1350	1325	531,3	3704,8	1959	-1503	456	1041,0	7552,1	-798,7	-3523,5	242,3	4028,6
1250	1300	1275	496,7	4201,6	1875	-1806	69	931,6	8483,7	-897,2	-4420,6	34,4	4063,0
1200	1250	1225	435,5	4637,1	1693	-2214	-521	737,7	9221,4	-964,7	-5385,3	-227,0	3836,0
1150	1200	1175	387,9	5025	1497	-2683	-1186	580,7	9802,1	-1041,2	-6426,5	-460,4	3375,6
1100	1150	1125	344,1	5369,1	1323	-3091	-1767	455,5	10257,6	-1063,5	-7490,0	-608,0	2767,6
1050	1100	1075	296,5	5665,6	1165	-3459	-2293	345,7	10603,3	-1025,9	-8515,9	-680,2	2087,4
1000	1050	1025	276,5	5942,1	996	-3809	-2813	275,5	10878,7	-1053,3	-9569,2	-777,8	1309,6
950	1000	975	247,4	6189,5	855	-4121	-3265	211,6	11090,4	-1019,6	-10588,8	-808,0	501,5
900	950	925	214	6403,6	714	-4397	-3682	153,0	11243,3	-941,1	-11529,9	-788,1	-286,6
850	900	875	184,3	6587,9	566	-4708	-4141	104,5	11347,8	-867,8	-12397,7	-763,3	-1049,9
800	850	825	166,7	6754,6	440	-5018	-4577	73,4	11421,2	-836,4	-13234,1	-763,0	-1812,9
750	800	775	145,4	6899,9	356	-5299	-4942	51,8	11473,1	-770,3	-14004,4	-718,5	-2531,4
700	750	725	114,8	7014,8	280	-5562	-5281	32,2	11505,2	-638,8	-14643,2	-606,6	-3138,0
650	700	675	95,1	7109,9	188	-5746	-5558	17,9	11523,2	-546,6	-15189,8	-528,7	-3666,6
600	650	625	64,3	7174,2	115	-5818	-5702	7,5	11530,6	-374,3	-15564,1	-366,9	-4033,5
550	600	575	52,7	7226,9	2	-6004	-6002	0,1	11530,7	-316,6	-15880,7	-316,5	-4350,0
500	550	525	53,6	7280,5	-142	-6307	-6449	-7,6	11523,1	-338,0	-16218,7	-345,6	-4695,6
450	500	475	37,9	7318,4	-289	-6623	-6912	-11,0	11512,1	-250,9	-16469,6	-261,9	-4957,5
400	450	425	34,7	7353,2	-453	-6895	-7348	-15,7	11496,4	-239,5	-16709,2	-255,3	-5212,8
350	400	375	38,9	7392	-652	-7218	-7871	-25,4	11471,0	-280,6	-16989,7	-305,9	-5518,7
300	350	325	35,2	7427,2	-870	-7640	-8511	-30,6	11440,4	-268,7	-17258,4	-299,3	-5818,0
250	300	275	31,9	7459,1	-1147	-8030	-9177	-36,6	11403,8	-256,2	-17514,7	-292,8	-6110,9
200	250	225	30,7	7489,8	-1526	-8406	-9933	-46,8	11357,0	-257,8	-17772,5	-304,7	-6415,5
150	200	175	29,6	7519,4	-1900	-8769	-10670	-56,3	11300,7	-259,9	-18032,4	-316,2	-6731,7
100	150	125	28,2	7547,6	-2288	-9124	-11413	-64,5	11236,1	-257,3	-18289,6	-321,8	-7053,5
50	100	75	22,2	7569,8	-2626	-9484	-12111	-58,3	11177,8	-210,5	-18500,1	-268,8	-7322,3
0	50	25	24,1	7593,9	-3074	-10150	-13224	-74,0	11103,8	-244,4	-18744,5	-318,4	-7640,7

Tungnaárjökull

Elevation (m a.s.l.)			ΔS (km^2)	$\sum\Delta S$ (km^2)	b_w (mm)	b_s (mm)	b_n (mm)	ΔB_w (10^6m^3)	$\sum\Delta B_w$ (10^6m^3)	ΔB_s (10^6m^3)	$\sum\Delta B_s$ (10^6m^3)	ΔB_n (10^6m^3)	$\sum B_n$ (10^6m^3)
1650	1700	1675	1,7	1,7	1923	-579	1343	3,3	3,3	-1,0	-1,0	2,3	2,3
1600	1650	1625	12,3	14	1901	-603	1297	23,4	26,7	-7,4	-8,4	16,0	18,3
1550	1600	1575	16,3	30,4	1856	-679	1176	30,3	57,0	-11,1	-19,5	19,2	37,5
1500	1550	1525	16,1	46,4	1826	-775	1050	29,3	86,3	-12,5	-32,0	16,9	54,4
1450	1500	1475	18,3	64,7	1775	-867	908	32,5	118,9	-15,9	-47,9	16,6	71,0
1400	1450	1425	23	87,8	1754	-1116	638	40,4	159,3	-25,7	-73,6	14,7	85,7
1350	1400	1375	21	108,8	1675	-1483	192	35,2	194,5	-31,2	-104,7	4,0	89,7
1300	1350	1325	27,1	135,9	1585	-1861	-275	43,0	237,4	-50,4	-155,2	-7,5	82,3
1250	1300	1275	20,3	156,2	1502	-2214	-711	30,5	268,0	-45,0	-200,2	-14,5	67,8
1200	1250	1225	22,2	178,4	1368	-2576	-1207	30,4	298,4	-57,2	-257,4	-26,8	41,0
1150	1200	1175	21	199,4	1175	-2935	-1759	24,7	323,0	-61,6	-319,0	-36,9	4,1
1100	1150	1125	17,6	217	935	-3266	-2331	16,5	339,6	-57,6	-376,6	-41,1	-37,1
1050	1100	1075	16,4	233,4	730	-3614	-2884	12,0	351,6	-59,4	-436,0	-47,4	-84,5
1000	1050	1025	16,7	250,2	579	-4001	-3421	9,7	361,3	-66,9	-503,0	-57,2	-141,7
950	1000	975	15,6	265,8	445	-4362	-3917	7,0	368,2	-68,2	-571,1	-61,2	-202,9
900	950	925	16	281,8	315	-4694	-4378	5,1	373,3	-75,3	-646,4	-70,2	-273,1
850	900	875	12,4	294,3	205	-5020	-4814	2,5	375,8	-62,4	-708,7	-59,8	-332,9
800	850	825	12,1	306,3	105	-5327	-5222	1,3	377,1	-64,2	-773,0	-63,0	-395,9
750	800	775	9,7	316	-8	-5632	-5640	-0,1	377,0	-54,4	-827,4	-54,5	-450,4
700	750	725	6,1	322	-123	-5904	-6027	-0,7	376,3	-35,8	-863,1	-36,5	-486,9
650	700	675	1,2	323,2	-199	-6191	-6391	-0,2	376,0	-7,2	-870,3	-7,4	-494,3

Sylgjujökull

Elevation (m a.s.l.)			ΔS (km^2)	$\sum\Delta S$ (km^2)	b_w (mm)	b_s (mm)	b_n (mm)	ΔB_w (10^6m^3)	$\sum\Delta B_w$ (10^6m^3)	ΔB_s (10^6m^3)	$\sum\Delta B_s$ (10^6m^3)	ΔB_n (10^6m^3)	$\sum B_n$ (10^6m^3)
1600	1650	1625	1,4	1,4	1700	-626	1074	2,3	2,3	-0,9	-0,9	1,5	1,5
1550	1600	1575	5,1	6,5	1661	-702	959	8,5	10,8	-3,6	-4,4	4,9	6,4
1500	1550	1525	18,8	25,3	1530	-880	649	28,8	39,6	-16,6	-21,0	12,2	18,6
1450	1500	1475	13,4	38,7	1497	-1047	450	20,1	59,8	-14,1	-35,1	6,0	24,7
1400	1450	1425	8,3	47,1	1499	-1281	217	12,5	72,2	-10,7	-45,8	1,8	26,5
1350	1400	1375	5,6	52,6	1492	-1491	1	8,3	80,6	-8,3	-54,1	0,0	26,5
1300	1350	1325	5,1	57,7	1442	-1932	-489	7,3	87,9	-9,8	-63,9	-2,5	24,0
1250	1300	1275	9,6	67,3	1322	-2355	-1033	12,7	100,6	-22,7	-86,6	-9,9	14,0
1200	1250	1225	11,4	78,7	1165	-2685	-1519	13,3	113,9	-30,6	-117,2	-17,3	-3,3
1150	1200	1175	12,8	91,5	1000	-2966	-1965	12,8	126,7	-38,0	-155,2	-25,2	-28,4
1100	1150	1125	12,1	103,6	824	-3279	-2455	10,0	136,7	-39,7	-194,8	-29,7	-58,1
1050	1100	1075	11,2	114,8	658	-3587	-2928	7,3	144,0	-40,0	-234,8	-32,7	-90,8
1000	1050	1025	9,9	124,7	464	-3888	-3423	4,6	148,7	-38,6	-273,5	-34,0	-124,8
950	1000	975	3,1	127,8	410	-4184	-3774	1,3	149,9	-13,0	-286,4	-11,7	-136,5
900	950	925	1,2	129,1	357	-4371	-4014	0,4	150,4	-5,4	-291,8	-4,9	-141,4

Köldukvíslarjökul

Elevation (m a.s.l.)			ΔS (km²)	∑ΔS (km²)	b_w (mm)	b_s (mm)	b_n (mm)	$ΔB_w$ (10^6m^3)	$∑ΔB_w$ (10^6m^3)	$ΔB_s$ (10^6m^3)	$∑ΔB_s$ (10^6m^3)	$ΔB_n$ (10^6m^3)	$∑B_n$ (10^6m^3)
1950	2000	1975	0,6	0,6	2094	221	2315	1,4	1,4	0,1	0,1	1,5	1,5
1900	1950	1925	13,7	14,4	1975	23	1999	27,1	28,5	0,3	0,5	27,4	28,9
1850	1900	1875	6,6	20,9	1830	-193	1637	12,1	40,5	-1,3	-0,8	10,8	39,7
1800	1850	1825	6,2	27,1	1769	-287	1482	10,9	51,5	-1,8	-2,6	9,2	48,9
1750	1800	1775	10,1	37,3	1752	-349	1402	17,8	69,2	-3,5	-6,1	14,2	63,1
1700	1750	1725	17,3	54,6	1660	-442	1217	28,7	97,9	-7,6	-13,8	21,0	84,1
1650	1700	1675	16	70,5	1571	-562	1008	25,1	123,0	-9,0	-22,7	16,1	100,2
1600	1650	1625	14,3	84,8	1514	-688	826	21,7	144,7	-9,9	-32,6	11,8	112,1
1550	1600	1575	18,4	103,3	1463	-868	594	27,0	171,7	-16,0	-48,6	11,0	123,0
1500	1550	1525	19,9	123,2	1420	-1070	350	28,3	200,0	-21,3	-69,9	7,0	130,0
1450	1500	1475	19,2	142,4	1388	-1298	90	26,7	226,7	-25,0	-94,9	1,7	131,8
1400	1450	1425	14,8	157,2	1329	-1577	-248	19,7	246,4	-23,4	-118,3	-3,7	128,1
1350	1400	1375	14,7	172	1247	-1982	-735	18,4	264,7	-29,2	-147,5	-10,8	117,2
1300	1350	1325	16,3	188,3	1174	-2489	-1315	19,1	283,9	-40,5	-188,1	-21,4	95,8
1250	1300	1275	17,3	205,6	1090	-2965	-1875	18,9	302,8	-51,4	-239,4	-32,5	63,3
1200	1250	1225	16,5	222,1	963	-3320	-2356	15,9	318,7	-54,9	-294,3	-39,0	24,4
1150	1200	1175	15,9	238	776	-3633	-2857	12,4	331,1	-57,8	-352,1	-45,5	-21,1
1100	1150	1125	14,1	252,1	579	-4079	-3499	8,2	339,2	-57,5	-409,6	-49,3	-70,4
1050	1100	1075	12,7	264,8	408	-4545	-4137	5,2	344,4	-57,5	-467,1	-52,4	-122,7
1000	1050	1025	10,2	275	277	-4836	-4559	2,8	347,2	-49,4	-516,5	-46,6	-169,3
950	1000	975	7,2	282,2	192	-4961	-4769	1,4	348,6	-35,9	-552,5	-34,6	-203,9
900	950	925	1,2	283,5	139	-5024	-4884	0,2	348,8	-6,1	-558,6	-5,9	-209,8

Dyngjujökull

Elevation (m a.s.l.)			ΔS (km^2)	$\sum \Delta S$ (km^2)	b_w (mm)	b_s (mm)	b_n (mm)	ΔB_w ($10^6 m^3$)	$\sum \Delta B_w$ ($10^6 m^3$)	ΔB_s ($10^6 m^3$)	$\sum \Delta B_s$ ($10^6 m^3$)	ΔB_n ($10^6 m^3$)	$\sum B_n$ ($10^6 m^3$)
1950	2000	1975	2,4	2,4	2081	79	2161	4,9	4,9	0,2	0,2	5,1	5,1
1900	1950	1925	17,7	20,1	2205	11	2216	39,0	44,0	0,2	0,4	39,2	44,3
1850	1900	1875	21,7	41,8	2066	-192	1873	44,9	88,9	-4,2	-3,8	40,7	85,1
1800	1850	1825	13,2	55	1964	-278	1685	25,9	114,8	-3,7	-7,5	22,3	107,3
1750	1800	1775	15,6	70,7	1916	-353	1562	30,0	144,8	-5,5	-13,0	24,4	131,8
1700	1750	1725	32,7	103,3	1918	-413	1504	62,7	207,5	-13,5	-26,5	49,1	180,9
1650	1700	1675	74,5	177,8	1951	-507	1444	145,4	352,9	-37,8	-64,3	107,6	288,5
1600	1650	1625	120,5	298,3	1987	-606	1380	239,5	592,4	-73,1	-137,5	166,4	454,9
1550	1600	1575	96,3	394,6	2013	-737	1275	193,9	786,3	-71,1	-208,5	122,8	577,7
1500	1550	1525	86,8	481,4	2023	-889	1134	175,7	962,0	-77,2	-285,8	98,5	676,2
1450	1500	1475	72,6	554	2001	-1053	947	145,3	1107,2	-76,5	-362,2	68,8	745,0
1400	1450	1425	60,3	614,3	1945	-1121	823	117,2	1224,4	-67,6	-429,8	49,6	794,6
1350	1400	1375	47,7	661,9	1834	-1225	609	87,5	1311,9	-58,4	-488,2	29,0	823,7
1300	1350	1325	36,1	698	1673	-1536	137	60,4	1372,3	-55,5	-543,7	4,9	828,6
1250	1300	1275	39,2	737,2	1477	-1982	-505	57,9	1430,2	-77,7	-621,4	-19,8	808,8
1200	1250	1225	43,5	780,7	1215	-2535	-1319	52,9	1483,0	-110,3	-731,6	-57,4	751,4
1150	1200	1175	43,3	824	914	-3209	-2295	39,6	1522,6	-139,0	-870,6	-99,4	652,0
1100	1150	1125	42,3	866,3	667	-3809	-3141	28,3	1550,9	-161,3	-1031,9	-133,0	519,0
1050	1100	1075	30,2	896,6	390	-4370	-3979	11,8	1562,7	-132,2	-1164,1	-120,4	398,6
1000	1050	1025	30,6	927,2	113	-4591	-4477	3,5	1566,2	-140,5	-1304,6	-137,0	261,6
950	1000	975	28,4	955,6	-123	-4900	-5024	-3,5	1562,7	-139,4	-1444,0	-142,9	118,7
900	950	925	24,3	979,9	-287	-5247	-5534	-7,0	1555,7	-127,5	-1571,5	-134,5	-15,8
850	900	875	20,4	1000,4	-397	-5621	-6018	-8,1	1547,6	-114,8	-1686,4	-122,9	-138,8
800	850	825	16,5	1016,9	-476	-6237	-6714	-7,9	1539,7	-103,0	-1789,4	-110,9	-249,6
750	800	775	8,5	1025,4	-557	-6892	-7449	-4,7	1535,0	-58,6	-1848,0	-63,3	-313,0
700	750	725	0,3	1025,7	-612	-7356	-7968	-0,2	1534,8	-2,5	-1850,5	-2,7	-315,7

Brúarjökull

Elevation (m a.s.l.)			ΔS (km^2)	∑ΔS (km^2)	b_w (mm)	b_s (mm)	b_n (mm)	$ΔB_w$ ($10^6 m^3$)	$∑ΔB_w$ ($10^6 m^3$)	$ΔB_s$ ($10^6 m^3$)	$∑ΔB_s$ ($10^6 m^3$)	$ΔB_n$ ($10^6 m^3$)	$∑B_n$ ($10^6 m^3$)
1900	1950	1925	0	0	1971	-514	1457	0,1	0,1	0,0	0,0	0,1	0,1
1850	1900	1875	1,2	1,3	2068	-441	1627	2,5	2,6	-0,5	-0,6	2,0	2,1
1800	1850	1825	4,4	5,6	2080	-344	1735	9,1	11,7	-1,5	-2,1	7,6	9,6
1750	1800	1775	2,8	8,5	2048	-378	1669	5,8	17,5	-1,1	-3,1	4,7	14,4
1700	1750	1725	4	12,5	2040	-427	1612	8,1	25,7	-1,7	-4,9	6,4	20,8
1650	1700	1675	5,6	18,1	2038	-490	1547	11,4	37,1	-2,8	-7,6	8,7	29,5
1600	1650	1625	51,6	69,6	2037	-632	1405	105,0	142,1	-32,6	-40,2	72,5	102,0
1550	1600	1575	47,7	117,3	1992	-702	1289	95,0	237,1	-33,5	-73,7	61,5	163,4
1500	1550	1525	73,6	190,9	1927	-784	1143	141,8	378,9	-57,7	-131,4	84,1	247,6
1450	1500	1475	80,1	271	2012	-897	1115	161,3	540,2	-71,9	-203,3	89,4	336,9
1400	1450	1425	114	385	2166	-970	1196	247,0	787,2	-110,6	-313,9	136,4	473,3
1350	1400	1375	157,5	542,4	2056	-1117	939	323,9	1111,0	-175,9	-489,8	147,9	621,3
1300	1350	1325	147,2	689,7	1897	-1330	567	279,4	1390,5	-195,9	-685,7	83,5	704,7
1250	1300	1275	137,9	827,6	1801	-1671	130	248,5	1638,9	-230,5	-916,2	17,9	722,7
1200	1250	1225	115,8	943,4	1641	-2152	-510	190,1	1829,0	-249,2	-1165,5	-59,2	663,5
1150	1200	1175	99,5	1042,9	1468	-2739	-1270	146,1	1975,1	-272,5	-1438,0	-126,4	537,1
1100	1150	1125	80,2	1123,1	1289	-3230	-1940	103,4	2078,6	-259,0	-1697,0	-155,6	381,6
1050	1100	1075	64,9	1188	1106	-3628	-2521	71,8	2150,4	-235,6	-1932,5	-163,7	217,9
1000	1050	1025	57,2	1245,2	900	-3979	-3079	51,4	2201,8	-227,5	-2160,0	-176,0	41,8
950	1000	975	51,6	1296,8	698	-4301	-3602	36,1	2237,9	-222,1	-2382,1	-186,0	-144,2
900	950	925	44,6	1341,4	542	-4607	-4065	24,2	2262,1	-205,5	-2587,6	-181,3	-325,5
850	900	875	38,4	1379,8	415	-4922	-4506	15,9	2278,0	-188,8	-2776,5	-172,9	-498,4
800	850	825	34,2	1414	317	-5259	-4941	10,9	2288,9	-180,1	-2956,6	-169,2	-667,6
750	800	775	30,9	1444,9	229	-5655	-5426	7,1	2296,0	-175,0	-3131,5	-167,9	-835,5
700	750	725	26,1	1471	157	-6132	-5974	4,1	2300,1	-160,0	-3291,6	-155,9	-991,4
650	700	675	9,5	1480,6	92	-6494	-6401	0,9	2301,0	-62,0	-3353,6	-61,1	-1052,5
600	650	625	0,5	1481,1	38	-6836	-6797	0,0	2301,0	-3,3	-3356,9	-3,3	-1055,8

Eyjabakkajökull

Elevation (m a.s.l.)			ΔS (km^2)	∑ΔS (km^2)	b_w (mm)	b_s (mm)	b_n (mm)	$ΔB_w$ ($10^6 m^3$)	$∑ΔB_w$ ($10^6 m^3$)	$ΔB_s$ ($10^6 m^3$)	$∑ΔB_s$ ($10^6 m^3$)	$ΔB_n$ ($10^6 m^3$)	$∑B_n$ ($10^6 m^3$)
1550	1600	1575	0	0	2799	-751	2047	0,0	0,0	0,0	0,0	0,0	0,0
1500	1550	1525	0,1	0,1	2795	-808	1986	0,2	0,3	-0,1	-0,1	0,2	0,2
1450	1500	1475	1,1	1,2	2719	-1033	1685	3,0	3,3	-1,2	-1,2	1,9	2,1
1400	1450	1425	2	3,3	2690	-1094	1595	5,5	8,8	-2,2	-3,5	3,3	5,3
1350	1400	1375	2,6	5,9	2632	-1201	1430	6,9	15,7	-3,1	-6,6	3,7	9,1
1300	1350	1325	4,2	10,1	2549	-1384	1165	10,7	26,4	-5,8	-12,4	4,9	14,0
1250	1300	1275	13,4	23,5	2420	-1833	586	32,4	58,8	-24,5	-37,0	7,8	21,8
1200	1250	1225	12,4	35,9	2318	-2384	-65	28,9	87,7	-29,7	-66,6	-0,8	21,0
1150	1200	1175	13,9	49,8	2108	-2978	-870	29,3	116,9	-41,3	-108,0	-12,1	8,9
1100	1150	1125	11,4	61,2	1872	-3414	-1541	21,4	138,3	-39,1	-147,1	-17,6	-8,7
1050	1100	1075	9,8	71,1	1627	-3733	-2105	16,0	154,3	-36,7	-183,7	-20,7	-29,4
1000	1050	1025	9,1	80,2	1384	-4038	-2654	12,7	167,0	-36,9	-220,7	-24,3	-53,7
950	1000	975	7,6	87,8	1139	-4387	-3248	8,7	175,7	-33,3	-254,0	-24,7	-78,3
900	950	925	5	92,8	930	-4710	-3780	4,7	180,3	-23,7	-277,7	-19,1	-97,4
850	900	875	3,9	96,7	811	-4916	-4105	3,2	183,5	-19,2	-297,0	-16,1	-113,5
800	850	825	2,9	99,6	731	-5142	-4410	2,1	185,6	-14,7	-311,7	-12,6	-126,1
750	800	775	1,8	101,4	626	-5483	-4856	1,1	186,7	-9,6	-321,3	-8,5	-134,6
700	750	725	1,6	103	514	-5752	-5237	0,8	187,6	-9,4	-330,7	-8,6	-143,2
650	700	675	0,6	103,6	370	-6105	-5734	0,2	187,8	-3,9	-334,6	-3,7	-146,8

Hoffellsjökull

Elevation (m a.s.l.)			ΔS (km^2)	∑ΔS (km^2)	b_w (mm)	b_s (mm)	b_n (mm)	$ΔB_w$ (10^6m^3)	$∑ΔB_w$ (10^6m^3)	$ΔB_s$ (10^6m^3)	$∑ΔB_s$ (10^6m^3)	$ΔB_n$ (10^6m^3)	$∑B_n$ (10^6m^3)
1450	1500	1475	1,2	1,2	2755	-1041	1714	3,2	3,2	-1,2	-1,2	2,0	2,0
1400	1450	1425	7,3	8,4	2853	-954	1899	20,8	24,0	-6,9	-8,2	13,8	15,8
1350	1400	1375	9,8	18,3	2781	-1073	1707	27,4	51,4	-10,6	-18,7	16,8	32,6
1300	1350	1325	16,1	34,4	2696	-1287	1409	43,4	94,8	-20,7	-39,4	22,7	55,3
1250	1300	1275	34,4	68,7	2418	-1632	786	83,1	177,9	-56,1	-95,5	27,0	82,3
1200	1250	1225	25,5	94,3	2257	-1800	457	57,6	235,5	-46,0	-141,5	11,7	94,0
1150	1200	1175	17,6	111,9	2041	-2083	-42	35,9	271,4	-36,6	-178,1	-0,8	93,3
1100	1150	1125	16,6	128,4	1752	-2379	-627	29,0	300,4	-39,4	-217,5	-10,4	82,9
1050	1100	1075	12,4	140,8	1454	-2792	-1338	18,1	318,5	-34,7	-252,2	-16,6	66,2
1000	1050	1025	9,4	150,3	1270	-3204	-1933	12,0	330,5	-30,2	-282,4	-18,2	48,0
950	1000	975	8,6	158,9	1131	-3545	-2414	9,8	340,2	-30,6	-313,1	-20,8	27,2
900	950	925	6,7	165,6	976	-3821	-2844	6,5	346,7	-25,4	-338,5	-18,9	8,2
850	900	875	4,2	169,7	806	-4089	-3282	3,4	350,1	-17,1	-355,6	-13,7	-5,5
800	850	825	3,4	173,2	686	-4313	-3627	2,4	352,5	-14,8	-370,4	-12,5	-17,9
750	800	775	2,9	176,1	616	-4458	-3841	1,8	354,3	-13,0	-383,4	-11,2	-29,1
700	750	725	2,9	179	416	-4883	-4467	1,2	355,5	-14,3	-397,7	-13,1	-42,2
650	700	675	3,2	182,2	223	-5349	-5126	0,7	356,2	-16,9	-414,6	-16,2	-58,5
600	650	625	2,5	184,7	92	-5651	-5558	0,2	356,4	-14,1	-428,8	-13,9	-72,4
550	600	575	1,8	186,5	-14	-5836	-5851	0,0	356,4	-10,5	-439,3	-10,5	-82,9
500	550	525	1,5	188	-134	-6014	-6149	-0,2	356,2	-9,1	-448,3	-9,3	-92,1
450	500	475	1,1	189	-335	-6327	-6663	-0,4	355,8	-6,7	-455,0	-7,1	-99,2
400	450	425	0,7	189,8	-539	-6691	-7230	-0,4	355,4	-4,8	-459,8	-5,2	-104,4
350	400	375	0,7	190,5	-787	-7120	-7908	-0,6	354,9	-5,1	-464,9	-5,7	-110,0
300	350	325	0,5	191	-1005	-7509	-8514	-0,5	354,4	-3,8	-468,7	-4,3	-114,3
250	300	275	0,6	191,6	-1226	-7860	-9086	-0,7	353,6	-4,8	-473,5	-5,5	-119,8
200	250	225	0,9	192,4	-1571	-8246	-9817	-1,3	352,3	-7,0	-480,5	-8,4	-128,2
150	200	175	1,8	194,2	-2020	-8671	-10692	-3,6	348,7	-15,5	-496,0	-19,1	-147,3
100	150	125	2,4	196,6	-2529	-9140	-11669	-6,0	342,7	-21,6	-517,7	-27,6	-175,0
50	100	75	2,2	198,8	-2972	-9559	-12531	-6,5	336,2	-20,9	-538,6	-27,4	-202,4
0	50	25	2,9	201,7	-3518	-10086	-13604	-10,2	326,0	-29,1	-567,7	-39,3	-241,7

Breiðamerkurjökull

Elevation (m a.s.l.)			ΔS (km²)	∑ΔS (km²)	b_w (mm)	b_s (mm)	b_n (mm)	ΔB_w ($10^6 m^3$)	$\sum\Delta B_w$ ($10^6 m^3$)	ΔB_s ($10^6 m^3$)	$\sum\Delta B_s$ ($10^6 m^3$)	ΔB_n ($10^6 m^3$)	$\sum B_n$ ($10^6 m^3$)
1900	1950	1925	0	0	5158	-242	4916	0,2	0,2	0,0	0,0	0,2	0,2
1850	1900	1875	0,4	0,4	5166	-129	5036	1,9	2,2	0,0	-0,1	1,9	2,1
1800	1850	1825	0,5	0,9	5066	-38	5027	2,4	4,6	0,0	-0,1	2,4	4,5
1750	1800	1775	0,9	1,8	4769	-60	4709	4,3	9,0	-0,1	-0,1	4,3	8,8
1700	1750	1725	2,6	4,4	3406	-360	3046	8,8	17,7	-0,9	-1,1	7,9	16,7
1650	1700	1675	6	10,4	2555	-550	2004	15,3	33,0	-3,3	-4,4	12,0	28,7
1600	1650	1625	18	28,3	2179	-615	1564	39,1	72,2	-11,0	-15,4	28,1	56,8
1550	1600	1575	26,4	54,7	2105	-698	1406	55,5	127,7	-18,4	-33,8	37,1	93,8
1500	1550	1525	31,8	86,5	2138	-826	1312	68,1	195,7	-26,3	-60,1	41,8	135,6
1450	1500	1475	46,6	133,1	2183	-934	1248	101,6	297,4	-43,5	-103,6	58,1	193,8
1400	1450	1425	57,5	190,6	2153	-1045	1107	123,8	421,2	-60,1	-163,7	63,7	257,5
1350	1400	1375	88,2	278,8	2111	-1225	886	186,4	607,6	-108,1	-271,9	78,2	335,7
1300	1350	1325	94,3	373,1	2058	-1438	620	194,1	801,6	-135,6	-407,4	58,5	394,2
1250	1300	1275	56,9	430	1968	-1571	396	111,9	913,6	-89,4	-496,8	22,6	416,8
1200	1250	1225	38,2	468,2	1855	-1741	113	71,0	984,6	-66,6	-563,4	4,4	421,1
1150	1200	1175	30,7	498,9	1716	-1978	-261	52,7	1037,3	-60,8	-624,2	-8,0	413,1
1100	1150	1125	25,1	524,1	1573	-2287	-713	39,5	1076,8	-57,5	-681,7	-17,9	395,2
1050	1100	1075	21,6	545,7	1448	-2574	-1126	31,4	1108,2	-55,7	-737,4	-24,4	370,8
1000	1050	1025	18,7	564,4	1350	-2842	-1491	25,3	1133,5	-53,2	-790,6	-27,9	342,9
950	1000	975	20,3	584,7	1256	-3225	-1969	25,5	1158,9	-65,4	-856,0	-39,9	302,9
900	950	925	21,9	606,6	1107	-3526	-2419	24,2	1183,2	-77,2	-933,2	-53,0	250,0
850	900	875	17,9	624,5	886	-3864	-2978	15,9	1199,1	-69,3	-1002,6	-53,4	196,5
800	850	825	20,8	645,4	703	-4202	-3499	14,7	1213,7	-87,6	-1090,1	-72,9	123,6
750	800	775	21,8	667,2	535	-4559	-4024	11,7	1225,4	-99,4	-1189,5	-87,7	35,9
700	750	725	16,7	683,8	385	-4893	-4508	6,4	1231,8	-81,5	-1271,0	-75,1	-39,2
650	700	675	22,4	706,3	264	-5215	-4950	5,9	1237,8	-117,0	-1388,0	-111,1	-150,2
600	650	625	25,4	731,6	141	-5510	-5368	3,6	1241,4	-139,8	-1527,8	-136,2	-286,5
550	600	575	22,5	754,2	-18	-5823	-5841	-0,4	1240,9	-131,3	-1659,1	-131,7	-418,2
500	550	525	21,2	775,4	-192	-6092	-6285	-4,1	1236,8	-129,2	-1788,3	-133,3	-551,5
450	500	475	12,1	787,5	-369	-6418	-6788	-4,5	1232,4	-77,8	-1866,1	-82,3	-633,8
400	450	425	13,3	800,8	-526	-6701	-7228	-7,0	1225,4	-89,0	-1955,1	-96,0	-729,8
350	400	375	14,7	815,5	-708	-7033	-7741	-10,4	1215,0	-103,3	-2058,4	-113,7	-843,4
300	350	325	11,6	827,1	-925	-7413	-8339	-10,8	1204,2	-86,2	-2144,6	-96,9	-940,4
250	300	275	9,8	836,9	-1218	-7780	-8999	-12,0	1192,2	-76,5	-2221,1	-88,5	-1028,8
200	250	225	9,9	846,8	-1673	-8206	-9879	-16,6	1175,6	-81,4	-2302,5	-98,1	-1126,9
150	200	175	8,9	855,7	-2167	-8619	-10786	-19,2	1156,4	-76,4	-2378,9	-95,7	-1222,5
100	150	125	9,1	864,8	-2600	-8978	-11578	-23,6	1132,8	-81,6	-2460,5	-105,2	-1327,7
50	100	75	7	871,8	-2936	-9387	-12324	-20,6	1112,1	-66,0	-2526,5	-86,6	-1414,4
0	50	25	3	874,8	-3130	-10168	-13299	-9,3	1102,9	-30,1	-2556,6	-39,4	-1453,8

Síðujökull

Elevation (m a.s.l.)			ΔS (km^2)	∑ΔS (km^2)	b_w (mm)	b_s (mm)	b_n (mm)	$ΔB_w$ (10^6m^3)	$∑ΔB_w$ (10^6m^3)	$ΔB_s$ (10^6m^3)	$∑ΔB_s$ (10^6m^3)	$ΔB_n$ (10^6m^3)	$∑B_n$ (10^6m^3)
1700	1750	1725	0,9	0,9	2356	-310	2046	2,2	2,2	-0,3	-0,3	1,9	1,9
1650	1700	1675	5,9	6,9	2377	-398	1979	14,1	16,3	-2,4	-2,7	11,8	13,7
1600	1650	1625	11,3	18,1	2215	-514	1700	24,9	41,2	-5,8	-8,5	19,1	32,8
1550	1600	1575	11,7	29,8	2220	-566	1654	25,9	67,1	-6,6	-15,1	19,3	52,1
1500	1550	1525	21,4	51,2	2196	-704	1491	47,1	114,2	-15,1	-30,2	32,0	84,1
1450	1500	1475	38	89,2	2129	-969	1159	80,9	195,1	-36,9	-67,0	44,1	128,1
1400	1450	1425	24,8	114	2037	-1166	870	50,5	245,6	-28,9	-95,9	21,6	149,7
1350	1400	1375	21	135	1928	-1468	460	40,5	286,1	-30,8	-126,7	9,7	159,3
1300	1350	1325	17,1	152	1833	-1826	6	31,3	317,4	-31,2	-157,9	0,1	159,5
1250	1300	1275	15,1	167,2	1760	-2176	-416	26,6	344,0	-32,9	-190,8	-6,3	153,2
1200	1250	1225	21,1	188,3	1687	-2527	-840	35,6	379,6	-53,4	-244,2	-17,7	135,4
1150	1200	1175	17,5	205,8	1552	-2953	-1401	27,2	406,9	-51,8	-296,0	-24,6	110,8
1100	1150	1125	16,6	222,5	1458	-3257	-1798	24,3	431,1	-54,2	-350,2	-29,9	80,9
1050	1100	1075	15	237,5	1379	-3594	-2215	20,8	451,9	-54,1	-404,3	-33,3	47,6
1000	1050	1025	18,5	256	1288	-3991	-2703	23,8	475,7	-73,7	-478,0	-49,9	-2,3
950	1000	975	19,4	275,4	1159	-4364	-3205	22,5	498,1	-84,5	-562,5	-62,1	-64,4
900	950	925	19,6	294,9	963	-4684	-3720	18,8	517,0	-91,6	-654,1	-72,8	-137,2
850	900	875	18,8	313,7	725	-5018	-4293	13,6	530,6	-94,2	-748,4	-80,6	-217,8
800	850	825	17,7	331,4	531	-5366	-4835	9,4	540,0	-94,8	-843,2	-85,5	-303,2
750	800	775	20,1	351,5	361	-5688	-5327	7,3	547,2	-114,4	-957,6	-107,1	-410,4
700	750	725	20	371,5	221	-5977	-5755	4,4	551,7	-119,9	-1077,5	-115,4	-525,8
650	700	675	19,9	391,4	100	-6341	-6240	2,0	553,7	-126,3	-1203,7	-124,2	-650,0
600	650	625	8,9	400,3	13	-6689	-6676	0,1	553,8	-59,6	-1263,3	-59,4	-709,5
550	600	575	0	400,4	-39	-6915	-6954	0,0	553,8	-0,3	-1263,6	-0,3	-709,8

Skaftárjökull

Elevation (m a.s.l.)			ΔS (km^2)	∑ΔS (km^2)	b_w (mm)	b_s (mm)	b_n (mm)	$ΔB_w$ (10^6m^3)	$∑ΔB_w$ (10^6m^3)	$ΔB_s$ (10^6m^3)	$∑ΔB_s$ (10^6m^3)	$ΔB_n$ (10^6m^3)	$∑B_n$ (10^6m^3)
1400	1450	1425	0	0	1871	-1289	581	0	0	-0	-0	0	0
1350	1400	1375	2,5	2,5	1798	-1510	287	4,4	4,4	-3,7	-3,7	0,7	0,7
1300	1350	1325	5,2	7,7	1720	-1812	-91	9	13,4	-9,5	-13,2	-0,5	0,2
1250	1300	1275	4	11,7	1647	-2204	-556	6,5	20	-8,7	-21,9	-2,2	-2
1200	1250	1225	6,3	17,9	1561	-2631	-1069	9,8	29,8	-16,5	-38,5	-6,7	-8,7
1150	1200	1175	7,4	25,3	1468	-2978	-1510	10,8	40,6	-21,9	-60,4	-11,1	-19,8
1100	1150	1125	10,6	35,9	1344	-3293	-1948	14,3	54,9	-35	-95,4	-20,7	-40,5
1050	1100	1075	11,7	47,6	1215	-3649	-2434	14,2	69,1	-42,7	-138,1	-28,5	-69
1000	1050	1025	12,7	60,4	1051	-4037	-2985	13,4	82,5	-51,4	-189,5	-38	-107
950	1000	975	8,8	69,2	856	-4450	-3594	7,6	90	-39,3	-228,8	-31,7	-138,7
900	950	925	5,8	75	712	-4776	-4064	4,1	94,2	-27,7	-256,5	-23,5	-162,3
850	900	875	4,7	79,7	558	-5074	-4516	2,6	96,8	-23,9	-280,4	-21,3	-183,6
800	850	825	4,8	84,5	413	-5373	-4959	2	98,8	-25,7	-306,1	-23,7	-207,3
750	800	775	4,5	88,9	289	-5657	-5367	1,3	100,1	-25,3	-331,4	-24	-231,3
700	750	725	3,9	92,9	155	-5899	-5743	0,6	100,7	-23,1	-354,4	-22,5	-253,8
650	700	675	2,8	95,7	21	-6173	-6152	0,1	100,7	-17,3	-371,7	-17,2	-271
600	650	625	0,5	96,2	10	-6342	-6332	0	100,8	-3,3	-375	-3,3	-274,2

Vestari Skaftárketill

Elevation (m a.s.l.)			ΔS (km^2)	$\sum\Delta S$ (km^2)	b_w (mm)	b_s (mm)	b_n (mm)	ΔB_w (10^6m^3)	$\sum\Delta B_w$ (10^6m^3)	ΔB_s (10^6m^3)	$\sum\Delta B_s$ (10^6m^3)	ΔB_n (10^6m^3)	$\sum B_n$ (10^6m^3)
1900	1950	1925	0,5	0,5	2003	-165	1837	1,1	1,1	-0,1	-0,1	1,0	1,0
1850	1900	1875	0,7	1,2	1957	-204	1753	1,3	2,3	-0,1	-0,2	1,1	2,1
1800	1850	1825	0,8	2	1893	-255	1637	1,5	3,8	-0,2	-0,4	1,3	3,4
1750	1800	1775	2,5	4,4	1775	-376	1399	4,4	8,2	-0,9	-1,3	3,4	6,8
1700	1750	1725	5,4	9,9	1699	-452	1247	9,2	17,4	-2,5	-3,8	6,8	13,6
1650	1700	1675	6,5	16,3	1652	-526	1126	10,7	28,1	-3,4	-7,2	7,3	20,9
1600	1650	1625	7,3	23,6	1632	-604	1027	11,9	40,0	-4,4	-11,6	7,5	28,4
1550	1600	1575	5	28,6	1587	-690	896	7,9	47,9	-3,4	-15,0	4,5	32,8
1500	1550	1525	2,7	31,2	1550	-746	804	4,1	52,0	-2,0	-17,0	2,1	35,0

Eystri Skaftárketill

Elevation (m a.s.l.)			ΔS (km^2)	$\sum\Delta S$ (km^2)	b_w (mm)	b_s (mm)	b_n (mm)	ΔB_w (10^6m^3)	$\sum\Delta B_w$ (10^6m^3)	ΔB_s (10^6m^3)	$\sum\Delta B_s$ (10^6m^3)	ΔB_n (10^6m^3)	$\sum B_n$ (10^6m^3)
1750	1800	1775	1,1	1,1	1742	-427	1315	1,9	1,9	-0,5	-0,5	1,5	1,5
1700	1750	1725	10	11,1	1734	-471	1262	17,3	19,2	-4,7	-5,2	12,6	14,1
1650	1700	1675	15,5	26,6	1798	-510	1287	27,8	47,1	-7,9	-13,1	19,9	34,0
1600	1650	1625	9,2	35,8	1783	-548	1235	16,4	63,5	-5,1	-18,1	11,4	45,4
1550	1600	1575	4,2	39,9	1773	-568	1205	7,4	70,9	-2,4	-20,5	5,0	50,4

Gjálp

Elevation (m a.s.l.)			ΔS (km^2)	$\sum\Delta S$ (km^2)	b_w (mm)	b_s (mm)	b_n (mm)	ΔB_w (10^6m^3)	$\sum\Delta B_w$ (10^6m^3)	ΔB_s (10^6m^3)	$\sum\Delta B_s$ (10^6m^3)	ΔB_n (10^6m^3)	$\sum B_n$ (10^6m^3)
1900	1950	1925	0,4	0,4	2031	-158	1873	0,7	0,700	-0,100	-0,100	0,700	0,700
1850	1900	1875	0,8	1,1	1961	-210	1750	1,5	2,200	-0,200	-0,200	1,300	2,000
1800	1850	1825	1,2	2,3	1871	-279	1592	2,2	4,400	-0,300	-0,500	1,900	3,900
1750	1800	1775	5,5	7,8	1753	-431	1322	9,7	14,100	-2,400	-2,900	7,300	11,200
1700	1750	1725	23,7	31,5	1806	-474	1331	42,9	57,000	-11,300	-14,200	31,600	42,800
1650	1700	1675	7,8	39,4	1884	-489	1394	14,8	71,800	-3,800	-18,000	10,900	53,700

Grímsvötn

Elevation (m a.s.l.)			ΔS (km^2)	$\sum\Delta S$ (km^2)	b_w (mm)	b_s (mm)	b_n (mm)	ΔB_w (10^6m^3)	$\sum\Delta B_w$ (10^6m^3)	ΔB_s (10^6m^3)	$\sum\Delta B_s$ (10^6m^3)	ΔB_n (10^6m^3)	$\sum B_n$ (10^6m^3)
1700	1750	1725	1,3	1,3	1927	-512	1415	2,6	2,6	-0,7	-0,7	1,9	1,9
1650	1700	1675	40,7	42,1	1973	-588	1384	80,4	83,0	-24,0	-24,7	56,4	58,3
1600	1650	1625	30,7	72,8	1985	-682	1303	60,9	143,9	-20,9	-45,6	40,0	98,3
1550	1600	1575	19,6	92,4	2021	-820	1201	39,6	183,5	-16,1	-61,7	23,5	121,8
1500	1550	1525	16,3	108,7	2064	-1001	1063	33,7	217,2	-16,3	-78,0	17,3	139,2
1450	1500	1475	9,5	118,2	2131	-1312	818	20,2	237,4	-12,5	-90,5	7,8	147,0
1400	1450	1425	13,7	131,9	2250	-1709	541	30,9	268,3	-23,5	-113,9	7,4	154,4
1350	1400	1375	1,2	133,1	2016	-1683	333	2,5	270,8	-2,1	-116,0	0,4	154,8

Appendix C: Coordinates of the velocity measurement stakes in 2023.

Position of the velocity measurement stakes determined by GPS sub-metre differential (I), fast static (FS) and kinematic (K). (Accuracy of horizontal position 0.5 – 1.0 m, and vertical accuracy 1-2 m for DGPS, about 1cm for fast static, and 3 cm for kinematic).
The station Hofn in Höfn í Hornafirði is used as a stationary reference for all measurements, ÍSN93 datum, h_l is elevation above ellipsoid, dL antenna height, N estimated difference between ellipsoid and sea-level, H elevation in metres above sea level (H= h_l+N+dL). X and Y are ÍSN93 Lambert conformal conic projected coordinates. M is a quality marker.

Site	time	Date		Calender Day #	Year	Latitude		Longitude		h_l (m a. e.)	dL (m)	N (m)	H (m a. s. l.)	X	Y	M
B07-23	11,72	4	5	124	2023	64	25,79652	16	17,48091	1425,86	0,00	-67,05	1358,81	630454,15	439244,78	K
B07-23	14,66	27	10	300	2023	64	25,79558	16	17,47997	1422,01	0,00	-67,05	1354,96	630454,97	439243,07	K
B09-23	12,52	5	5	125	2023	64	44,48331	16	6,18820	792,97	0,00	-66,68	726,28	637922,21	474330,23	K
B09-23	18,34	24	10	297	2023	64	44,48316	16	6,18824	785,91	0,00	-66,68	719,23	637922,20	474329,95	K
B10-23	12,87	5	5	125	2023	64	43,68247	16	6,70405	823,90	0,00	-66,71	757,19	637581,12	472825,09	K
B10-23	19,00	24	10	297	2023	64	43,68247	16	6,70405	817,50	0,00	-66,71	750,79	637581,12	472825,09	K
B11-23	10,61	5	5	125	2023	64	40,93875	16	10,48385	1011,44	0,00	-66,81	944,63	634810,08	467596,73	K
B11-23	19,25	24	10	297	2023	64	40,94359	16	10,47997	1006,27	0,00	-66,81	939,46	634812,77	467605,85	K
B12-23	10,13	5	5	125	2023	64	38,26171	16	14,14876	1144,89	0,00	-66,90	1077,99	632114,81	462498,71	K
B12-23	19,63	24	10	297	2023	64	38,26979	16	14,14172	1140,78	0,00	-66,90	1073,88	632119,76	462513,95	K
B13-23	19,71	4	5	124	2023	64	34,57784	16	19,63675	1289,43	0,00	-67,01	1222,42	628035,10	455472,21	K
B13-23	17,43	26	10	299	2023	64	34,58619	16	19,62759	1285,61	0,00	-67,01	1218,60	628041,75	455488,03	K
B13ror15	17,75	4	5	124	2023	64	34,65271	16	19,57542	1286,54	0,00	-67,01	1219,53	628078,16	455613,27	K
B13ror15	16,74	26	10	299	2023	64	34,66130	16	19,56503	1285,09	0,00	-67,01	1218,08	628085,77	455629,55	K
B14-23	16,36	4	5	124	2023	64	31,65039	16	24,77175	1391,49	0,00	-67,11	1324,38	624160,14	449867,02	K
B14-23	18,65	23	10	296	2023	64	31,65696	16	24,75936	1389,30	0,00	-67,11	1322,20	624169,55	449879,61	K
B15-23	15,49	4	5	124	2023	64	28,51272	16	30,03180	1472,91	0,00	-67,21	1405,70	620185,53	443872,53	K
B15-23	20,66	24	10	297	2023	64	28,51716	16	30,02018	1469,11	0,00	-67,21	1401,90	620194,51	443881,14	K
B16-23	15,49	8	5	128	2023	64	24,12250	16	40,92038	1596,01	0,00	-67,33	1528,68	611762,44	435388,49	K
B16-23	19,63	23	10	296	2023	64	24,12277	16	40,91989	1594,65	-1,08	-67,33	1526,24	611762,81	435389,00	K
B17-23	17,15	4	5	124	2023	64	36,73298	16	28,79729	1284,46	0,00	-67,12	1217,34	620565,67	459172,88	K
B17-23	18,85	23	10	296	2023	64	36,74267	16	28,79082	1280,36	0,00	-67,12	1213,24	620570,11	459191,07	K
B18-23	21,19	3	5	123	2023	64	31,57695	16	0,12051	1383,79	0,00	-66,92	1316,87	643870,26	450601,67	K
B18-23	16,02	23	10	296	2023	64	31,58259	16	0,12373	1379,62	0,00	-66,92	1312,70	643867,20	450612,02	K
B19-23	13,20	3	5	123	2023	64	27,97835	15	56,00763	1507,47	0,00	-66,89	1440,58	647481,46	444081,14	K
B19-23	15,54	23	10	296	2023	64	27,97867	15	56,00814	1502,79	0,00	-66,89	1435,90	647481,02	444081,72	K
Bb0-23	10,73	4	5	124	2023	64	22,70700	16	5,04118	1585,41	0,00	-66,85	1518,56	640697,38	433954,77	K
Bb0-23	14,20	23	10	296	2023	64	22,70683	16	5,04228	1580,97	0,00	-66,85	1514,12	640696,51	433954,41	K
Barc-23	14,11	31	5	151	2023	64	38,40650	17	26,76249	1974,21	-1,65	-67,87	1904,69	574281,29	460791,90	K
Barc-23	15,64	24	10	297	2023	64	38,40626	17	26,75635	1971,88	-1,35	-67,87	1902,66	574286,20	460791,56	K
Bb02-23	14,39	31	5	151	2023	64	38,42457	17	26,76060	1974,14	-1,65	-67,87	1904,62	574281,97	460825,50	K
Bb02-23	15,90	12	9	255	2023	64	38,42440	17	26,75629	1971,34	-1,00	-67,87	1902,47	574285,41	460825,26	K
Bb02-23	15,23	24	10	297	2023	64	38,42435	17	26,75470	1973,03	-2,70	-67,87	1902,46	574286,68	460825,20	K
Bb08-23	14,71	31	5	151	2023	64	39,02326	17	23,21833	1939,34	-1,65	-67,84	1869,84	577075,05	462008,18	K
Bb08-23	16,63	12	9	255	2023	64	39,02357	17	23,21351	1936,61	-1,00	-67,87	1867,74	577078,87	462008,86	K
Bb08-23	16,37	24	10	297	2023	64	39,02348	17	23,21185	1937,34	-2,40	-67,87	1867,07	577080,20	462008,73	K
Bb09-23	15,07	31	5	151	2023	64	39,66595	17	28,01689	1983,95	-1,65	-67,87	1914,43	573225,38	463106,86	K
Bb09-23	17,54	24	10	297	2023	64	39,66574	17	28,01388	1981,79	-2,20	-67,87	1911,72	573227,79	463106,54	K
Bb05-23	15,41	31	5	151	2023	64	36,59093	17	30,78860	1982,95	-1,65	-67,87	1913,43	571153,67	457342,36	K
Bb05-23	18,88	24	10	297	2023	64	36,58916	17	30,78989	1980,74	-2,25	-67,87	1910,62	571152,72	457339,04	K
Bb07-23	15,78	31	5	151	2023	64	36,56588	17	25,04511	1951,47	-1,65	-67,86	1881,96	575734,83	457407,03	K
Bb10-23	16,11	31	5	151	2023	64	36,32061	17	15,64637	1685,34	-1,65	-67,72	1615,96	583241,88	457148,45	K
Bb10-23	19,89	24	10	297	2023	64	36,31825	17	15,63749	1683,01	-2,05	-67,72	1613,24	583249,08	457144,27	K
Bb10-23	15,35	12	9	255	2023	64	36,32077	17	15,63689	1681,85	-0,85	-67,72	1613,27	583249,43	457148,96	K
Bor-23	14,12	2	6	153	2023	64	24,93782	17	20,15447	1480,56	-1,26	-67,70	1411,60	580203,31	435909,79	K
Bor-23	12,83	27	10	300	2023	64	24,93314	17	20,15922	1496,23	0,00	-67,70	1428,53	580199,73	435901,00	K

Br1-23	12,35	22	6	173	2023	64	5,95858	16	19,81973	137,00	-1,06	-65,90	70,04	630134,01	402338,50	K
Br1-23	17,97	22	10	295	2023	64	5,96327	16	19,82096	131,57	-1,55	-65,90	64,12	630132,65	402347,16	K
Br2-22	19,30	21	6	172	2023	64	6,35483	16	22,52633	217,27	-1,06	-66,03	150,18	627905,83	402982,04	K
Br2-23	19,80	21	6	172	2023	64	6,35398	16	22,52332	217,14	-1,06	-66,03	150,04	627908,33	402980,56	K
Br2-23	14,54	22	10	295	2023	64	6,35358	16	22,52295	211,42	-1,55	-66,03	143,84	627908,67	402979,83	K
Br3-22	17,00	21	6	172	2023	64	8,41263	16	23,96994	415,63	-1,06	-66,26	348,31	626576,70	406753,83	K
Br3-23	17,50	21	6	172	2023	64	8,41308	16	23,97076	415,68	-1,06	-66,26	348,36	626576,00	406754,63	K
Br3-23	15,56	22	10	295	2023	64	8,41016	16	23,96632	412,03	-1,55	-66,26	344,22	626579,82	406749,36	K
Br7-23	14,30	4	5	124	2023	64	22,14259	16	16,93857	1312,10	0,00	-67,01	1245,10	631180,98	432480,73	K
Br7-23	16,17	23	10	296	2023	64	22,11530	16	16,93063	1308,74	-1,98	-67,01	1239,75	631189,55	432430,35	K
Bru-23	19,77	3	5	123	2023	64	39,75323	15	56,53495	958,13	0,00	-66,78	891,35	646001,32	465912,77	K
Bru-23	17,26	23	10	296	2023	64	39,76363	15	56,53151	953,21	0,00	-66,78	886,42	646003,12	465932,19	K
Bud-23	19,86	3	5	123	2023	64	35,98984	15	59,88663	1205,05	0,00	-66,88	1138,17	643667,99	458800,44	K
Bud-23	16,86	23	10	296	2023	64	36,00147	15	59,88466	1200,24	0,00	-66,88	1133,36	643668,53	458822,10	K
D01-23	17,53	5	5	125	2023	64	47,86795	16	49,97493	906,50	0,00	-67,05	839,45	602977,18	479223,49	K
D05-23	16,86	5	5	125	2023	64	42,22496	16	54,68882	1274,11	0,00	-67,35	1206,76	599591,58	468618,84	K
D05-23	17,30	26	10	299	2023	64	42,24186	16	54,66462	1272,04	-2,23	-67,35	1202,46	599609,76	468650,85	K
D07-23	17,89	5	5	125	2023	64	38,28941	16	59,25843	1446,36	0,00	-67,50	1378,86	596193,84	461192,51	K
D07-23	15,61	26	10	299	2023	64	38,30935	16	59,23880	1444,16	-2,44	-67,50	1374,22	596208,29	461230,03	K
D08-23	18,59	5	5	125	2023	64	34,68189	17	1,51937	1556,43	0,00	-67,56	1488,87	594602,50	454436,20	K
D08-23	14,86	26	10	299	2023	64	34,69128	17	1,51695	1554,81	-2,30	-67,56	1484,95	594603,88	454453,71	K
D09	14,86	26	10	299	2023	64	34,69128	17	1,51695	1554,81	-2,30	-67,56	1484,95	594603,88	454453,71	K
D12-23	19,30	5	5	125	2023	64	28,97478	17	0,18444	1719,13	0,00	-67,55	1651,58	596002,94	443871,20	K
D12-23	11,19	24	10	297	2023	64	28,97532	17	0,18424	1716,10	0,00	-67,55	1648,55	596003,06	443872,21	K
E01-22	18,53	3	5	123	2023	64	40,65000	15	34,84254	818,43	0,00	-66,72	751,72	663158,10	468460,83	K
E01-23	18,53	3	5	123	2023	64	40,65000	15	34,84254	818,43	0,00	-66,72	751,72	663158,10	468460,83	K
E01-23	17,03	24	10	297	2023	64	40,66066	15	34,83391	813,37	0,00	-66,72	746,66	663163,88	468480,98	K
E02-23	18,19	3	5	123	2023	64	39,10820	15	35,99632	1016,88	0,00	-66,79	950,10	662395,40	465550,82	K
E02-23	16,69	24	10	297	2023	64	39,12654	15	35,98950	1011,25	0,00	-66,79	944,46	662398,99	465585,14	K
E03-23	16,62	3	5	123	2023	64	36,60342	15	36,90205	1258,54	0,00	-66,85	1191,69	661924,17	460864,92	K
E03-23	14,83	24	10	297	2023	64	36,60921	15	36,90590	1252,32	0,00	-66,85	1185,47	661920,53	460875,50	K
E04-23	15,68	3	5	123	2023	64	34,93758	15	37,17934	1356,15	0,00	-66,83	1289,32	661868,72	457762,39	K
E04-23	13,96	24	10	297	2023	64	34,93827	15	37,17891	1351,03	0,00	-66,83	1284,20	661869,00	457763,70	K
E07-23	16,75	3	5	123	2023	64	38,41193	15	24,70313	1136,68	0,00	-66,62	1070,07	671449,23	464756,11	K
E07-23	15,71	24	10	297	2023	64	38,41668	15	24,69403	1130,47	0,00	-66,62	1063,85	671455,97	464765,34	K
E08-23	17,34	3	5	123	2023	64	39,72010	15	23,84813	1014,92	0,00	-66,55	948,37	671990,94	467221,47	K
E08-23	16,15	24	10	297	2023	64	39,72246	15	23,84788	1009,03	0,00	-66,55	942,48	671990,88	467225,86	K
Fl01-23	12,85	3	5	123	2023	64	26,16388	15	55,63150	1415,44	0,00	-66,82	1348,61	647946,52	440728,47	K
Fl01-23	14,88	23	10	296	2023	64	26,15738	15	55,61613	1409,86	0,00	-66,82	1343,04	647959,43	440717,01	K
G02-23	19,45	7	5	127	2023	64	26,84696	17	17,71810	1635,34	0,00	-67,73	1567,61	582064,28	439507,82	K
G02-23	11,15	24	10	297	2023	64	26,84273	17	17,72185	1634,66	-1,77	-67,73	1565,17	582061,48	439499,89	K
G03-23	18,81	7	5	127	2023	64	28,44152	17	16,33470	1729,51	0,00	-67,74	1661,78	583092,99	442499,54	K
G03-23	11,49	24	10	297	2023	64	28,43946	17	16,33598	1728,79	-2,10	-67,74	1658,95	583092,07	442495,69	K
G04-23	10,38	6	5	126	2023	64	30,02476	17	15,02675	1758,88	0,00	-67,73	1691,15	584059,71	445468,90	K
G04-23	12,45	24	10	297	2023	64	30,02508	17	15,02649	1758,43	-2,35	-67,72	1688,36	584059,90	445469,50	K
Go1-23	11,25	6	5	126	2023	64	33,96748	17	24,92679	1829,56	0,00	-67,84	1761,72	575950,18	452583,10	K
Go1-23	13,10	24	10	297	2023	64	33,96599	17	24,92618	1829,43	-2,40	-67,86	1759,17	575950,74	452580,34	K
Haab-23	10,95	6	5	126	2023	64	20,96631	17	24,11018	1798,70	0,00	-67,54	1731,16	577213,02	428451,08	K
Haab-23	10,80	25	10	298	2023	64	20,96676	17	24,10999	1795,33	0,00	-67,54	1727,79	577213,15	428451,92	K
Hof01-23	14,33	3	5	123	2023	64	32,34928	15	35,83025	1209,56	0,00	-66,67	1142,89	663203,11	453018,07	K
Hof01-23	14,25	24	10	297	2023	64	32,34295	15	35,83034	1204,55	0,00	-66,67	1137,87	663203,68	453006,33	K
K01-23	17,91	6	5	126	2023	64	35,17679	17	51,88038	1103,74	0,00	-67,58	1036,16	554380,46	454366,41	K
K01-23	15,47	25	10	298	2023	64	35,17796	17	51,88690	1098,61	0,00	-67,58	1031,03	554375,22	454368,50	K
K02-23	17,28	6	5	126	2023	64	34,80440	17	49,67746	1235,64	0,00	-67,61	1168,02	556151,70	453706,72	K
K02-23	15,00	25	10	298	2023	64	34,80774	17	49,69254	1230,80	0,00	-67,61	1163,18	556139,55	453712,72	K
K03-23	16,59	6	5	126	2023	64	34,23421	17	46,39332	1359,51	0,00	-67,67	1291,84	558794,28	452697,27	K
K03-23	14,11	25	10	298	2023	64	34,23727	17	46,41187	1355,43	0,00	-67,67	1287,76	558779,36	452702,67	K
K04-23	15,57	6	5	126	2023	64	33,21107	17	42,24640	1554,76	0,00	-67,73	1487,02	562145,20	450862,78	K
K04-23	13,20	25	10	298	2023	64	33,21487	17	42,27205	1550,11	0,00	-67,73	1482,37	562124,56	450869,41	K
K05-23	14,34	6	5	126	2023	64	33,44646	17	35,45784	1746,98	0,00	-67,82	1679,16	567560,40	451416,09	K
K05-23	11,91	25	10	298	2023	64	33,44370	17	35,47278	1743,61	0,00	-67,82	1675,79	567548,58	451410,70	K
K06-23	12,70	6	5	126	2023	64	38,35357	17	31,31262	2014,24	0,00	-67,88	1946,37	570659,23	460606,65	K
K06-23	17,81	24	10	297	2023	64	38,35319	17	31,31006	2014,66	-2,55	-67,88	1944,23	570661,29	460605,98	K
K07-23	18,78	6	5	126	2023	64	29,11538	17	42,03620	1598,96	0,00	-67,68	1531,28	562469,58	443258,05	K
K07-23	12,50	25	10	298	2023	64	29,11556	17	42,03785	1595,69	0,00	-67,68	1528,01	562468,26	443258,37	K

Kverk-23	17,50	1	6	152	2023	64	38,65917	16	40,53513	1893,83	-0,32	-67,38	1826,13	611079,01	462390,70	K
Kverk-23	12,21	24	10	297	2023	64	38,65941	16	40,53518	1889,29	0,00	-67,38	1821,91	611078,96	462391,14	K
S01-23	13,91	6	5	126	2023	64	7,01626	17	49,97436	765,42	0,00	-66,84	698,58	556867,79	402080,46	K
S02-23	13,19	6	5	126	2023	64	12,16517	17	48,98648	1066,44	0,00	-67,05	999,40	557490,85	411660,57	K
S02-23	12,45	25	10	298	2023	64	12,15120	17	48,99325	1060,88	0,00	-67,04	993,84	557485,86	411634,51	K
S04-23	12,49	6	5	126	2023	64	16,18145	17	48,19226	1223,58	0,00	-67,21	1156,37	557992,49	419133,67	K
S04-23	11,87	25	10	298	2023	64	16,16264	17	48,21241	1217,98	0,00	-67,21	1150,78	557976,88	419098,43	K
S05-23	11,66	6	5	126	2023	64	20,51465	17	33,99310	1518,88	0,00	-67,51	1451,36	569275,50	427421,30	K
S05-23	11,19	25	10	298	2023	64	20,51258	17	34,01067	1515,16	0,00	-67,51	1447,64	569261,43	427417,14	K
SkGPS-23	13,43	2	6	153	2023	64	15,47584	17	14,73302	1027,39	-1,30	-67,01	959,08	585044,98	418453,87	K
Ske02-23	11,40	8	5	128	2023	64	15,91232	17	0,06565	1246,20	0,00	-67,07	1179,13	596865,37	419616,22	K
Ske03-23	12,80	8	5	128	2023	64	18,05267	16	56,16229	1365,66	0,00	-67,20	1298,45	599887,02	423692,21	K
Ske03-23	14,78	26	10	299	2023	64	18,02757	16	56,22648	1358,51	0,00	-67,20	1291,31	599836,78	423643,90	K
Ske04-23	13,24	8	5	128	2023	64	20,14603	16	51,80617	1466,85	0,00	-67,30	1399,56	603267,90	427696,21	K
Ske04-23	13,58	26	10	299	2023	64	20,13582	16	51,83282	1462,96	0,00	-67,30	1395,67	603247,08	427676,52	K
Ske05-23	13,92	8	5	128	2023	64	22,23402	16	47,23409	1540,72	0,00	-67,35	1473,37	606813,74	431700,01	K
Ske05-23	15,79	26	10	299	2023	64	22,22984	16	47,24418	1537,26	0,00	-67,35	1469,91	606805,90	431691,97	K
Skf00-23	20,99	2	5	122	2023	64	15,48130	15	54,09593	1011,07	0,00	-66,03	945,03	650150,17	420964,14	K
Skf00-23	11,58	23	10	296	2023	64	15,48292	15	54,09271	1004,88	0,00	-66,03	938,85	650152,63	420967,28	K
Skf01-23	9,95	3	5	123	2023	64	18,01726	16	5,02291	1349,99	0,00	-66,64	1283,36	641113,89	425251,13	K
Skf01-23	13,74	23	10	296	2023	64	18,01480	16	5,00810	1344,86	0,00	-66,64	1278,23	641126,03	425247,13	K
T01-23	15,29	7	5	127	2023	64	19,15529	18	6,52452	828,29	0,00	-67,25	761,04	543110,47	424414,05	K
T02-23	14,32	7	5	127	2023	64	19,47945	18	4,54734	948,08	0,00	-67,27	880,82	544695,50	425039,16	K
T03-23	12,54	7	5	127	2023	64	20,19899	17	58,61111	1129,37	0,00	-67,30	1062,07	549458,13	426449,60	K
T03-23	14,89	25	10	298	2023	64	20,19630	17	58,62751	1124,63	0,00	-67,30	1057,33	549445,00	426444,39	K
T04-23	11,42	7	5	127	2023	64	21,33609	17	51,52929	1286,66	0,00	-67,36	1219,30	555124,90	428659,66	K
T04-23	14,46	25	10	298	2023	64	21,33178	17	51,54574	1282,32	0,00	-67,36	1214,96	555111,81	428651,41	K
T05-23	10,83	7	5	127	2023	64	22,26332	17	43,00304	1411,86	0,00	-67,47	1344,39	561953,42	430513,72	K
T05-23	13,85	25	10	298	2023	64	22,25949	17	43,01894	1409,80	-1,72	-67,47	1340,62	561940,76	430506,36	K
T06-23	17,91	6	5	126	2023	64	24,27135	17	36,52699	1535,23	0,00	-67,61	1467,62	567081,28	434353,98	K
T06-23	12,53	25	10	298	2023	64	24,26702	17	36,53949	1535,15	-2,90	-67,61	1464,64	567071,41	434345,70	K
T07-23	15,36	6	5	126	2023	64	25,29334	17	31,21459	1631,41	0,00	-67,70	1563,71	571305,27	436349,26	K
T07-23	11,60	25	10	298	2023	64	25,29120	17	31,22372	1629,94	-1,90	-67,70	1560,34	571298,03	436345,11	K
T08-23	16,03	6	5	126	2023	64	26,29828	17	27,75570	1704,46	0,00	-67,75	1636,71	574037,23	438282,17	K
T08-23	11,11	25	10	298	2023	64	26,29798	17	27,75821	1701,57	0,00	-67,75	1633,82	574035,23	438281,57	K

Appendix D: Measured surface velocity at marked sites on Vatnajökull in 2023.

Site	Calendar day date	#	Calendar day date	#	# of days	translation (m)	(°)	velocity (cm/day)	(m/annum)
B07-23	230504	124	231027	300	176	1,90	157	1,08	3,93
B09-23	230505	125	231024	297	172	0,28	187	0,16	0,59
B10-23	230505	125	231024	297	172	0,00	270	0,00	0,00
B11-23	230505	125	231024	297	172	9,48	19	5,51	20,12
B12-23	230505	125	231024	297	172	15,98	21	9,29	33,91
B13-23	230504	124	231026	299	175	17,11	25	9,77	35,68
B13ror15	221017	290	230504	124	199	5,65	27	2,84	10,36
B13ror15	230504	124	231026	299	175	17,94	28	10,25	37,42
B14-23	230504	124	231023	296	172	15,69	39	9,12	33,30
B15-23	230504	124	231024	297	173	12,42	49	7,18	26,21
B16-23	230508	128	231023	296	168	0,64	38	0,38	1,38
B17-23	230504	124	231023	296	172	18,67	16	10,86	39,62
B18-23	230503	123	231023	296	173	10,76	346	6,22	22,70
B19-23	230503	123	231023	296	173	0,72	325	0,42	1,52
Bb0-23	230504	124	231023	296	172	0,94	250	0,55	1,99
Barc-23	230531	151	231024	297	146	4,91	95	3,36	12,28
Bb02-23	230531	151	230912	255	104	3,45	95	3,31	12,10
Bb02-23	230912	255	231024	297	42	1,27	94	3,02	11,03
Bb08-23	230531	151	230912	255	104	3,88	81	3,73	13,62
Bb08-23	230912	255	231024	297	42	1,33	97	3,17	11,58
Bb09-23	230531	151	231024	297	146	2,43	99	1,66	6,07
Bb05-23	230531	151	231024	297	146	3,44	197	2,35	8,59
Bb10-23	230531	151	231024	297	146	8,32	122	5,70	20,80
Bb10-23	231024	297	230912	255	-42	4,69	6	-11,17	-40,77
Bor-23	230602	153	231027	300	147	9,47	204	6,44	23,51
Br1-23	230622	173	231022	295	122	8,74	353	7,17	26,16
Br2-22	220330	89	230621	172	448	4,28	150	0,96	3,49
Br2-23	230621	172	231022	295	123	0,80	158	0,65	2,37
Br3-22	220330	89	230621	172	448	24,67	149	5,51	20,10
Br3-23	230621	172	231022	295	123	6,50	146	5,28	19,28
Br7-23	230504	124	231023	296	172	50,94	173	29,62	108,11
Bru-23	230503	123	231023	296	173	19,45	8	11,25	41,05
Bud-23	230503	123	231023	296	173	21,60	4	12,48	45,56
D05-23	230505	125	231026	299	174	36,73	32	21,11	77,06
D07-23	230505	125	231026	299	174	40,10	23	23,05	84,12
D08-23	230505	125	231026	299	174	17,50	6	10,06	36,70
D12-23	230505	125	231024	297	172	1,01	9	0,59	2,15
E01-22	221017	290	230503	123	198	15,05	276	7,60	27,74
E01-23	230503	123	231024	297	174	20,90	19	12,01	43,84
E02-23	230503	123	231024	297	174	34,40	9	19,77	72,15
E03-23	230503	123	231024	297	174	11,15	344	6,41	23,40
E04-23	230503	123	231024	297	174	1,32	15	0,76	2,78
E07-23	230503	123	231024	297	174	11,40	39	6,55	23,91
E08-23	230503	123	231024	297	174	4,38	3	2,51	9,18
Fl01-23	230503	123	231023	296	173	17,23	134	9,96	36,36
G02-23	230507	127	231024	297	170	8,39	201	4,94	18,02
G03-23	230507	127	231024	297	170	3,95	195	2,32	8,48
G04-23	230506	126	231024	297	171	0,63	19	0,37	1,34
Go1-23	230506	126	231024	297	171	2,80	170	1,64	5,98
Haab-23	230506	126	231025	298	172	0,85	10	0,49	1,80
Hof01-23	230503	123	231024	297	174	11,72	180	6,74	24,59

K01-23	230506	126	231025	298	172	5,64	293	3,28	11,96
K02-23	230506	126	231025	298	172	13,53	297	7,87	28,72
K03-23	230506	126	231025	298	172	15,86	291	9,22	33,65
K04-23	230506	126	231025	298	172	21,67	289	12,60	45,98
K05-23	230506	126	231025	298	172	12,98	247	7,55	27,55
K06-23	230506	126	231024	297	171	2,16	109	1,26	4,60
K07-23	230506	126	231025	298	172	1,36	284	0,79	2,89
Kverk-23	230601	152	231024	297	145	0,45	355	0,31	1,12
S02-23	230506	126	231025	298	172	26,45	192	15,38	56,12
S04-23	230506	126	231025	298	172	38,45	205	22,35	81,59
S05-23	230506	126	231025	298	172	14,66	255	8,52	31,10
Ske03-23	230508	128	231026	299	171	69,57	228	40,69	148,50
Ske04-23	230508	128	231026	299	171	28,60	229	16,73	61,06
Ske05-23	230508	128	231026	299	171	11,22	226	6,56	23,94
Skf00-23	230502	122	231023	296	174	3,97	41	2,28	8,33
Skf01-23	230503	123	231023	296	173	12,78	111	7,39	26,97
T03-23	230507	127	231025	298	171	14,12	249	8,26	30,13
T04-23	230507	127	231025	298	171	15,46	239	9,04	33,00
T05-23	230507	127	231025	298	171	14,62	241	8,55	31,22
T06-23	230506	126	231025	298	172	12,85	231	7,47	27,27
T07-23	230506	126	231025	298	172	8,33	242	4,84	17,68
T08-23	230506	126	231025	298	172	2,09	255	1,21	4,43

Appendix E: Melt water runoff to selected rivers in summer 2023, derived from summer surface balance.

ΔS: area in each elevation range where summer balance is negative, **∑ΔS**: cumulative area above a given elevation, **ΔQ$_s$**: melt water runoff from a given elevation range, **∑ΔQ$_s$**: cumulative melt water runoff from an area above given elevation.

Tungnaá water drainage basin

Elevation (m a. s. l.)		ΔS km^2	∑ΔS km^2	ΔQ$_s$ ($10^6 m^3$)	∑ΔQ$_s$ ($10^6 m^3$)
1350	1400	0,3	0,3	0,5	0,5
1300	1350	6	6,3	11,8	12,4
1250	1300	9,8	16,1	22,6	35,0
1200	1250	10,7	26,8	27,9	62,9
1150	1200	9,5	36,4	28,2	91,1
1100	1150	11	47,4	36,0	127,1
1050	1100	10,3	57,7	37,4	164,5
1000	1050	9,5	67,2	38,1	202,6
950	1000	8,8	76,1	38,2	240,8
900	950	8,5	84,6	39,6	280,4
850	900	6,3	90,9	31,8	312,2
800	850	6,3	97,1	33,8	346,0
750	800	4,6	101,8	26,2	372,2
700	750	2,5	104,2	14,5	386,7
650	700	0,1	104,4	0,8	387,5

Sylgja water drainage basin

Elevation (m a. s. l.)		ΔS km^2	∑ΔS km^2	ΔQ$_s$ ($10^6 m^3$)	∑ΔQ$_s$ ($10^6 m^3$)
1300	1350	1,1	1,1	2,3	2,3
1250	1300	3,4	4,5	8,2	10,5
1200	1250	5,3	9,7	14,2	24,7
1150	1200	8	17,8	23,5	48,2
1100	1150	5,8	23,5	18,9	67,2
1050	1100	6	29,5	21,5	88,7
1000	1050	5,7	35,3	22,5	111,1
950	1000	1,8	37,1	7,7	118,8
900	950	0,7	37,8	2,9	121,7

Western Skaftá cauldron water drainage basin

Elevation (m a. s. l.)		ΔS km^2	∑ΔS km^2	ΔQ$_s$ ($10^6 m^3$)	∑ΔQ$_s$ ($10^6 m^3$)
1700	1750	2,3	2,3	1,1	1,1
1650	1700	7,1	9,4	3,7	4,8
1600	1650	7,9	17,4	4,8	9,6
1550	1600	5	22,4	3,4	13,1
1500	1550	2,6	25,0	2,0	15,0

Eastern Skaftár cauldron water drainage basin

Elevation (m a. s. l.)		ΔS km^2	∑ΔS km^2	ΔQ_s ($10^6 m^3$)	$\sum\Delta Q_s$ ($10^6 m^3$)
1700	1750	2,3	2,3	1,1	1,1
1650	1700	7,1	9,4	3,7	4,8
1600	1650	7,9	17,4	4,8	9,6
1550	1600	5	22,4	3,4	13,1
1500	1550	2,6	25,0	2,0	15,0

Grímsvötn water drainage basin

Elevation (m a. s. l.)		ΔS km^2	∑ΔS km^2	ΔQ_s ($10^6 m^3$)	$\sum\Delta Q_s$ ($10^6 m^3$)
1900	1950	0,4	0,4	0,1	0,1
1850	1900	1,4	1,8	0,3	0,4
1800	1850	1,7	3,5	0,5	0,8
1750	1800	4,9	8,3	2,1	2,9
1700	1750	24	32,3	11,4	14,4
1650	1700	48	80,3	27,4	41,8
1600	1650	30,7	111,0	21,0	62,7
1550	1600	19,6	130,6	16,1	78,8
1500	1550	16,2	146,8	16,2	95,0
1450	1500	9,5	156,3	12,5	107,5
1400	1450	13,7	170,0	23,5	130,9
1350	1400	1,2	171,3	2,1	133,0

Kaldakvísl water drainage basin

Elevation (m a. s. l.)		ΔS km^2	∑ΔS km^2	ΔQ_s ($10^6 m^3$)	$\sum\Delta Q_s$ ($10^6 m^3$)
1950	2000	0,1	0,1	0,0	0,0
1900	1950	6,5	6,6	0,5	0,5
1850	1900	6,5	13,1	1,2	1,7
1800	1850	6,2	19,3	1,8	3,5
1750	1800	10,9	30,2	3,8	7,4
1700	1750	20,3	50,5	9,0	16,3
1650	1700	16,8	67,3	9,4	25,8
1600	1650	14,5	81,8	10,0	35,7
1550	1600	18,4	100,2	16,0	51,7
1500	1550	24,1	124,3	25,6	77,3
1450	1500	27,8	152,1	34,5	111,8
1400	1450	22,3	174,4	33,1	144,9
1350	1400	20,5	194,9	37,9	182,8
1300	1350	19,2	214,1	45,9	228,7
1250	1300	20,5	234,7	58,7	287,4
1200	1250	20	254,6	64,2	351,6
1150	1200	19	273,6	67,2	418,8
1100	1150	17	290,6	67,1	485,9
1050	1100	15,7	306,4	68,5	554,3
1000	1050	12,9	319,2	59,6	613,9
950	1000	7,2	326,5	35,9	649,9
900	950	1,2	327,7	6,1	656,0

Jökulsá á Fjöllum water drainage basin

Elevation (m a. s. l.)		ΔS km^2	∑ΔS km^2	ΔQ_s $(10^6 m^3)$	$\sum \Delta Q_s$ $(10^6 m^3)$
1950	2000	0,9	0,9	0,0	0,0
1900	1950	11,5	12,4	0,9	1,0
1850	1900	25	37,4	5,2	6,1
1800	1850	18,4	55,8	5,3	11,5
1750	1800	21,9	77,7	7,9	19,4
1700	1750	39,3	117,0	16,4	35,8
1650	1700	81	198,0	41,2	77,1
1600	1650	122	320,3	73,7	150,8
1550	1600	101	421,2	74,1	224,9
1500	1550	92,6	513,8	82,1	307,0
1450	1500	79,5	593,3	83,6	390,6
1400	1450	68,7	662,0	77,0	467,6
1350	1400	54,2	716,2	66,5	534,1
1300	1350	42,7	758,9	65,4	599,5
1250	1300	46,3	805,2	91,1	690,5
1200	1250	49,3	854,4	122,9	813,4
1150	1200	48,7	903,1	152,5	965,9
1100	1150	44,1	947,2	166,1	1132,1
1050	1100	31	978,2	134,5	1266,6
1000	1050	31,1	1009,3	142,3	1408,9
950	1000	28,9	1038,1	141,2	1550,0
900	950	24,7	1062,8	129,2	1679,2
850	900	20,5	1083,3	115,3	1794,5
800	850	16,5	1099,8	103,0	1897,5
750	800	8,5	1108,4	58,6	1956,1
700	750	0,3	1108,7	2,5	1958,6

Kreppa and Kverká water drainage basin

Elevation (m a. s. l.)		ΔS km^2	∑ΔS km^2	ΔQ_s ($10^6 m^3$)	$\sum\Delta Q_s$ ($10^6 m^3$)
1900	1950	0,1	0,1	0,1	0,1
1850	1900	1,4	1,5	0,6	0,7
1800	1850	4,4	5,9	1,5	2,2
1750	1800	2,7	8,6	1,0	3,2
1700	1750	3,8	12,4	1,6	4,9
1650	1700	5,3	17,7	2,6	7,5
1600	1650	41,6	59,3	25,9	33,4
1550	1600	20,4	79,7	14,1	47,5
1500	1550	13,4	93,1	10,8	58,2
1450	1500	16,3	109,4	14,9	73,1
1400	1450	20,1	129,5	20,7	93,9
1350	1400	25,9	155,4	29,3	123,2
1300	1350	20,3	175,7	27,0	150,2
1250	1300	15,3	191,0	26,2	176,4
1200	1250	17,7	208,7	43,0	219,4
1150	1200	17,2	225,8	52,9	272,3
1100	1150	16,1	242,0	55,3	327,6
1050	1100	10,4	252,4	38,7	366,3
1000	1050	11,6	263,9	46,6	412,8
950	1000	12,7	276,6	55,1	468,0
900	950	12,8	289,4	59,4	527,4
850	900	11,9	301,1	58,8	586,2
800	850	9,8	311,0	52,3	638,5
750	800	6,7	317,7	38,4	676,9
700	750	3,4	33,9	20,9	176,3
650	700	0,2	34,1	1,0	177,3

Hálslón water drainage basin

Elevation (m a. s. l.)		ΔS km^2	∑ΔS km^2	ΔQ_s ($10^6 m^3$)	$\sum\Delta Q_s$ ($10^6 m^3$)
1600	1650	11,7	11,7	7,8	7,8
1550	1600	33,6	45,3	24,0	31,8
1500	1550	65,2	110,6	51,1	82,9
1450	1500	70	180,6	62,7	145,6
1400	1450	98,9	279,5	94,7	240,4
1350	1400	133	412,4	148,2	388,5
1300	1350	129	541,5	171,8	560,3
1250	1300	122	663,9	203,7	764,0
1200	1250	97,2	761,1	204,0	968,1
1150	1200	81,9	843,1	218,5	1186,6
1100	1150	64	907,0	203,5	1390,2
1050	1100	54,6	961,6	197,1	1587,3
1000	1050	45,8	1007,5	181,7	1769,0
950	1000	39,1	1046,6	167,6	1936,6
900	950	31,9	1078,4	146,2	2082,8
850	900	26,6	1105,0	130,3	2213,1
800	850	24,4	1129,5	127,9	2341,1
750	800	24,2	1153,7	136,4	2477,5
700	750	22,7	1176,4	139,0	2616,4
650	700	9,4	1185,8	61,0	2677,4
600	650	0,5	1186,3	3,3	2680,7

Jökulsá á Fljótsdal water drainage basin

Elevation (m a. s. l.)		ΔS km^2	∑ΔS km^2	ΔQ_s $(10^6 m^3)$	$\sum \Delta Q_s$ $(10^6 m^3)$
1550	1600	0	0,0	0,0	0,0
1500	1550	0,1	0,1	0,1	0,1
1450	1500	1,1	1,2	1,1	1,2
1400	1450	2	3,2	2,2	3,5
1350	1400	2,8	6,1	3,4	6,9
1300	1350	5,4	11,5	7,6	14,4
1250	1300	15,8	27,3	28,9	43,3
1200	1250	14,8	42,1	35,3	78,6
1150	1200	16,4	58,6	48,9	127,6
1100	1150	14	72,6	47,9	175,5
1050	1100	11,7	84,3	43,8	219,3
1000	1050	10,8	95,1	43,7	262,9
950	1000	8,7	103,8	38,4	301,4
900	950	5,5	109,3	26,0	327,4
850	900	4,2	113,5	20,7	348,1
800	850	2,9	116,5	15,0	363,1
750	800	1,8	118,2	9,6	372,7
700	750	1,6	119,8	9,4	382,1
650	700	0,6	120,5	3,9	386,0

Hornafjarðarfljót water drainage basin

Elevation (m a. s. l.)		ΔS km^2	∑ΔS km^2	ΔQ_s ($10^6 m^3$)	$\sum \Delta Q_s$ ($10^6 m^3$)
1450	1500	1,2	1,2	1,3	1,3
1400	1450	8,3	9,5	7,9	9,2
1350	1400	12,4	21,9	13,2	22,4
1300	1350	18,9	40,8	23,9	46,3
1250	1300	37,3	78,1	60,1	106,4
1200	1250	28,7	106,8	51,1	157,5
1150	1200	19,9	126,7	41,6	199,1
1100	1150	18,3	145,0	43,9	243,0
1050	1100	13,8	158,8	38,7	281,7
1000	1050	10,6	169,4	34,0	315,6
950	1000	10,1	179,5	35,9	351,5
900	950	8,1	187,5	30,9	382,4
850	900	5,1	192,6	20,9	403,3
800	850	4,2	196,8	18,3	421,6
750	800	3,3	200,1	14,7	436,3
700	750	3,1	203,2	15,0	451,3
650	700	3,3	206,4	17,5	468,8
600	650	2,6	209,0	14,6	483,4
550	600	1,9	210,9	11,1	494,5
500	550	1,7	212,7	10,3	504,9
450	500	1,3	214,0	8,4	513,3
400	450	1	215,0	6,9	520,1
350	400	1	216,0	6,8	527,0
300	350	0,6	216,6	4,4	531,4
250	300	0,7	217,2	5,3	536,7
200	250	0,9	218,1	7,3	544,0
150	200	1,8	219,9	15,5	559,6
100	150	2,4	222,3	21,6	581,2
50	100	2,2	224,5	20,9	602,1
0	50	2,9	227,4	29,1	631,2

Jökulsá á Breiðamerkursandi water drainage basin

Elevation (m a. s. l.)		ΔS km^2	∑ΔS km^2	ΔQ_s ($10^6 m^3$)	$\sum\Delta Q_s$ ($10^6 m^3$)
1700	1750	1	1,0	0,6	0,6
1650	1700	4,2	5,2	2,6	3,3
1600	1650	14,4	19,5	9,2	12,5
1550	1600	19,1	38,6	13,3	25,8
1500	1550	22,7	61,3	18,7	44,6
1450	1500	36,2	97,6	33,8	78,3
1400	1450	50,9	148,5	52,7	131,1
1350	1400	83	231,5	99,6	230,7
1300	1350	82,6	314,1	112,1	342,8
1250	1300	51	365,1	76,6	419,4
1200	1250	33,6	398,7	57,3	476,7
1150	1200	27,2	425,9	54,4	531,1
1100	1150	22,1	448,0	51,6	582,7
1050	1100	18,4	466,4	48,5	631,2
1000	1050	14,5	480,9	42,6	673,8
950	1000	15,2	496,1	49,4	723,2
900	950	15,5	511,7	54,8	778,0
850	900	13,1	524,7	50,5	828,5
800	850	15,2	539,9	63,7	892,2
750	800	16,9	556,9	77,1	969,3
700	750	12,9	569,8	63,4	1032,6
650	700	20,3	590,1	105,7	1138,3
600	650	20,9	611,0	114,8	1253,2
550	600	15,9	626,9	92,7	1345,9
500	550	14,1	641,0	85,6	1431,5
450	500	4,8	645,8	30,8	1462,3
400	450	6,1	651,9	41,2	1503,5
350	400	5,7	657,6	39,9	1543,4
300	350	4,5	662,1	32,9	1576,3
250	300	4,6	666,7	36,0	1612,3
200	250	4,9	671,6	40,4	1652,7
150	200	4,4	676,0	37,7	1690,4
100	150	4,7	680,7	42,1	1732,4
50	100	4,1	684,8	38,4	1770,8
0	50	1,2	686,0	12,1	1782,9

Breiðárlón/Fjallsárlón water drainage basin

Elevation (m a. s. l.)		ΔS km²	∑ΔS km²	ΔQs (10⁶m³)	∑ΔQs (10⁶m³)
2000	2050	0,1	0,1	0,0	0,0
1950	2000	0,6	0,7	0,2	0,2
1900	1950	0,9	1,7	0,2	0,4
1850	1900	1,6	3,2	0,2	0,7
1800	1850	2	5,2	0,1	0,8
1750	1800	2,5	7,7	0,2	1,0
1700	1750	3	10,7	0,6	1,5
1650	1700	3,1	13,8	1,0	2,5
1600	1650	4,3	18,0	1,9	4,5
1550	1600	4,3	22,3	2,6	7,1
1500	1550	5,7	28,1	4,6	11,7
1450	1500	5	33,1	4,8	16,6
1400	1450	5,1	38,1	5,9	22,4
1350	1400	6,3	44,5	9,8	32,2
1300	1350	12,5	57,0	24,6	56,8
1250	1300	6,4	63,4	13,6	70,4
1200	1250	5,5	68,9	11,1	81,5
1150	1200	4,7	73,6	9,3	90,7
1100	1150	4,2	77,8	9,3	100,0
1050	1100	4,6	82,5	11,2	111,2
1000	1050	5,6	88,0	14,9	126,1
950	1000	6,2	94,3	20,1	146,1
900	950	7,2	101,5	25,5	171,6
850	900	5,7	107,2	21,9	193,5
800	850	6,8	114,0	28,7	222,1
750	800	7,9	121,9	35,9	258,1
700	750	6,2	128,1	30,6	288,6
650	700	5,1	133,2	26,6	315,2
600	650	6,2	139,4	34,0	349,3
550	600	7	146,4	41,0	390,3
500	550	7,6	154,0	46,3	436,6
450	500	7,9	162,0	50,9	487,6
400	450	8	169,9	53,5	541,0
350	400	9,9	179,8	69,5	610,5
300	350	8	187,8	59,4	669,9
250	300	6	193,8	46,9	716,8
200	250	6	199,8	49,0	765,8
150	200	5,6	205,4	47,9	813,7
100	150	5,6	211,0	50,5	864,2
50	100	3,9	214,9	37,4	901,6
0	50	5	220,0	52,9	954,5

Skeiðarársandur (Gígja) water drainage basin

Elevation (m a. s. l.)		ΔS km^2	∑ΔS km^2	ΔQ_s $(10^6 m^3)$	$\sum \Delta Q_s$ $(10^6 m^3)$
1700	1750	1,8	1,8	0,9	0,9
1650	1700	21,9	23,8	13,3	14,2
1600	1650	83,1	106,8	52,5	66,7
1550	1600	85,8	192,6	61,9	128,7
1500	1550	111	303,3	90,8	219,5
1450	1500	106	409,7	102,3	322,0
1400	1450	104	513,3	119,4	441,4
1350	1400	90,7	604,0	123,2	564,7
1300	1350	77,4	681,4	118,8	683,5
1250	1300	68,7	750,1	123,3	806,8
1200	1250	59,7	809,8	127,2	934,0
1150	1200	54,1	863,8	134,5	1068,5
1100	1150	50,3	914,2	139,7	1208,1
1050	1100	45,4	959,5	140,3	1348,4
1000	1050	40	999,5	134,6	1482,9
950	1000	39,4	1039,0	143,3	1626,2
900	950	35,8	1074,8	142,8	1769,0
850	900	37,6	1112,4	163,2	1932,2
800	850	32,1	1144,4	149,2	2081,4
750	800	28,3	1172,7	140,3	2221,6
700	750	23,6	1196,3	124,4	2346,1
650	700	21,9	1218,2	123,6	2469,6
600	650	14,5	1232,8	86,9	2556,6
550	600	20	1252,7	124,9	2681,6
500	550	21,9	1274,7	144,6	2826,1
450	500	16,5	1291,1	112,9	2939,0
400	450	11,4	1302,6	82,5	3021,5
350	400	11,5	1314,1	86,4	3107,9
300	350	12,9	1327,0	101,2	3209,1
250	300	13,1	1340,2	108,1	3317,2
200	250	11,6	1351,7	100,2	3417,3
150	200	11,6	1363,3	103,2	3520,5
100	150	9,6	1372,8	88,5	3609,0
50	100	6,8	1379,6	64,0	3673,0
0	50	3,5	1383,3	34,2	3707,2

Djúpá water drainage basin

Elevation (m a. s. l.)		ΔS km^2	∑ΔS km^2	ΔQ$_s$ ($10^6 m^3$)	∑ΔQ$_s$ ($10^6 m^3$)
1450	1500	0,1	0,1	0,1	0,1
1400	1450	0,3	0,4	0,4	0,5
1350	1400	0,6	1,0	1,0	1,5
1300	1350	3,4	4,4	6,4	7,9
1250	1300	3,2	7,5	6,8	14,7
1200	1250	2,9	10,4	7,1	21,8
1150	1200	3,2	13,6	8,8	30,6
1100	1150	5	18,7	15,6	46,3
1050	1100	5	23,6	17,8	64,1
1000	1050	8,4	32,1	33,6	97,6
950	1000	7,3	39,3	32,2	129,9
900	950	7,4	46,7	35,0	164,8
850	900	6	52,7	30,7	195,6
800	850	5,8	58,5	31,2	226,8
750	800	5,9	64,4	33,8	260,6
700	750	3,6	68,1	22,0	282,6
650	700	2	70,1	12,7	295,3
600	650	0,1	70,1	0,6	295,9

Brunná water drainage basin

Elevation (m a. s. l.)		ΔS km^2	∑ΔS km^2	ΔQ$_s$ ($10^6 m^3$)	∑ΔQ$_s$ ($10^6 m^3$)
1000	1050	0,7	0,7	2,7	2,7
950	1000	1,8	2,4	7,8	10,5
900	950	3,8	6,2	17,7	28,2
850	900	3,9	10,1	19,4	47,6
800	850	3,6	13,7	19,7	67,2
750	800	3,9	17,7	22,4	89,6
700	750	4,4	22,1	26,3	116,0
650	700	5,2	27,2	33,1	149,1
600	650	2,5	29,8	17,0	166,1
550	600	0	29,8	0,0	166,1

Hverfisfljót water drainage basin

Elevation (m a. s. l.)		ΔS km^2	∑ΔS km^2	$ΔQ_s$ (10^6m^3)	$∑ΔQ_s$ (10^6m^3)
1700	1750	1	1,0	0,3	0,3
1650	1700	5,9	6,9	2,4	2,7
1600	1650	9,1	16,0	4,5	7,2
1550	1600	10,6	26,6	5,9	13,1
1500	1550	20,8	47,5	14,7	27,8
1450	1500	40,1	87,6	39,4	67,2
1400	1450	26,5	114,1	30,8	98,0
1350	1400	24	138,1	35,2	133,2
1300	1350	22,5	160,6	40,8	174,1
1250	1300	17,2	177,8	37,4	211,5
1200	1250	20,3	198,1	51,2	262,7
1150	1200	14,2	212,4	42,1	304,8
1100	1150	10,6	223,0	34,8	339,6
1050	1100	9,4	232,4	33,8	373,4
1000	1050	8,4	240,8	33,5	406,9
950	1000	8,5	249,3	37,2	444,1
900	950	7,5	256,8	34,9	479,0
850	900	7,9	264,7	39,3	518,3
800	850	6,7	271,3	35,8	554,1
750	800	7,5	278,9	42,7	596,8
700	750	9,5	288,3	56,2	653,0
650	700	11,1	299,5	70,2	723,1
600	650	6,3	305,7	41,7	764,9
550	600	0	305,8	0,3	765,1

Skaftá water drainage basin

Elevation (m a. s. l.)		ΔS km^2	∑ΔS km^2	$ΔQ_s$ (10^6m^3)	$∑ΔQ_s$ (10^6m^3)
1650	1700	2	2,0	1,2	1,2
1600	1650	14,9	16,9	9,0	10,2
1550	1600	22,9	39,8	15,7	25,9
1500	1550	31,9	71,7	25,7	51,6
1450	1500	24,6	96,3	21,6	73,3
1400	1450	22,4	118,6	25,1	98,3
1350	1400	20,4	139,0	30,2	128,6
1300	1350	22,1	161,1	40,6	169,2
1250	1300	14,8	175,9	32,5	201,7
1200	1250	20,2	196,1	52,1	253,8
1150	1200	22	218,0	64,8	318,7
1100	1150	23,1	241,1	75,7	394,4
1050	1100	21,8	262,9	79,1	473,5
1000	1050	24,8	287,8	99,5	573,0
950	1000	20	307,8	88,2	661,1
900	950	16,6	324,5	78,5	739,6
850	900	13,6	338,0	68,0	807,6
800	850	13,5	351,5	71,8	879,4
750	800	12,5	364,0	70,3	949,7
700	750	10,1	374,1	59,7	1009,4
650	700	5,5	379,5	33,9	1043,3
600	650	0,6	380,1	3,5	1046,8

Appendix F: Records of surface elevation change a surface velocity at mass balance survey sites on Vatnajökull.

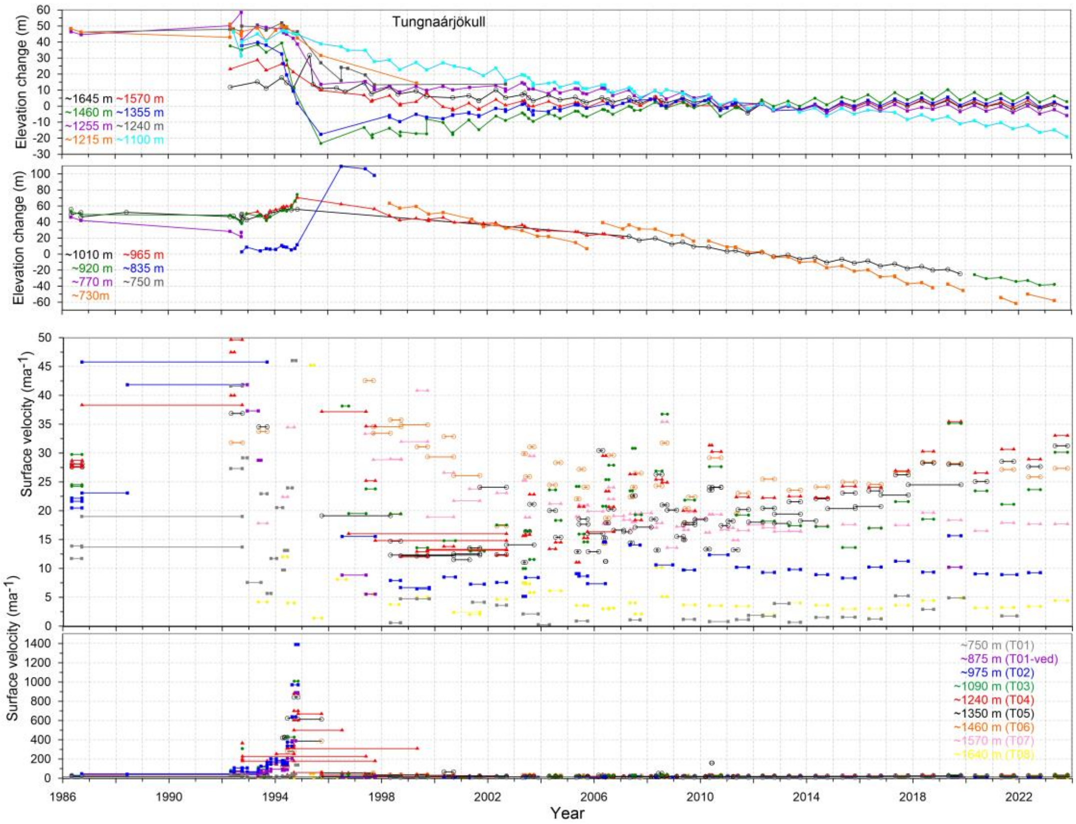

Surface elevation change relative to summer 2012 (upper panel) and average surface velocity (lower panel) at mb sites on Tungnaárjökull in 1986 to 2023.

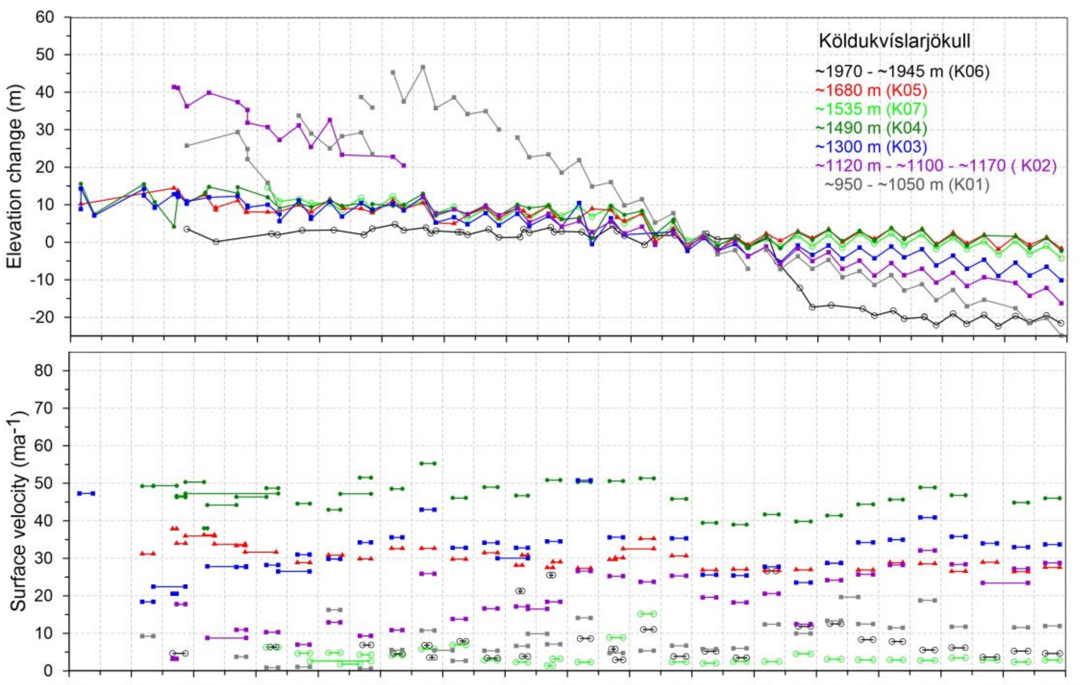

Surface elevation change relative to summer 2011-12 (upper panel) and average surface velocity (lower panel) at mb sites on Köldukvíslarjökull in 1992 to 2023.

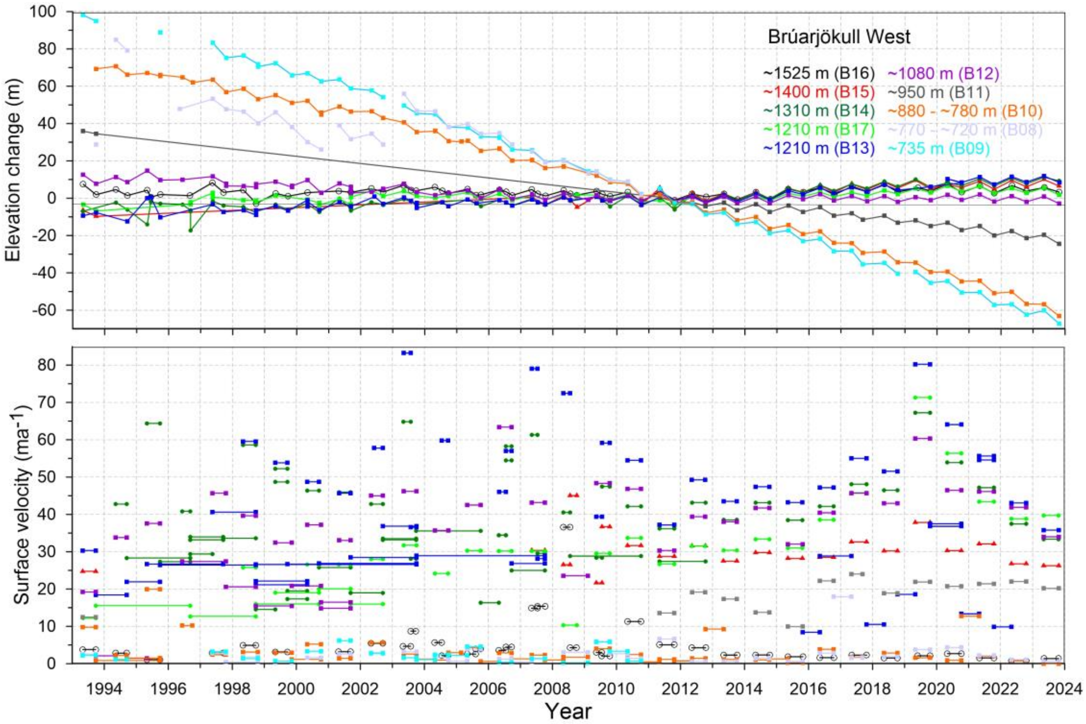

Surface elevation change relative to summer 2011 (upper panel) and average surface velocity at mb sites (lower panel) on W-Brúarjökull in 1993 to 2023.

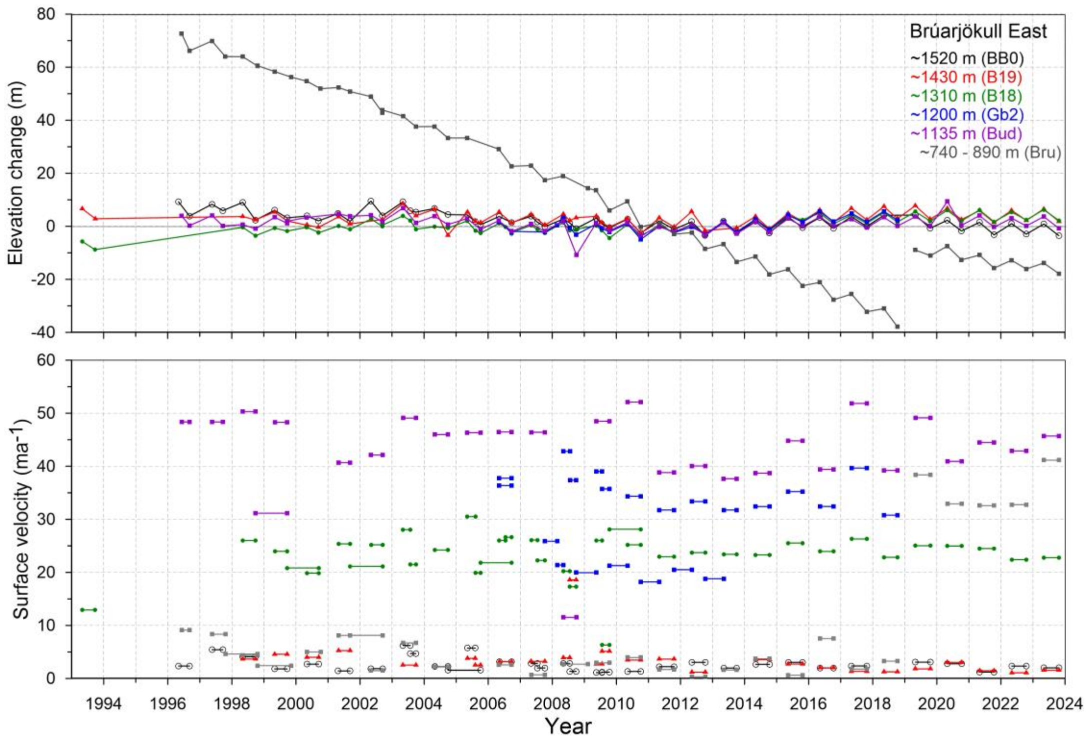

Surface elevation change relative to summer 2010 (upper panel) and average surface velocity at mb sites (lower panel) on E-Brúarjökull in 1993 to 2023.

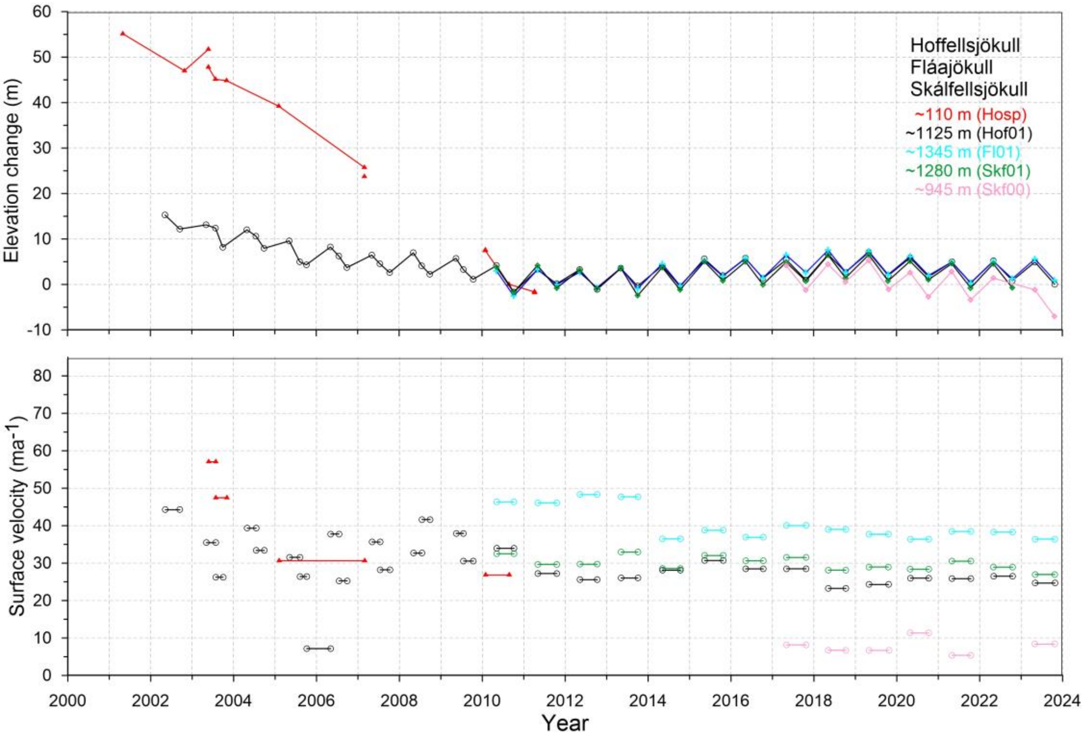

Surface elevation change relative to summer 2010 (upper panel) and average surface velocity) at mb sites (lower panel) on SE-Vatnajökull outlets in 2000 to 2023.

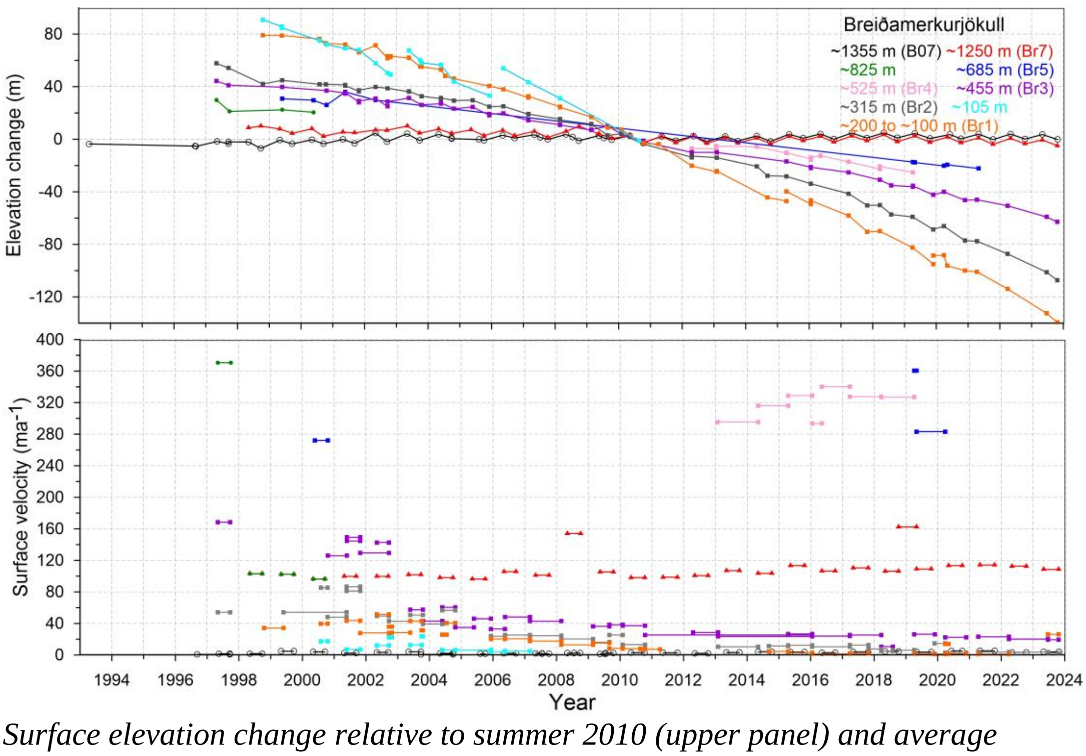

Surface elevation change relative to summer 2010 (upper panel) and average surface velocity at mb sites (lower panel) on Breiðamerkurjökull in 1993 to 2022.

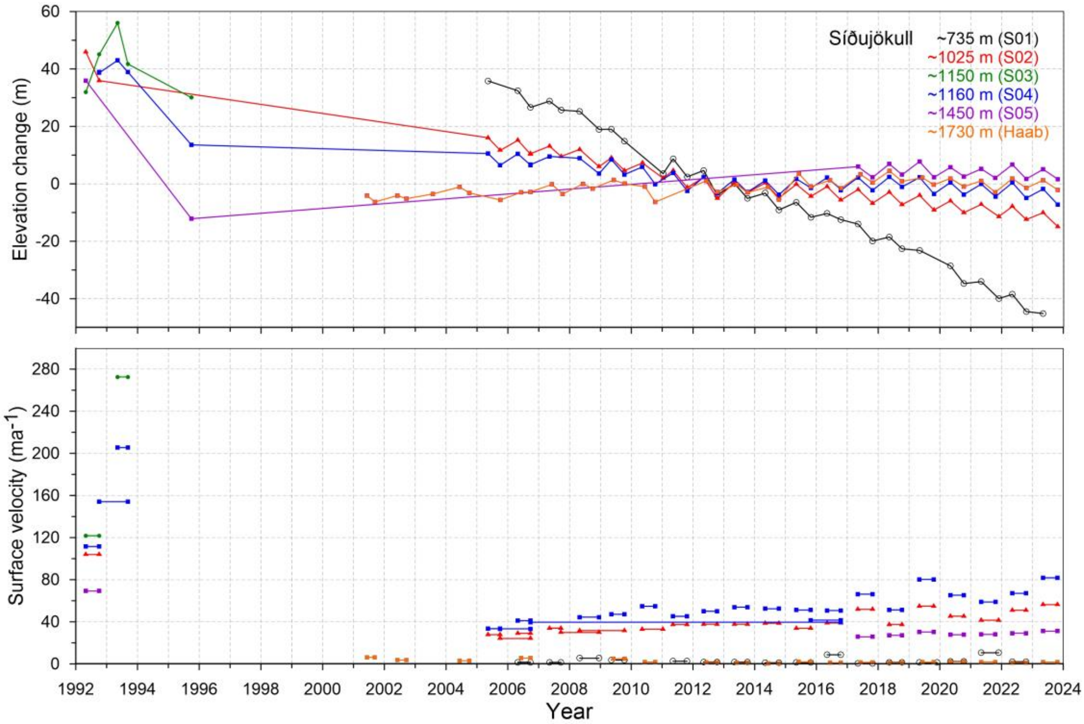

Surface elevation change relative to summer 2012 (upper panel) and average surface velocity at mb sites (lower panel) on Síðujökull in 1992 to 2023.

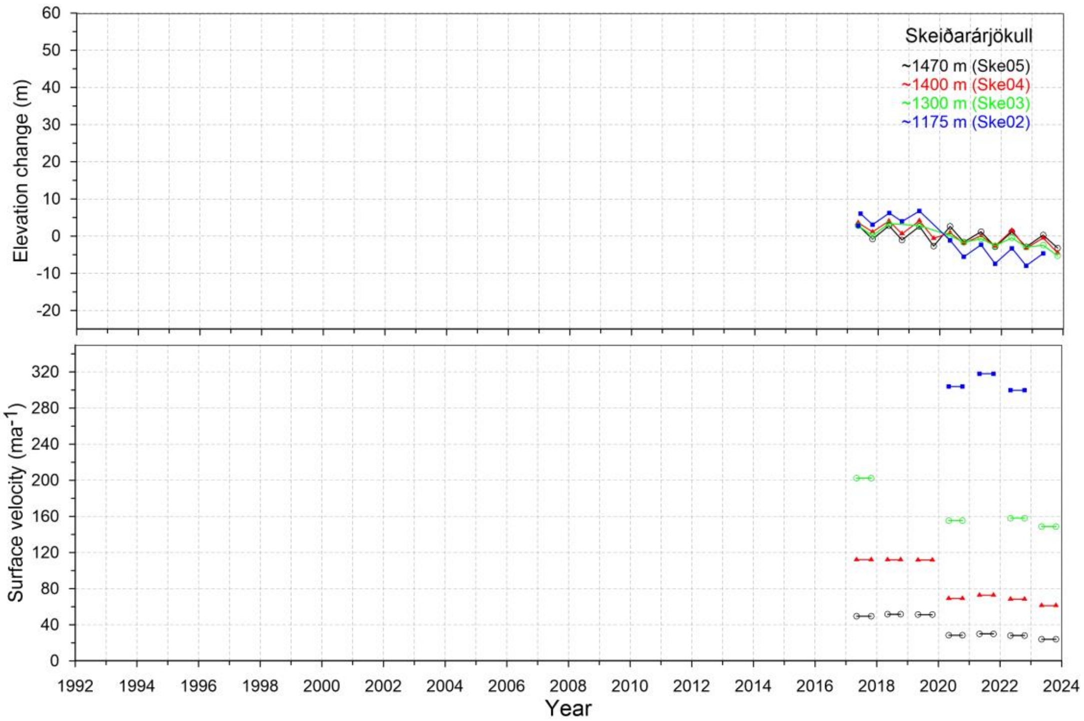

Surface elevation change relative to summer 2011-12 (upper panel) and average surface velocity at mb sites (lower panel) on Skeiðarárjökull in 2017 to 2023.

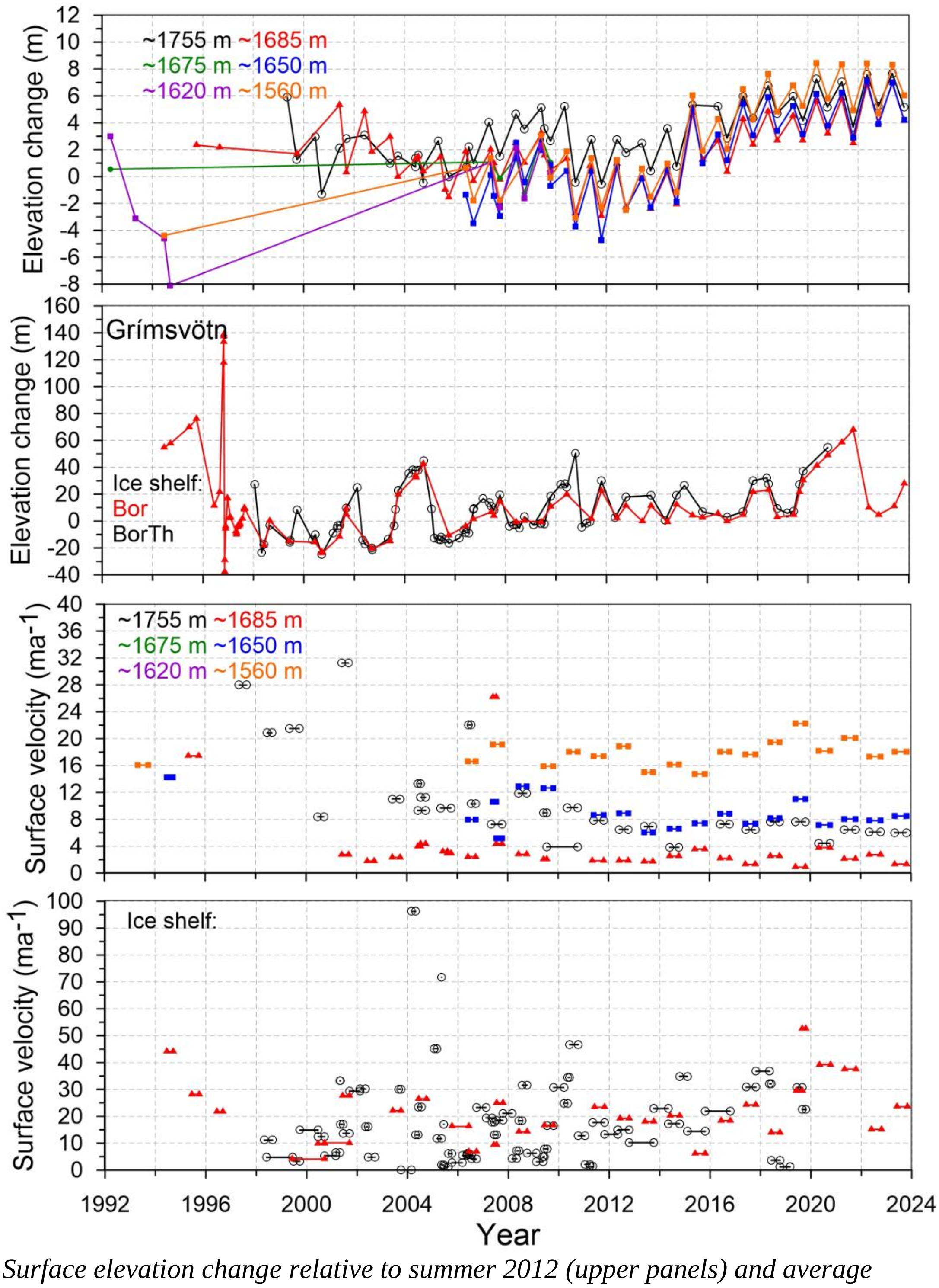

Surface elevation change relative to summer 2012 (upper panels) and average surface velocity at mb sites (lower panels) in Grímsvötn ice catchment in 1993 to 2023.